391/D-263

U.S. Department
of the Interior
National Park Service
Cultural Resources

ENVIRONMENT AND CULTURAL RESOURCES

DRAFT

PHILADELPHIA MERCHANTS' EXCHANGE

CONSERVATION STRATEGY

William D. Brookover

Elaine S. McGee

Victor G. Mossotti

Donald A. Dolske

Susan I. Sherwood

Anett Andersen, Candace Clifford, Jeffrey Coe, Frank Doyle, Cornelius Dugan, Raouf Eldeeb, James Messerich, Mary Oerhlein, Charles Pilmore, Robert Ryan, Kathryn Sather, William Schaub, Mary Woodruff, and NPS Air Quality Staff

ENVIRONMENT AND
CULTURAL RESOURCES
RESEARCH MONOGRAPH # 1

Preservation Assistance Division
Washington, DC

September 1992
Draft

Color Scans
8/22/2003



U.S. Department
of the Interior
National Park Service
Cultural Resources

ENVIRONMENT AND CULTURAL RESOURCES

DRAFT

PHILADELPHIA MERCHANTS' EXCHANGE

CONSERVATION STRATEGY

William D. Brookover

Elaine S. McGee

Victor G. Mossotti

Donald A. Dolske

Susan I. Sherwood

Anett Andersen, Candace Clifford, Jeffrey Coe, Frank Doyle, Cornelius Dugan, Raouf Eldeeb, James Messerich, Mary Oerhlein, Charles Pilmore, Robert Ryan, Kathryn Sather, William Schaub, Mary Woodruff, and NPS Air Quality Staff

ENVIRONMENT AND
CULTURAL RESOURCES
RESEARCH MONOGRAPH # 1

Preservation Assistance Division
Washington, DC

September 1992
Draft

PHILADELPHIA MERCHANTS' EXCHANGE

CONSERVATION STRATEGY

William D. Brookover
Independence NHP, NPS, Philadelphia, PA

Elaine S. McGee
U. S. Geological Survey, Reston, VA

Victor G. Mossotti
U. S. Geological Survey, Menlo Park, CA

Donald A. Dolske
Illinois State Water Survey, Champaign, IL

Susan I. Sherwood
Preservation Assistance Division, NPS, Washington, DC

Anett Andersen[1], Candace Clifford[2], Jeffrey Coe[3], Frank Doyle[4], Cornelius Dugan[5], Raouf Eldeeb[6], James Messerich[3], Mary Oerhlein[7], Charles Pilmore[3], Robert Ryan[8], Kathryn Sather[2], William Schaub[9], Mary Woodruff[10], and NPS Air Quality Staff[11]

1. ICOMOS Intern, Washington, DC
2. NCSHPO Consultant, Washington, DC
3. USGS-Photogrammetric Plotter Lab, Denver, CO
4. Independence NHP, NPS, Philadelphia, PA
5. Air Management Services, City of Philadelphia, PA
6. USGS-Branch of Geochemistry, Menlo Park, CA
7. Oerhlein and Associates, Washington, DC
8. Berger/Ryan and Associates, Ltd, Iowa City, IA
9. Preservation Assistance Division, NPS, Washington, DC
10. USGS-Geologic Division, Reston, VA
11. Research Branch, Air Quality Division, NPS, Denver, CO

ENVIRONMENT AND
CULTURAL RESOURCES
RESEARCH MONOGRAPH # 1

National Park Service
Preservation Assistance Division
Washington, DC
Draft, September 1992

TABLE OF CONTENTS

Executive Summary i

List of Figures iii

List of Tables vi

Introduction 1

Chapter One: Building History and Alterations 5

Chapter Two: Marble Characteristics and Deterioration 13

Chapter Three: Photogrammetric Description of Marble Decay 29

Chapter Four: Environmental Exposure 41

Chapter Five: Implications of Building History, Exposure and Weathering Pattterns 67

Chapter Six: Conservation Treatment Options 75

References 78

Appendix A: X-ray and Scanning Electron Microscopic Study of Alteration Crust 81

Appendix B: Photogrammetric Project Methodology 85

Appendix C: 19th-Century Pollution Estimates for Philadelphia 93

Appendix D: Microclimate/Pollution Measurement Methods 111

Appendix E: Estimating Sulfur Deposition to the Marbles 117

Plates in Stereo, with viewers

EXECUTIVE SUMMARY

There are three types of marble found in the 160 year old Philadelphia Merchants Exchange: Pennsylvania marble (walls, columns, antefixes), Carrara marble (column and pilaster capitals, cheek block lions), and Georgia marble (restorations on the east facade). Most of the exterior marble features have been unaltered since the original construction. The building was well cared for except in the 1920s-40s, during its use as a produce market. The East entrance stairs and marble lions were removed and the marble portico was used as a support structure for a broad metal awning or shed roof. The National Park Service (NPS) restoration in the 1950s and 1960s, included replacement of the East entrance stairs and selective infill in the east wall with Georgia marble, return of the lions from the Philadelphia Museum of Art, removal of copper bird netting from the capitals, and overall repointing and cleaning with high-pressure water.

The condition of these marbles vary as a function of exposure and, to a lesser extent, the type of marble. Where protected from the rain, the Carrara marble is more discolored, but overall is in better condition than the Pennsylvania marble. Where washed by rain, both marbles have suffered extreme decay, which is more pronounced in the Pennsylvania marble. The marbles on the west facade are in significantly better condition than on the east. Within the semi-circular east portico, the condition of the marbles decreases from north to south. The coarse texture, porous nature, and diverse mix of minerals of the Pennsylvania marble make it more susceptible to dissolution and related decay processes. The relatively impervious Carrara marble may be particularly susceptible to decay associated with sulfur deposition.

In 1986/7, a program was designed to monitor the condition of the marbles and evaluate the role of environment agents of decay. Marble measurements consist of mineralogical characteristics, analysis of stereophotogrammetry to measure stone loss, and washdown experiments to determine sulfate and nitrate concentrations in the near surface of the marbles. Environmental measurements include a short-term moisture survey on east and west facades, a rooftop meteorological station (rain chemistry began in 1988), and detailed microclimate and pollution concentration measurements at the north and south ends of the east portico at the third story level.

The environmental context of the Exchange is relatively straightforward to understand because it is not overshadowed by nearby buildings. Rather, it is surrounded by open spaces of at least 100 meters except to the south. Differences in temperature cycling (on average 10°C per day) between the north and south facades may explain the relative fragility of the rain-sheltered marble, which tends to be mostly disaggregated grains beneath a gypsum crust. The greatest volume of rain comes from the southeast, with the pattern of relative volumes related to the pattern of marble erosion. The most acidic rains come from the southwest and northwest, but do not account for much of the rain volume (3% and 12% respectively). In terms of stone moisture, the southeastern exposure is wetter than the northeast; the west facade is typically dryer than all aspects of the east. This difference in stone wetness causes a significant difference in the amount of SO_2 deposited to the marble surfaces; a 15% increase in time of wetness south to north causes a 60% increase in pollutant flux. Further, the Pennsylvania marble tends to absorb as much as three times more SO_2 than the Carrara marble.

A preliminary investigation of the pollution levels over the life of the building indicates that the Exchange was immediately surrounded by some of the densest pollutant emissions in late 19th-century Philadelphia. In addition, it is located directly east of the harbor, where marine boiler emissions are thought to rival that of industry. Perhaps most importantly, tracks along Dock Street within 20 m of the Exchange constituted one of three links

between the Port of Philadelphia and the PRR, Reading, and B & O railroad systems between the 1850s until World War II.

Analysis of detailed stereophotogrammetric recordings indicate that the recent rate of marble loss (between 1987 and 1991) is approximately the same as the loss rates in the first 150 years. The erosion rates for Pennsylvania marble are estimated to be 75-100 μm per year or about 8-10 mm/century. With the reference controls designed into this project, the detection limits range from 130 - 210 μm; thus erosion of 500 μm can be reliably detected in photogrammetry taken at five-year intervals. Historic erosion rates can be estimated in the absence of pre-existing, baseline stereoimagery with permanent reference points; however, the detection limit is about 8 mm. With this approach, typical marble erosion rates can be detected at 35-40 intervals.

In May 1992, a meeting of architects, engineers, conservators, conservation scientists, and NPS cultural resource managers was convened to review the research results to date and to begin to develop a decision framework for the conservation of the Exchange. The planned approach is to continue the initial environmental and marble monitoring; adding a microclimate/pollution station to the West facade and particle measurements at all locations, mapping the alteration crusts overall, and a crack survey. In addition, a program to evaluate potential conservation treatments is envisioned, including traditional methods such as limewater consolidation as well as emerging technologies such as cleaning with pelletized CO_2. The purpose of the testing program is to evaluate the suitability of candidate cleaning, consolidation, and repair materials and methods for the specific conditions at the Exchange; i.e., Pennsylvania and Carrara marbles that are eroded, encrusted, disaggregated, and cracked. The criteria for evaluation have yet to be fully developed, but are envisioned to explicitly include consideration of the performance of treated substrates under conditions of temperature and moisture cycling, as well as pollutant deposition typical of the Exchange.

LIST OF FIGURES

1. Detail view of east colonnade column capitals, November 1964 2
2. View from east, 1988 3
3. View from west, 1988 4
4. View from southeast, June 1869 7
5. Newspaper photo, c. 1901 7
6. View from northeast, Spring 1951 7
7. View from northwest, September 3, 1954 8
8. East facade after removal of produce sheds, May 1963 8
9. Recarving column on north side, May 1953 9
10. Scaffolding for masonry cleaning on west side, June 1965 10
11. South lion being hoisted back into position, June 3, 1965 10
12. Detail of Column 10, April 1989 11
13. Detail of Column 10 capital under repair, June 1989 12
14. Calcite grain size for Pennsylvania and Carrara marble samples 15
15. Typical grain shapes and boundaries in Pennsylvania and Cararra marble 16
16. Backscattered electron image of a Pennsylvania marble calcite grain with attached muscovite grains 17
17. Weathering has accentuated the natural foliation of the Pennsylvania marble and resulted in spalling and loss of layers of stone material 19
18. The Pennsylvania marble in the column shafts is grainier and has lost more of the original carved details compared to the similarly-exposed Carrara marble 20
19. Column shafts of Pennsylvania marble on the east facade have developed rounded, wavy edges 21
20. Pennsylvania marble column shaft shows a transition from exposed to sheltered areas 22
21. Orange alteration crust on the east facade portico wall 23
22. Carrara marble underneath a black alteration crust on the east facade is completely disaggregated into loose grains 23

23. Scanning electron micrograph of black alteration crusts on Pennsylvania marble 25

24. The blackened alteration crust on a ground level column has blistered off, exposing white, newly-revealed and disaggregated Pennsylvania marble underneath 26

25. New gypsum crystals have formed on a calcite grain that was underneath a black alteration crust 26

26. Column 12 showing the various profiles 29

27. Comparison between 2 replicate profiles 30

28. Comparison of inside Column 3 and inside Column 10 32

29. Morphology audits, comparison with lower flute profiles 34

30. Morphology audits, lower flute profiles 36

31. Morphology audits, upper flute profiles 36

32. Erosion roses - Pennsylvania marble, upper and lower flutes 37

33. Erosion rose - Carrara marble 38

34. Pollution concentrations in Philadelphia - 1965-1986 a) sulfur dioxide b) nitrogen dioxide c) particles 42

35. Estimates of historic sulfur dioxide levels 43

36. Hexamer Insurance Map, Vol. 1, 1865 45

37. SO_2 emissions density map for 1890s 46

38. Precipitation pH for Philadelphia - 1978-1992 47

39. Rain chemistry roses for the Exchange 48

40. SO_2 fluxes to marble and limestone 49

41. Moisture patterns for Exchange 50

42. Microclimate data - annual averages a) ambient b) stone 52

43. Microclimate data - seasonal averages 55

44. Pollutant concentrations at the Exchange a) total nitrate b) particulate sulfate c) SO_2 61

45. NO_x concentrations at the Exchange 62

46. Volumes of washdown solutions - a) North capital b) South capital c) North column d) South column 63

47. Encrustion on columns; distribution and composition 69

48. Progression of volute failure 70

49. Composition of crusts on east portico walls 72

50. Monthly averages of stone temperature excursions 73

A-1. Scanning electron micrograph (SEM) of alteration crust sample 4/5 81

A-2. SEM micrograph of a typical quartz particle in an alteration crust sample 82

B-1. Location of the stereoimagery from 1987 and 1991. 85

B-2. Location of sapphire microbenchmarks in capitals and columns 86

B-3. Digital terrain models 88

C-1. Hexamer Insurance Surveys 94

C-2. Particulate matter emission density 97

C-3. Nitrogen oxide emission density 98

C-4. Sulfur dioxide emission density 99

C-5. Hexamer General Survey 100

C-6. Location of selected industries listed in Table C-3 101

D-1. Microclimate and pollution sensor array 112

E-1. Washdown locations at the Exchange 118

E-2. Excess sulfate concentrations in runoff by Gettysburg monument 119

LIST OF TABLES

1. Calcite composition 15

2. Flute/Arris los per flute in 160 years 33

3. Sulfate concentrations in washdown solutions 64

4. Relating marble decay at the Exchange to potential causes 67

A-1. Summary of the Exchange alteration crust samples 83

B-1. Data availability for stereoimage analysis 89

B-2. Classification of erosion rates 91

C-1. Hexamer Insurance Classification System 95

C-2. Emission factors used for calculating strength of area sources in 1890s Philadelphia 96

C-3. Selected industries used for estimating point source emissions 107

C-4. Port of Philadelphia marine traffic and associated emission estimates 109

D-1. Locations os sensors in 1987 ten-point moisture cycle survey 113

E-1. Values of parameters used to estimate dry deposition velocities 120

E-2. Calculated sulfur fluxes to the north and south sides of the Exchange 121

INTRODUCTION

William D. Brookover

The Philadelphia Merchants' Exchange in Independence National Historical Park (INHP), central Philadelphia, is one of the most significant architectural resources under the care of the National Park Service. The management objectives for the building are to preserve the historic structure and to interpret its historical and architectural significance to park visitors. The building was built in 1833-34 of local Pennsylvania blue marble, with column and pilaster capitals imported from Italy of carved Carrara marble.

During its history the building has suffered many alterations and changes. It was restored to its original appearance by the National Park Service in 1964. The decorative stone is severely deteriorated. Many carved details of the capitals and antefixes are eroded and in some cases missing. Since 1986 the building has been the subject of detailed condition surveys and scientific studies to determine the cause of the deterioration and to lay the foundation for eventual repair and conservation of the historic masonry in the building. The results of these studies are presented in this monograph.

One of the first steps in this program of detailed studies was to document the existing appearance and condition of the masonry and to set a base line of information for the condition of the exterior masonry. The building was recorded using close-range photogrammetry as a supplement to the measured drawings produced by the Historic American Building Survey (HABS) in 1951. The project also included molds and casts of portions of the Corinthian column capitals. The stereopairs and castings record the condition and appearance of the building prior to any conservation work and also provide detailed information on the extent of deterioration. The advantages of recording the masonry with stereophotogrammetry include the ability to produce very large scale detail drawings at any time in the future as required, as well as to monitor changes in the condition with great precision.

Another early study was a moisture monitoring project. Moisture meters were placed at ten points on the columns and capitals, distributed on both the east and west porticos of the building. This project revealed that there was a significant variation in the frequency and length of moisture cycling between the east and west porticos. The east showed significantly greater variation. The east portico thus became the focus of the following stages of investigation.

During these investigations the building has been examined from several points of view. Geologists have examined the characteristics of the stone and its deterioration processes at a microscopic level. The building has also been examined by photogrammetrist who have measured minute changes in the surface of the stone. A second point of view is that of the physical scientist who has examined the interaction of environmental forces to which the building is subjected, including rain, wind, temperature, relative humidity, solar radiation, and pollutants.
The stone elements of the building need attention. In priority order these include:

- the Carrara marble column capitals at the east portico where there has been the greatest loss of ornamental detail (Figure 1); those at the west portico are in danger of similar catastrophic loss and need protection;

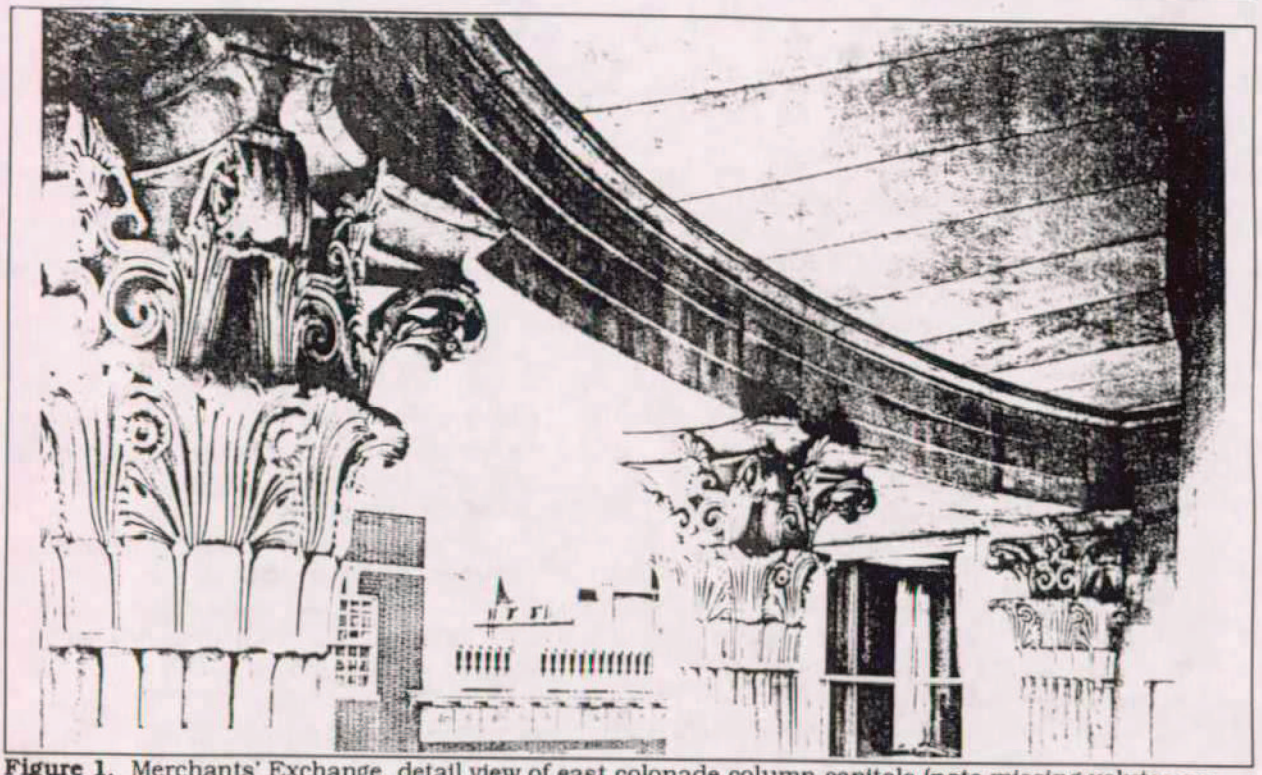


Figure 1. Merchants' Exchange, detail view of east colonade column capitals (note missing volutes on outside faces of capitals), November 1964. Courtesy of INHP Photo Collection.

• the Pennsylvania blue marble antefixes surmounting the cornice of the east portico which are subject to the most extreme combinations of wind, water, and temperature (Figure 2);

• the Pennsylvania blue marble first floor columns, particularly facing Walnut and Third Streets, whose location at ground level subjects them to vehicular exhaust; the overhanging cornice at the second floor level protects them from the washing action of rain, creating a build-up of dirt (Figure 3);

• the Pennsylvania blue marble column shafts at the east portico, which have lost the edges of their fluting;

• the projecting cornice at the second floor level where the loss of the outer edge contributes to a haphazard washing pattern of the wall below; the appearance of a green algae indicates that this cornice no longer promotes water run-off as it was originally designed;

• the lions flanking the east portico which are exposed to wind and rain from several sides;

• the Pennsylvania blue marble walls of the building where there has been a build-up of dirt and soiling; and

• the paving of the east and west porticos where there is a build-up of pigeon droppings from uncontrolled nests in the entablature above;

The park is in the process of developing a conservation strategy for the building. This monograph forms the basis of a decision making process to be presented May 22, 1992, at a Stone Conservation Strategy Workshop to a group of architects, conservators, and National Park Service managers responsible for the building. The

presentations and resulting discussion will form the basis for developing a conservation plan for the building. The following issues will be addressed by the group:

- need for additional documentation;

- discussion of treatment options, and materials to be used, including consolidation, washing, replacement, dutchman repairs, and criteria to be used to evaluate the appropriateness of these options; questions to be discussed include whether routine cleaning is helpful in areas that are not rain washed; whether routine removal of gypsum prolongs the life of the stone; whether a sacrificial coating should be applied if the stone were to be cleaned; whether consolidation with silanes or acrylic silanes are useful; what kind of fillings perform best and without creating new problems; whether replacement carvings should be executed in original stone, more durable stone, cast stone, resin carvings, or in fiberglass molds;

- development of a testing procedure for proposed treatments;

- development of documentation standards as treatments are implemented;

- development of a preventive maintenance program;

- approaches to pigeon control, including removal of nests, deterrent chemicals, permanently installed netting, and criteria to be used to evaluate the appropriateness of these options; and

- management considerations.

From the discussions to be held at this workshop, the park will develop a treatment plan for the masonry. The plan will identify individual work tasks, placed



Figure 2. *Merchants' Exchange, view from east, 1988. Courtesy INHP Photo Collection.*

in order of priority and construction sequence, broken into one-year phases. Each phase will form the basis for funding requests from the park's operating budget and special funding programs within the National Park Service. The building currently houses the Mid-Atlantic Regional Office of the National Park Service. The regional office has plans to vacate the building in the next few years, which will allow for a major rehabilitation of mechanical and electrical systems on the interior of the building. This will provide somewhat greater flexibility for scheduling major items of masonry repair.

The carefully detailed program of stone treatment must deal with the full range of stone deterioration problems, from simple cleaning and protection from pigeons and environmental pollutants, to more intensive treatments such as stone consolidation and replacement.

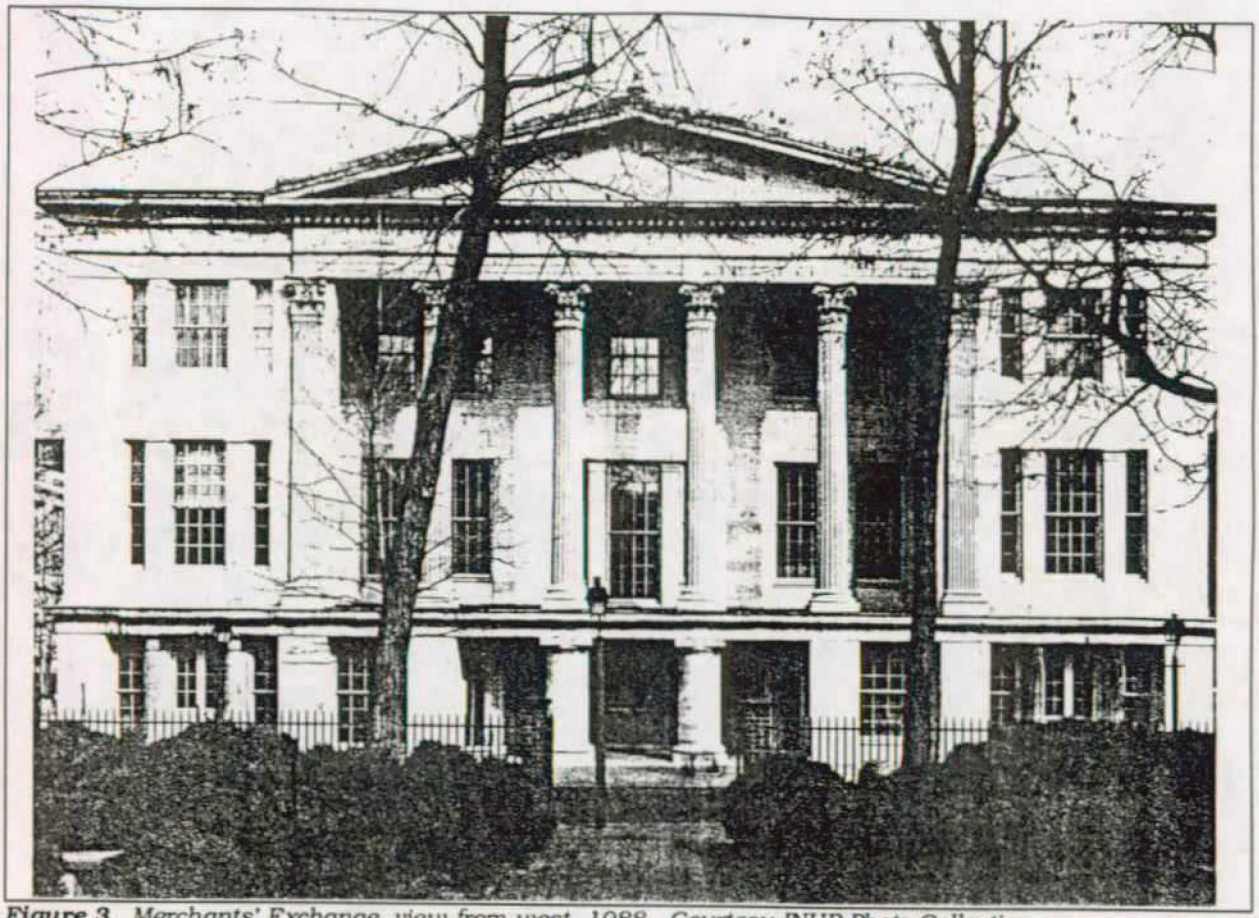


Figure 3. *Merchants' Exchange, view from west, 1988. Courtesy INHP Photo Collection.*

BUILDING HISTORY AND ALTERATIONS

William D. Brookover

ORIGINAL CONSTRUCTION

The Philadelphia Merchants' Exchange with its massive classical design in marble underscores the significance of this financial institution in the early history of the nation and the city. The building was built in 1834 to house the newly formed Philadelphia Exchange Company. From the middle of the 18th century, merchants had met in small coffee houses near the waterfront to conduct business. By the early 19th century, Philadelphia's merchants had grown to the point of needing a larger home to accommodate their transactions. They commissioned William Strickland, one of the United States' earliest native born professional architects to design a new building on a triangular lot bounded by Dock, Walnut, and Third Streets. This location was conveniently near the waterfront and the financial district, and presented Strickland with an elevated, relatively isolated site (Webster 1976, pp. 290-291).

Strickland took full advantage of the architectural possibilities of the site and designed a free-standing monumental structure in the Greek Revival style, with the main entrance facing east toward Dock Street. The design combined elements of ancient Greek architecture gleaned from the pages of *The Antiquities of Athens*, by James Stuart and Nicholas Revett, with early 19th-century construction techniques and materials (Figure 4). The column capitals are based on Stuart and Revett's plates of the Corinthian order found at the Choragic Monument of Lysicrates in Athens. The portico's eight Corinthian capitals were designed to visually harmonize with those supporting the portico of the nearby First Bank of the United States a short way up Dock Street. Strickland's design for the Exchange was boldly innovative with its placement of one structure, a lantern-shaped copy of the same Choragic Monument used for the main order of the buildng, on top of a three-story semicircular portico. The building presented a memorable sight with its curving colonnade flanked by monumental exterior stairs, topped by the notable lantern (Petrak 1963).

During construction 30,811 cubic feet of marble were delivered from Montgomery County for John Struthers and his Italian masons hired to put up the marble facade on the building's thick brick walls, and to carve embellishments at the cornice, the water belt, the portico, and west facade. The marble for the exterior was supplied by Samuel Henderson & Son from their quarry operating in Upper Merion Township. The Hendersons operated one of the principal quarries in Montgomery County near Philadelphia. This quarry produced mostly blue marble, but also some pure white. Both varieties were used in the building. The belt of Pennsylvania marble in nearby Montgomery County is described as limestone in 19th century geological literature. David Henderson is listed as the marble quarrier on the cornerstone (Simon 1961).

The column capitals were carved in Italy of Carrara marble. Strickland sent full size drawings and insisted that the proportions and dimensions be strictly followed (Gilchrist 1953, pp. 86-95). In 1838 the east portico received marble lions to embellish the staircases at either end. These were copied from Canova's lions sculpted for the tomb of Pope Clement XII at St. Peter's in Rome. They were a gift to the city from John Moss, who commissioned them from Signor Fiorelli, an Italian stone carver working in Philadelphia (Fairmount Park Art Association 1974, p.60).

ALTERATIONS

1901 Alterations

Until the Civil War the Exchange served its original purpose as a center for commerce and as well as a home for the Philadelphia Post Office. As the century waned, the Exchange suffered increasing neglect as commerce moved west, away from the Delaware River, and decreasing popularity as its Greek Revival architecture fell out of fashion. In 1900 a group of capitalists purchased the building and donated it to the Philadelphia Stock Exchange Company. Louis C. Hickman won the competition to design alterations to the building. His design for the building removed the roof and lantern and much of the original interior (Figure 5). The entrance was shifted to the west side of the building facing Third Street. The work carried out in 1901 consisted of gutting the interior, removing the roof, installing a new roof and tower of a different design and placement, the addition of the round piers and recessed entry on the west entrance, the insertion of a new window configuration for the west facade behind the portico, and the replacement of the outermost marble panels on the east portico with windows (Petrak 1963).

1922 Alterations

S. W. Hollowell bought the building in 1922 and converted it into a produce market. Drawings in park archives dated 1922-25 document the addition of the metal awning and produce stalls that were constructed around the east and north facades (Figure 6), and the alteration of the interior spaces for office use. Hollowell inserted windows in place of the recessed marble panels along the third floor of the east portico and cut into the shafts of the fur northernmost columns at the east end to receive iron straps and rods to support the produce shed roofs below. Sometime prior to 1947 copper netting was placed over the column capitals on both the east and the west facades (Figure 7). The stairs flanking the east portico were demolished and the lion sculptures located there were removed to the grounds of the Philadelphia Museum of Art. The Museum of Art was under construction at that time, and the lions were placed on platforms flanking monumental exterior steps on the west side of the grounds, towards Fairmount Park.

National Park Service Restoration

Charles Oeslanger produced a set of drawings, dated April 3, 1950, to document the existing structure, and the building was measured and drawn by the Historic American Buildings Survey (HABS) during the summer of 1951. The National Park Service purchased the building in 1952. The sheds from the produce market were torn down between May and December, 1953 (Figure 8).

As part of the restoration of the building, the National Park Service cleaned the exterior masonry. Several different cleaning methods were sampled on the building. First floor columns on the north side of the building were cleaned by recutting in May 1953 (Figure 9) and sandblasting in December 1953.

Both of these methods were determined to be unacceptable. Instead, the entire building was cleaned using a high pressure water spray aimed at the building for lengthy periods of time (24-36 hours). The work was undertaken by the Day Labor force of Independence National Historical Park. The Weekly Field Reports and Day Labor Daily Logs both document the cleaning process but do not specify the pressure of the water spray. The day laborcarpenters put up the scaffolding, the painters did the cleaning, and the masons did the pointing work following the cleaning. A memorandum from August 22, 1963, in the park's correspondence file describes a program of cleaning and pointing and waterproofing to start that year. No reference has been found in the available files to clarify what was intended as waterproofing, or that the waterproofing was carried out. The cleaning began along Dock Street, or north side of the building,

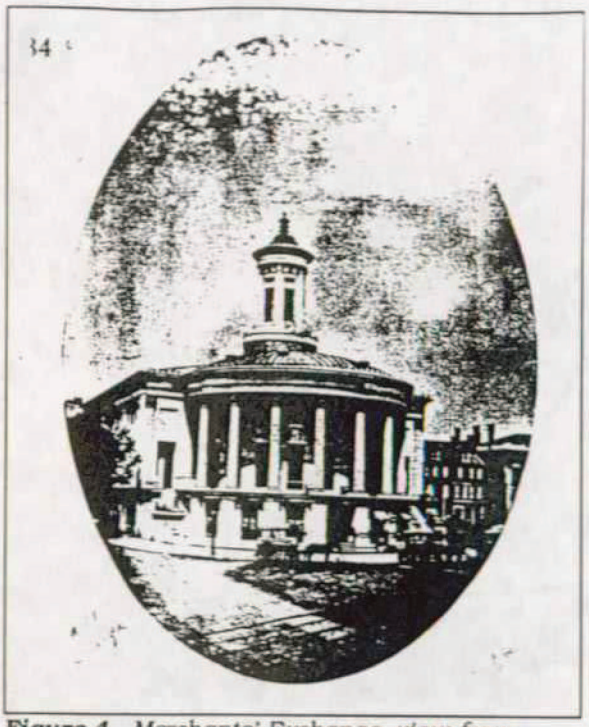


Figure 4. *Merchants' Exchange, view from southeast, June 1869. Courtesy Print Collection, Library of Congress.*

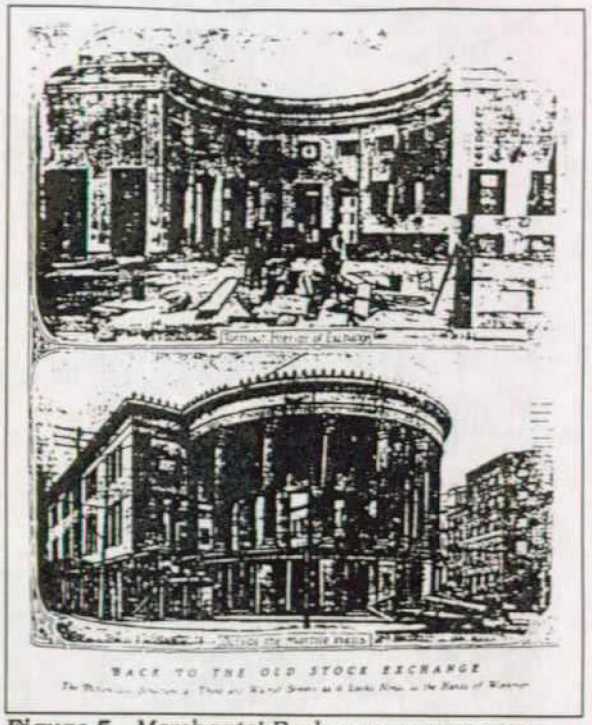


Figure 5. *Merchants' Exchange, newspaper photo, c. 1901. Courtesy Free Library of Philadelphia.*

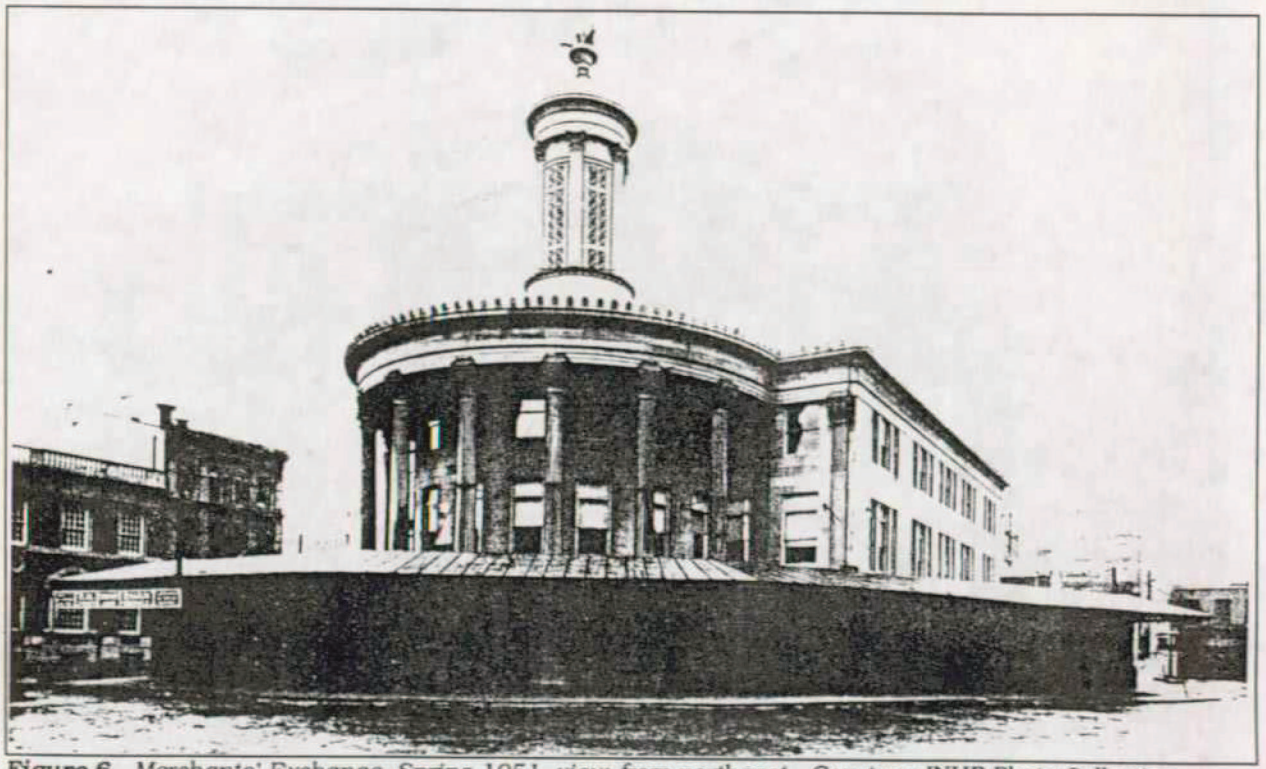


Figure 6. *Merchants' Exchange, Spring 1951, view from northeast. Courtesy INHP Photo Collection.*

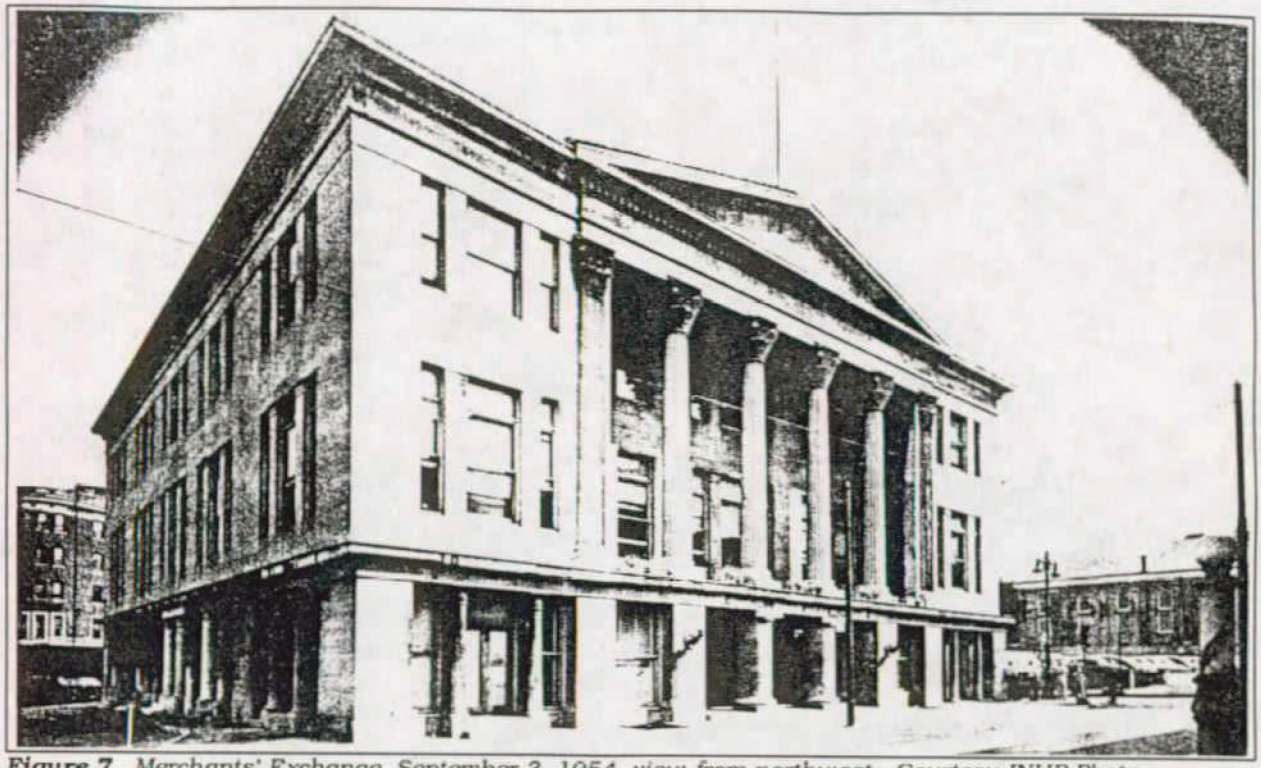


Figure 7. *Merchants' Exchange, September 3, 1954, view from northwest. Courtesy INHP Photo Collection.*

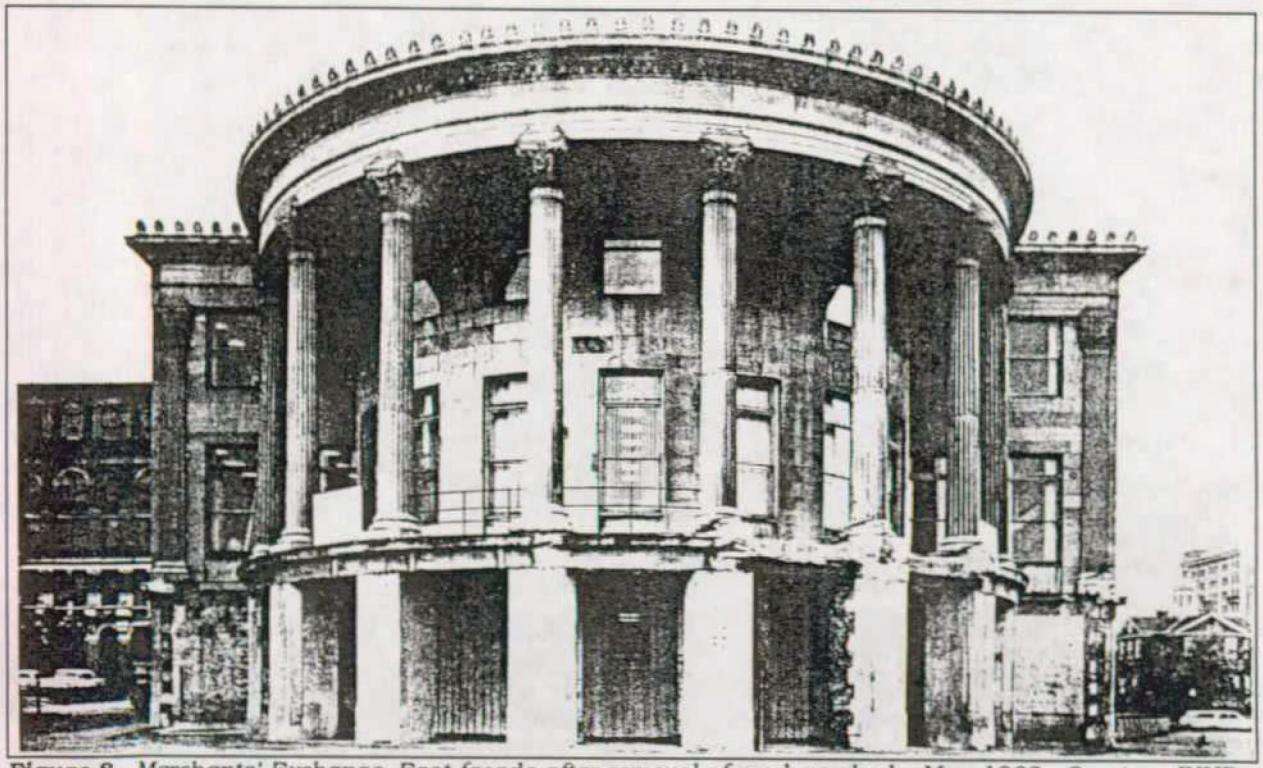


Figure 8. *Merchants' Exchange, East facade after removal of produce sheds, May 1963. Courtesy INHP Photo Collection.*

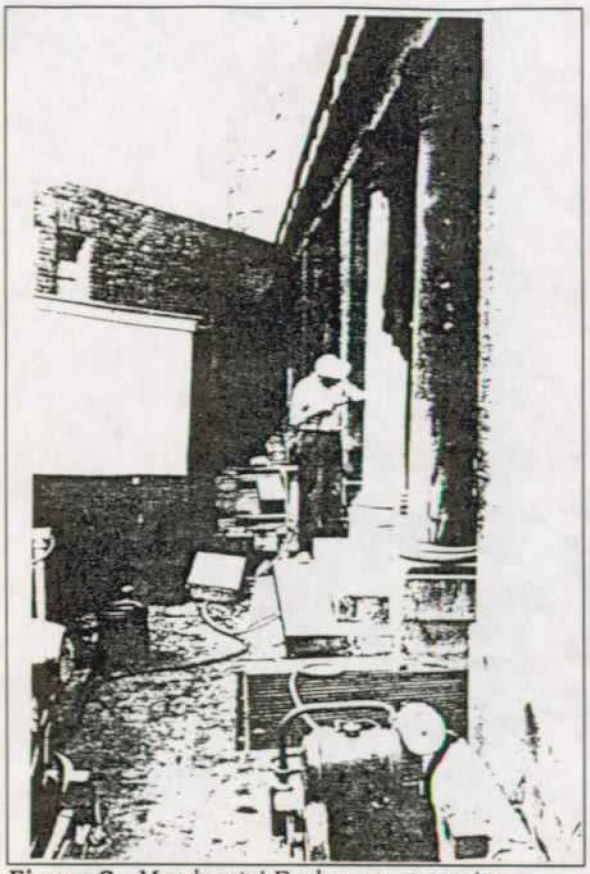


Figure 9. *Merchants' Exchange, recarving column on north side, May 1953. Courtesy INHP Photo Collection.*

then progressed to the east side inside the portico. Next, the outer face of the columns were cleaned, at which time the copper netting was removed. The work then moved to Walnut Street, or the south side, and then to Third Street, or the west side (Figure 10). The whole process started in August 1963 and continued until September 1965 with a few months off each winter (NPS Weekly Field Reports 1963-1965).

A restoration program was developed to return the architectural emphasis of the building to its east or portico end, based largely on photographic evidence. Under a separate construction contract, the east stairs flanking the portico were rebuilt, stone columns damaged where iron straps had been cut into the stone were repaired with epoxy patches, the tar was removed from the portico flooring and replaced with new marble, and the roof with its lantern was restored to the building. The lions were moved back into position on June 3, 1965 (Figure 11). Management considerations dictated that the west facade retain the 1901 alterations which made it the front entrance (Petrak 1963).

Recent Repairs

By 1984, the epoxy patches on stone Columns 9, 10, 11, and 12 installed in 1965 had begun to fail. The epoxy had shrunk and pulled away from the stone at the thin tapered sections where the patches had been feathered into the arrises of the flutes. Because the adhesive strength of the epoxy was greater than that of the stone, a thin section of stone pulled away with the patch. These patches were removed in 1984 and replaced with lime-cement mortar patches, tinted to match the color of the stone.

During field work associated with the current program of environmental monitoring, Park Mason Frank Doyle identified a serious crack in a projecting abacus and volute in the southwest corner of the capital of Column 10 (Figure 12). In consultation with Conservator Virginia Naude', it was determined that the crack was almost continuous and required immediate repair. A stategy was devised to 1) provide support for the weight of the piece in danger of falling; 2) reattach the cracked segment securely to the stone entablature above; 3) fill the major cracks between the capital and the stone volute; and 4) stabilize and fill the damaged volute. Figure 13 shows the repair in progress. Two stainless steel rods were inserted into holes drilled through the cracked piece up into the entablature. The round hole is visible in the curved face of the abacus just to the right of the mason's hand in the photograph. Three small holes were drilled into the cracks on each side of the capital and the figure illustrates the mason injecting an epoxy resin into the cracks and drilled holes. The resin flowed into the crack and filled the drilled holes, acting as

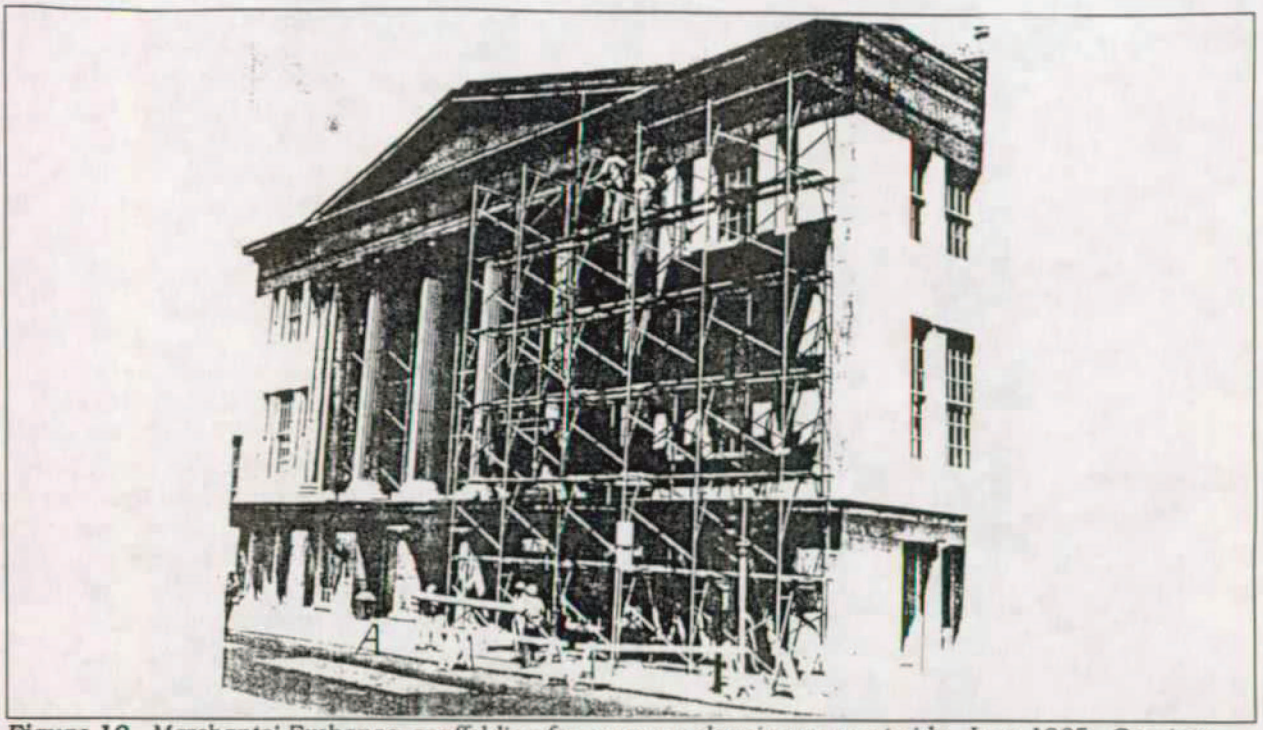


Figure 10. *Merchants' Exchange, scaffolding for masonry cleaning on west side, June 1965. Courtesy INHP Photo Collection.*

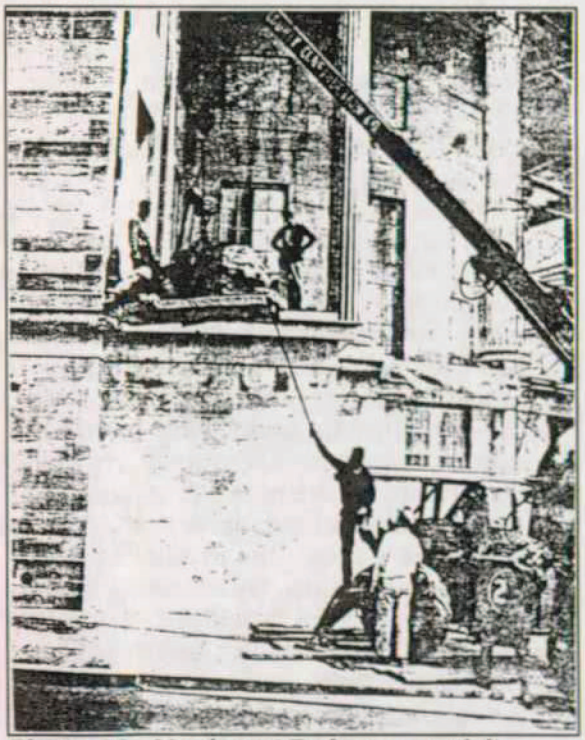


Figure 11. *Merchants' Exchange, south lion being hoisted back into position on top of rebuilt stair cheek walls, June 3, 1965. Courtesy INHP Photo Collection.*

small reinforcing rods. Next, the voids in the volute were filled with masonry patching compound to reestablish the original profiles and forms and to prevent further water penetration through the cracks.

ACKNOWLEDGMENTS

My sincere thanks to Kathryn Sather for her diligent research work in the park's archives during the summer of 1991.



Figure 12. *Merchants' Exchange, detail view of Column 10 (note crack in abacus molding above volutes), April 1989. Photo courtesy of INHP Photo Collection.*

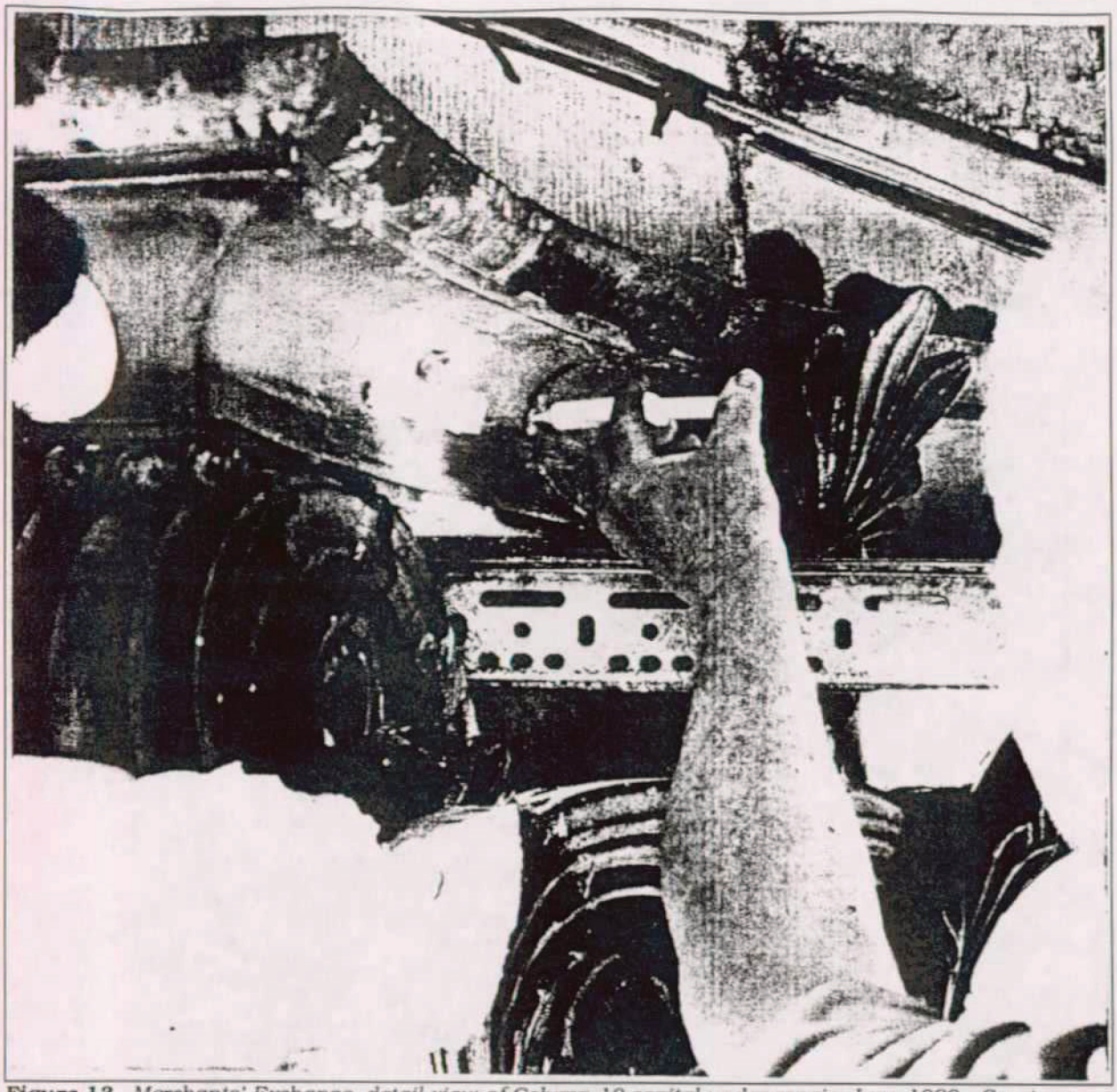


Figure 13. *Merchants' Exchange, detail view of Column 10 capital under repair, June 1989. Courtesy INHP Photo Collection.*

MARBLE CHARACTERISTICS AND DETERIORATION

Elaine S. McGee

Characteristics of the stone used in a building influence its deterioration and are important in choosing appropriate stone treatments. The Philadelphia Merchants' Exchange uses three marbles. A local marble from Pennsylvania and Carrara marble from Italy were used in original construction. A marble from Georgia used in the 1960s restoration. While the marbles are predominantly composed of calcite, they differ in the amount and type of inclusions, grain size distribution, and original stone fabric. These characteristics may influence the manner in which the marbles deteriorate and may also influence the effectiveness of treatments that may be applied to the deteriorated stone.

The form of visible deterioration of the marble varies. The architectural features have weathered differently; sheltered and exposed areas show pronounced contrast in the form of deterioration, and some of the decay appears to correlate with position. These varied forms of deterioration indicate the need for treatments that are aimed at each specific problem.

DESCRIPTION OF THE STONE

Marble is a metamorphic rock, predominantly composed of the mineral calcite (calcium carbonate). Three characteristics of marble may contribute to variations in the appearance and durability of different marbles: 1) the presence of inclusions, 2) the grain size of the calcite, and 3) how strongly the marble was metamorphosed (recrystallized) during its original formation. Inclusions in marble occur as isolated grains or as clusters that form streaks or swirls of contrasting color in the stone. Mineral inclusions tend to weather differently from the calcite. The boundaries between calcite grains and inclusions may also permit easier penetration of water into the stone than inclusion-free areas, and thus contribute to the stone deterioration. Grain size and texture of the marble reflect its formation; weakly metamorphosed stone may be loose textured, with many inclusions, whereas more strongly metamorphosed marble will be tightly compacted and the recrystallized calcite will be tightly locked together. Although fine grain size presents more surface area in the stone, coarse grain size has been cited as contributing to marble deterioration (Julian, 1884), possibly because loose-textured, coarse-grained marbles permit greater accessibility of water than fine grained marbles (Dale, 1912).

Pennsylvania Marble

The Pennsylvania marble was quarried in nearby Montgomery County from the Conestoga formation of Cambro-Ordovician age in southeastern Pennsylvania. Trade names "King of Prussia marble" or "Pennsylvania Blue marble" were used for this stone. The quarries were opened around the time of the American Revolution and the marble was used widely for buildings in and around Philadelphia until about 1840, when marbles from other eastern states became more readily available (Merrill, 1889). Both white and blue marbles were quarried near King of Prussia, Pennsylvania (Stone, 1932). Marble from these quarries has been described as "beautiful coarse grained marble, white, gray, blue and mottled" (Miller, 1934) and "...light blue, semi-crystalline texture, with signs of irregular stratification, evenly bedded, and in medium to thick courses" (Census, 1884). Bascom and others (1909) describe the marble as a white or blue magnesian limestone that is highly siliceous. It varies from blue to white within one quarry, contains disseminated inclusions of quartz, feldspar, phlogopite, graphite, pyrite, and

siderite, and it may have calcite and quartz veins (Bascom et al, 1909). Marble from Montgomery County quarries is described in the 10th U.S. Census Report (Census, 1884) as "distinguished from other marbles in use here [Philadelphia] by its bluish color and coarser texture...". Some of the many public buildings constructed in Philadelphia of Montgomery County marble include Girard Bank (1798), United States Custom-House (1819), United States Mint (1829), United States Naval Asylum (1830), Philadelphia Merchants' Exchange (1832), and Girard College (1833). After 1840, the stone was used mostly for sills, ledges, and curbing in the Philadelphia area.

Park archives contain the business records of the Henderson Quarry. They document that the marble used in the Exchange came from the Henderson Quarry, located west of the Schuylkill River near King of Prussia; about one half mile south of Henderson Station in Montgomery County, Pennsylvania. The Henderson Quarry was one of the principal quarries in the marble beds located in Upper Merion Township of Montgomery County (Hall, 1881). The marble beds are located near the southern margin of the limestone area and near an area of slate and limestone alternations (Hall, 1881). Miller (1934) gives the following description of the stone from the Henderson Quarry:

> The stone in this property consists of interbedded coarsely crystalline white to white and light blue banded or mottled marble in parallel beds interbedded with dark blue to black hard silicious dolomite. The strata have a strike of approximately east-west and dip about 60° S. The largest and most southern bed worked varies from 20 to 25 feet in thickness. It is underlain by 30 feet of silicious dolomite and then the second marble bed formerly worked is found. It is similar to the first marble band; but only 10 to 12 feet thick.

The Pennsylvania marble used in the Exchange is predominantly blue gray in color but in some areas it has a mottled, streaked appearance of light gray or blue gray areas with white. There is no regularity to the streak pattern and generally the mottling is neither large nor continuous, but streaks are more apparent on flat wall areas than on carved features. The stone is weakly metamorphosed; it contains abundant micaceous inclusions and the calcite is not strongly recrystallized. The marble is loosely textured, with a marked foliation (or planar) fabric forming a series of parallel planes that are weakly held together. The loose texture and pronounced foliation of this marble have been accentuated by exposure, as weathering and deterioration have concentrated at weak points in the stone. Light blue gray calcite is the dominant mineral in this stone; the longest dimension of the grains range from about 40 µm to 1060 µm, but most grains are 100 to 400 µm (Figure 14). The calcite grains are angular to subrounded in shape (Figure 15a) and are nearly pure $CaCO_3$, with minor amounts of magnesium and a trace of iron (Table 1). Muscovite (a mica) and apatite (a calcium phosphate) are common inclusion phases in the marble, visible with the scanning electron microscope (SEM) but difficult to see visually or optically because they are small and similar in color to the calcite. Muscovite occurs as small (10-50 µm) isolated grains and in linear clusters, often with apatite. Small grains of muscovite are commonly found still attached to loose grains of calcite (Figure 16) that have disaggregated from exposure. Minor pyrite, sphene, zircon, and tourmaline are also present in inclusion rich areas.

Carrara Marble

Carrara marble from the Adriatic coast in northern Italy has been widely used for statuary and buildings since Roman times. The marble, taken from a number of quarries near the town of Carrara, is varied and abundant (Merrill, 1889). It has been noted and admired for its appearance,

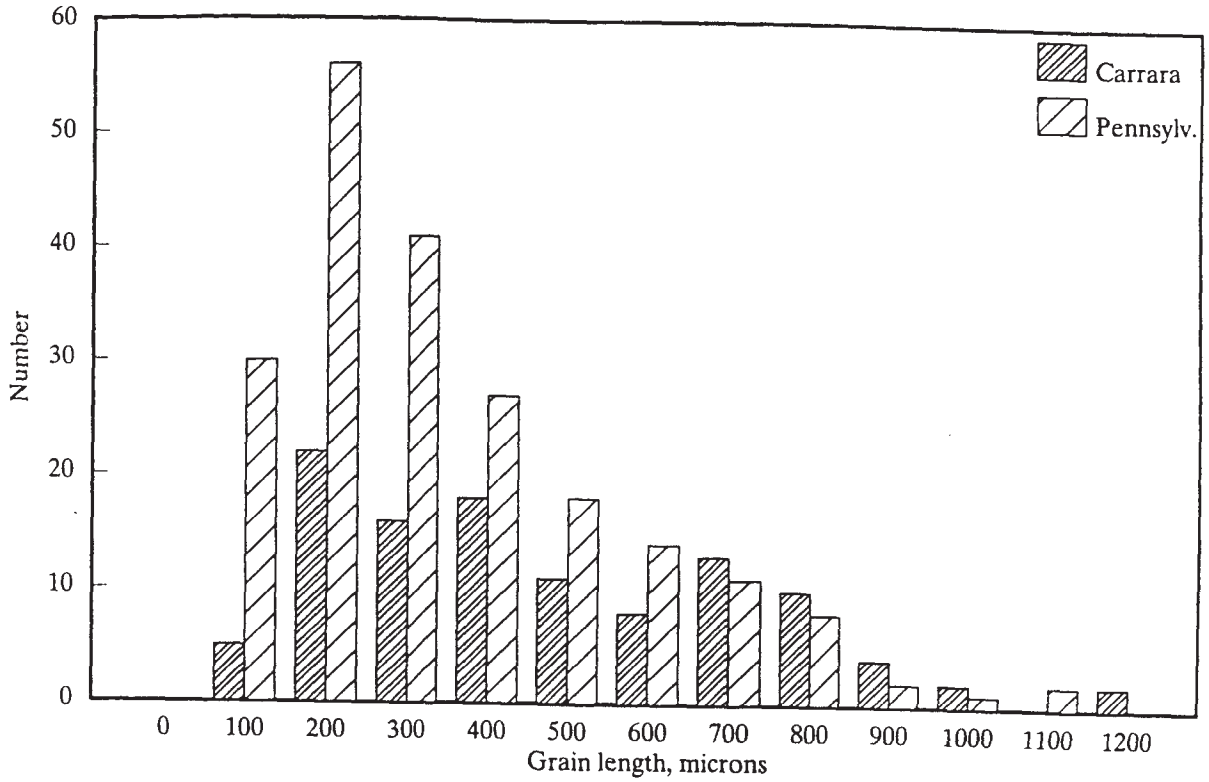


Figure 14. *Calcite grain size for Pennsylvania and Carrara marble samples; longest dimension of grains measured in microns vs. number of grains in each size range.*

Table 1. Calcite composition

Pennsylvania marble

	Average	Minimum	Maximum
CaO	56.22	55.90	56.60
MgO	0.25	0.14	0.32
MnO	0.00	0.00	0.00
FeO	0.08	0.01	0.13
SrO	0.00	0.00	0.02
BaO	0.01	0.00	0.06

Carrara marble

	Average	Minimum	Maximum
CaO	55.89	54.78	56.78
MgO	0.19	0.10	0.26
MnO	0.00	0.00	0.00
FeO	0.05	0.00	0.13
SrO	0.00	0.00	0.03
BaO	0.02	0.00	0.43

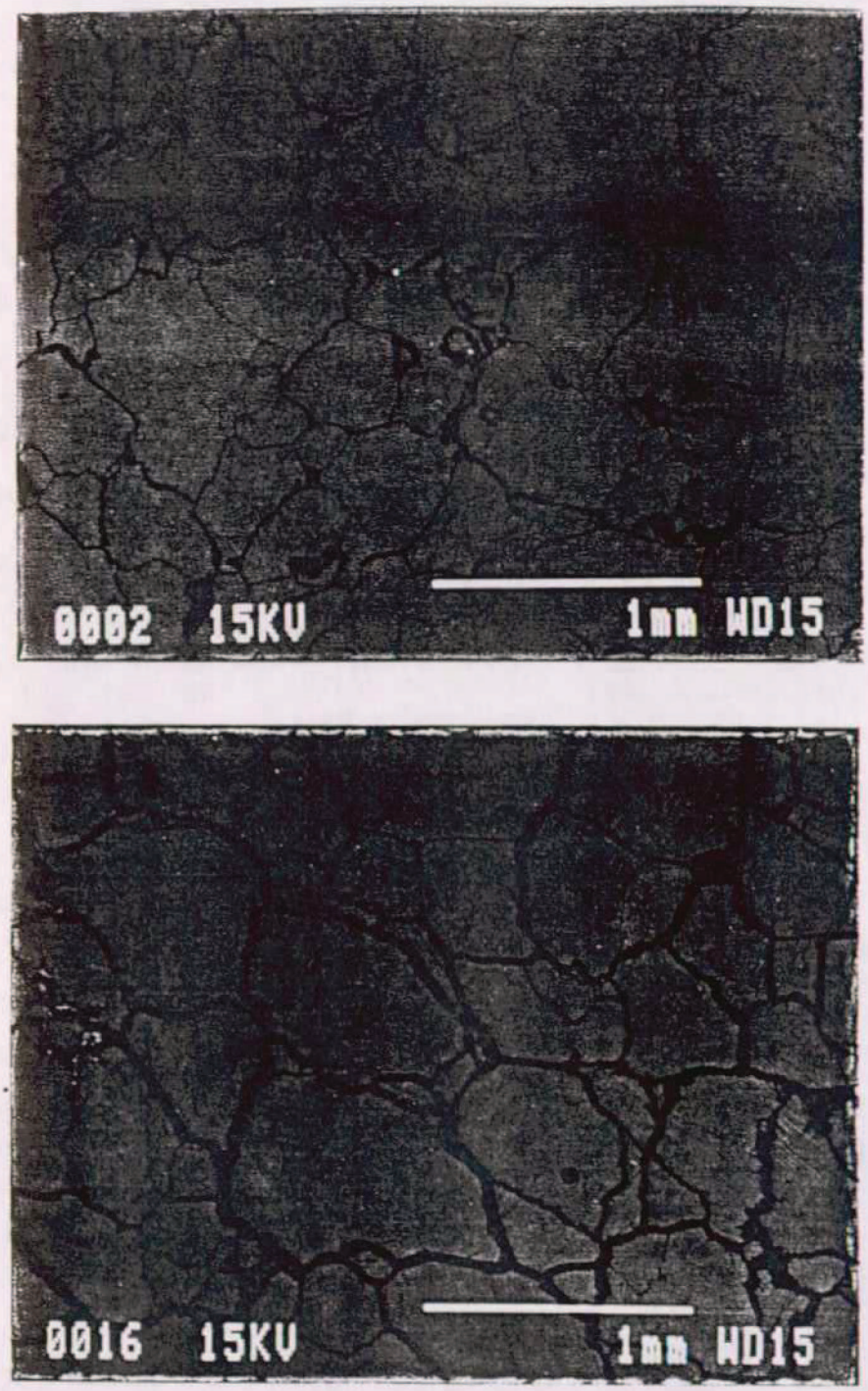


Figure 15. *Typical grain shapes and boundaries in a) Pennsylvania marble and b) Carrara marble. The Pennsylvania marble sample is from a small spalled piece on the wall of the east facade portico with no visible alteration crust; the Carrara marble sample is a cross section of an alteration-covered carved piece that fell from an east facade column capital. Photos are scanning electron micrographs from polished sections; scale at lower right.*

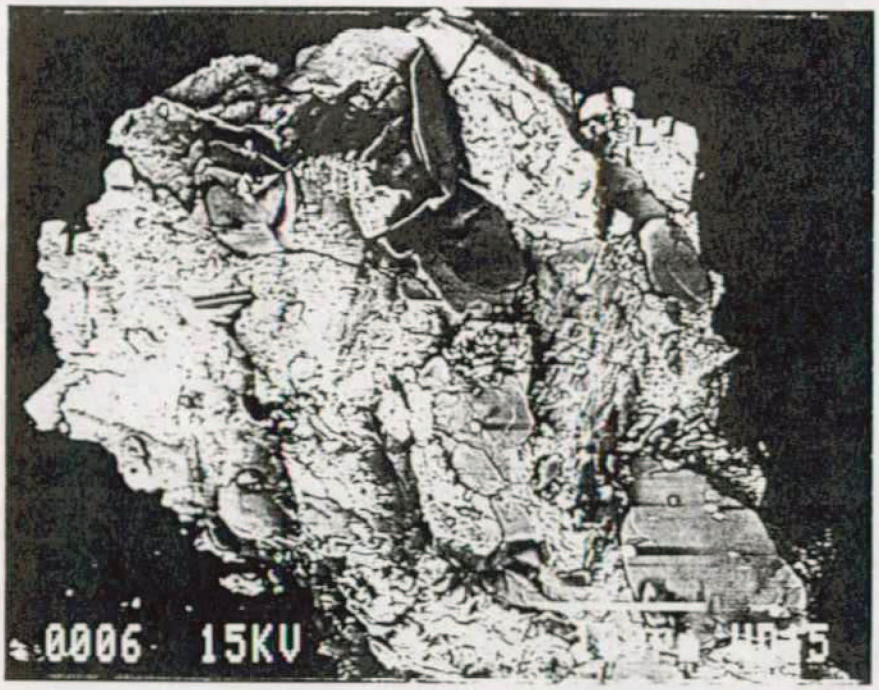


Figure 16. *Backscattered electron image of a Pennsylvania marble calcite grain with attached (platy, darker gray) muscovite grains. Small bright white dots are apatite grains. The sample is from an antefix.*

particularly for the fine grained and lustrous varieties that could be delicately carved. Many descriptions of marble in the literature compare the qualities of other marbles to marble from Carrara, but few are able to measure up to it, as illustrated by the following quote from Burnham (1883, p. 49). "The white, statuary marble of this State [Vermont] has been compared to the Carrara of Italy, but any marble-worker knows that the latter is greatly superior to the former for art purposes. It is softer, more translucent, and freer from siliceous and other foreign substances."

The Carrara is quite homogeneous in texture and mineralogy, although weathering has obscured the original character. It is even grained and tightly textured, suggesting that it was strongly metamorphosed. The Carrara marble consists almost entirely of calcite with a few rare inclusions of muscovite mica that form thin, light gray veins. The calcite is of nearly pure $CaCO_3$ but it also contains minor magnesium (Table 1). The calcite is now beige to light buff in color in contrast to its original white color (Dean, 1988). The grains are angular to subrounded in shape (Figure 15b), and range in size from about 60 µm to 1120 µm with most grains between 200 and 500 µm (Figure 14). The stone has a slight, subtle foliation, reflected in the alignment of the slightly elongate calcite grains. The foliation, however, does not appear to be significant in the weathering response of the stone; the Carrara marble has weathered evenly but shows pronounced deterioration effects from extremes in exposure to and sheltering from water.

DETERIORATION OF MARBLE

When stone is exposed to the effects of wind, rain, and temperature, weaknesses in the stone are attacked by a combination of chemical, physical, and biological processes. In an urban setting, these deterioration processes may be exaggerated by contributions from pollutants. Marble is particularly susceptible to the effects of both weather and pollutants because it is predominantly composed of the mineral calcite (calcium carbonate). Calcite readily dissolves in weak acids such as carbonic acid (that forms from carbon dioxide plus water in air) and sulfuric and nitric acids. In the presence of sulfur dioxide gas and moisture, calcite will react to form the

alteration mineral phase, gypsum (hydrated calcium sulfate). Two forms of pollutant-accelerated decay are recognized on marble buildings; those resulting from dissolution, and those resulting from chemical alteration of the stone. Dissolution effects are seen in stone exposed to washing by rain. Because gypsum is very soluble in water, it does not tend to accumulate where it is exposed to water; thus surficial alteration crusts tend to form in rain-sheltered areas (Amoroso and Fassina, 1983).

Carved details are particularly vulnerable to dissolution deterioration because of the number of facets and sharp edges presented to rain. The edges are readily rounded as water flows over the stone; here the loss of individual grains is most likely to occur. The carved surfaces also experience more turbulent flows around the edges and over the surface of the stone, thus increasing the impact of dissolution to the stone (Sherwood, et al, 1990). The effects of dissolution are visible in the loss of sharp edges, softening of carved details, and sugaring (a loosening of individual grains) and subsequent loss, making the surface rough. Two other forms of deterioration which may begin with dissolution of the calcite grains and then be exacerbated by temperature and freeze-thaw cycles include splitting of the stone along foliation planes and loss of partial or entire architectural details.

Carved details are also particularly vulnerable to alteration deterioration because the shape of the surface (with nooks and crannies) allows moisture to linger, and thus promotes gypsum growth in the restricted and protected areas. As the alteration crusts grow thicker, cracks are likely to develop. When portions of the encrusted features crack, there is significant and irreparable loss. The process by which the stone beneath these crusts disaggregates is not yet understood, but the thickest crusts seem to cover the most severely affected stone.

Dissolution

Various architectural details at the Exchange have suffered from dissolution deterioration that varies with the exposure to rain. The antefixes are the architectural detail most fully exposed to rain. Roughened surfaces and loss of much of the carved detail on the antefix faces (see Plate 9) are typical features of dissolution deterioration that result from the full exposure as well as from characteristics of the stone. Although some antefixes show preferential weathering around inclusions (see Plate 9), most have suffered from a more general loss of stone material. The natural foliation of the marble has led to a common form of antefix deterioration; thin layers of stone spalled along weakened foliation planes on the backs of the antefixes (Figure 17).

The columns and capitals show the most dramatic deterioration (Figure 18). Many of the exterior volutes on the east facade column capitals are missing, as are much of the carved details between the volutes. Where the volutes are fully exposed to washing from rain, the surface is whitened and covered with loosened grains of calcite. The Carrara marble in the capitals has weathered homogeneously with no indication of preferential loss of inclusions. The Pennsylvania marble columns have nearly all lost the upper edge of the flutes in exposed areas. On the outward facing sides of the column shaft, the arrises no longer have smooth surfaces or sharp edges; the surface is sugared and rough, and the arrises are rounded or wavy where the stone has split along the foliation that runs vertically in the column (Figure 19). Around a given column, the impact from dissolution on the stone integrity is quite notable; zones of rain-exposed and rain-sheltered flutes can be readily identified (Figure 20) and mapped (see Chapter 5). Dissolution effects on the column bases are far less pronounced than on the shafts, possibly because on the bases the foliation in the stone is horizontal or because there may be less variation in the stone selected for bases.

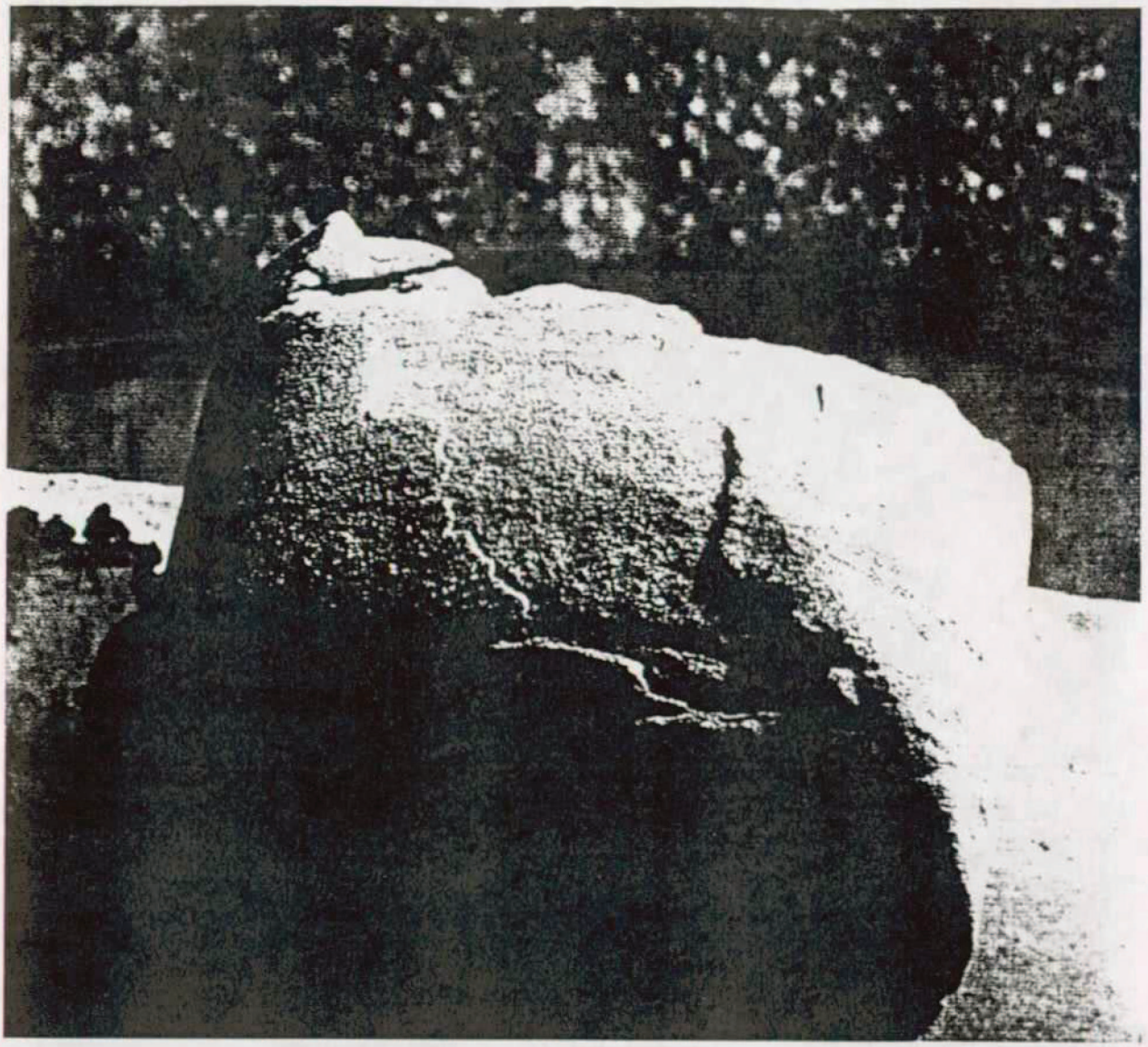


Figure 17. *Weathering has accentuated the natural foliation (plannar texture) of the Pennsylvania marble and resulted in spalling and loss of layers of stone material on this antefix.*

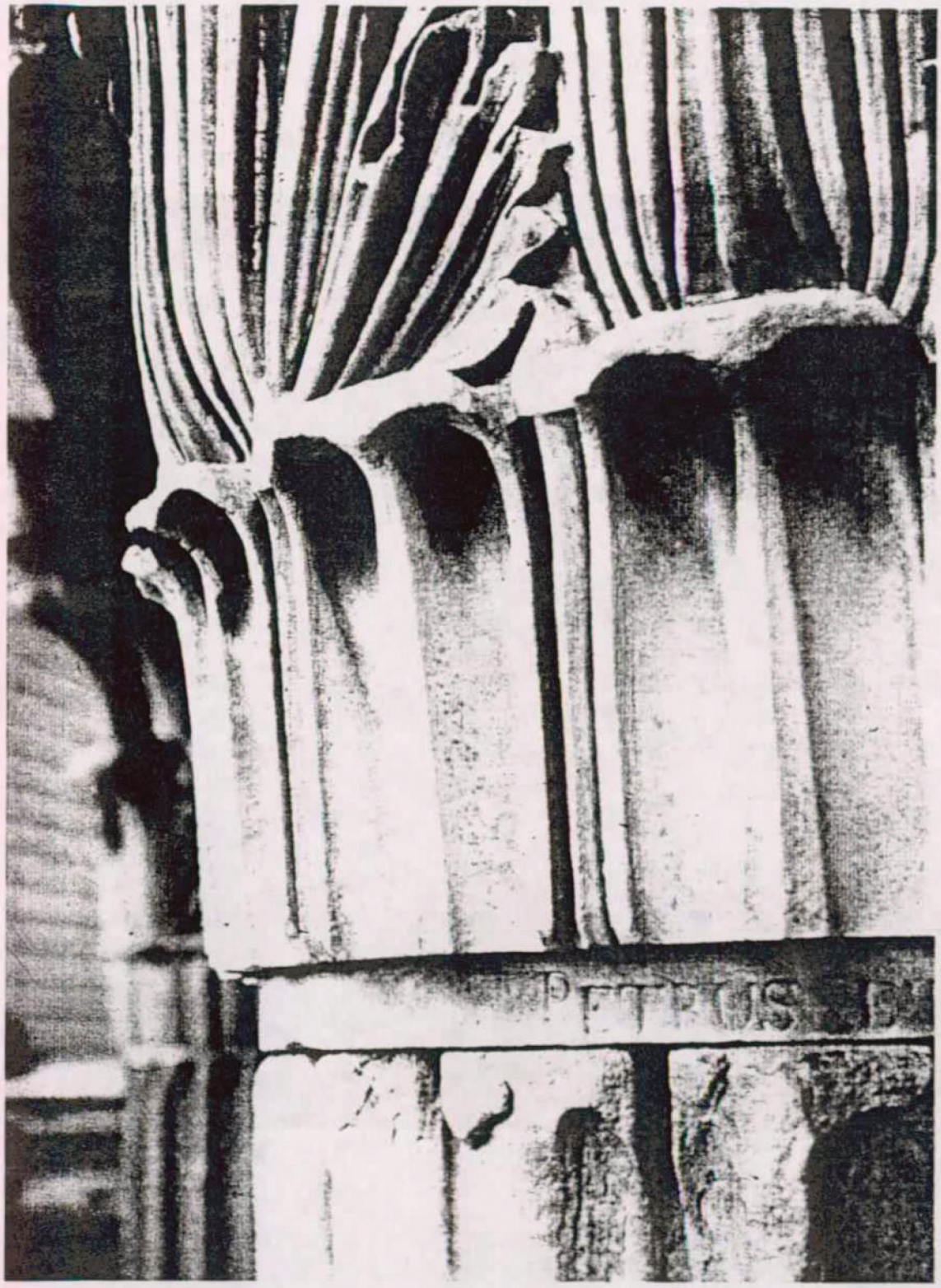


Figure 18. *The Pennsylvania marble in the column shafts is grainier and has lost more of the original carved details compared to the similarly-exposed Carrara marble.*

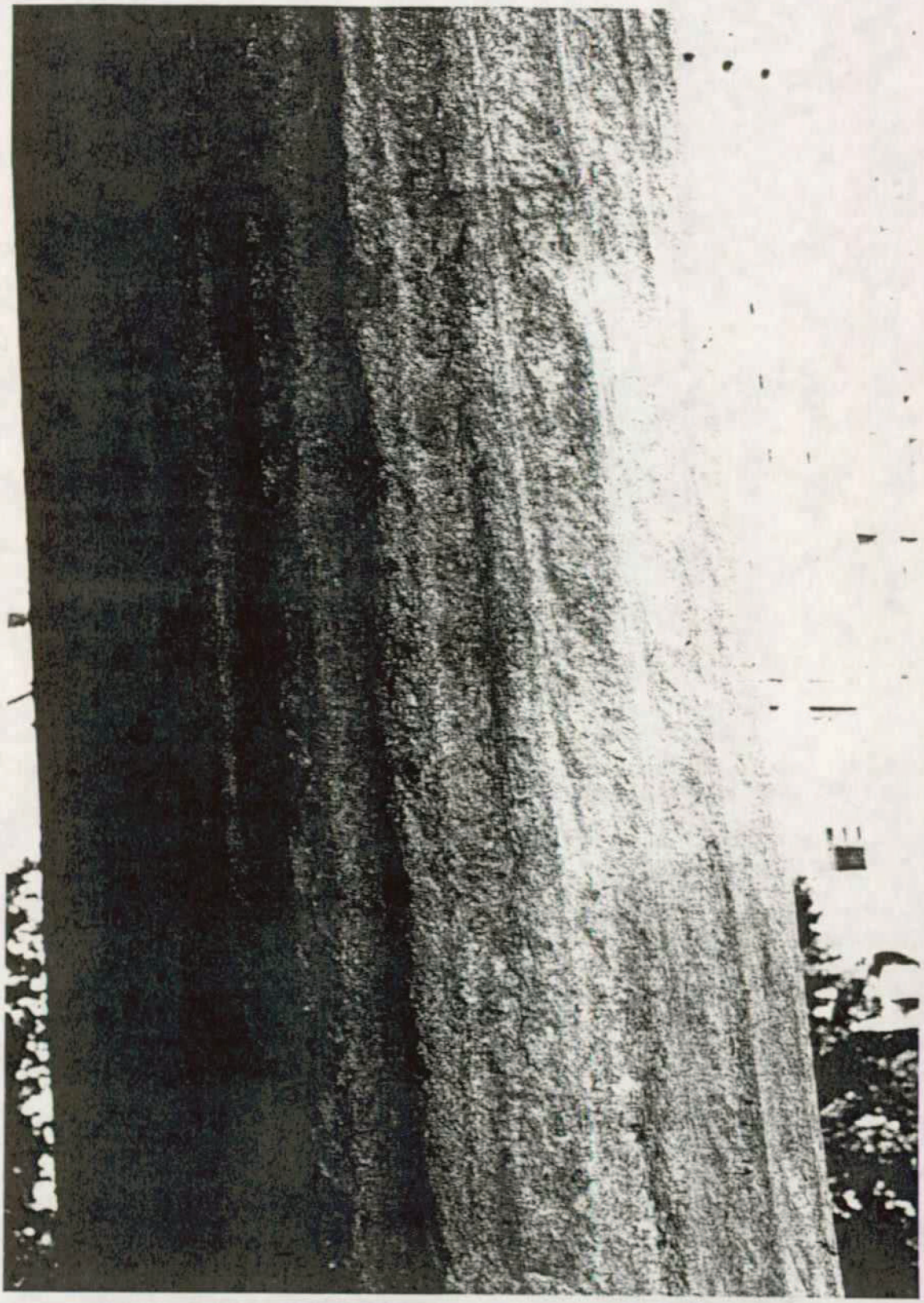


Figure 19. *Column shafts of Pennsylvania marble on the east facade have developed rounded, wavy edges. Where the foliation of the original stone lies parallel to the exposed stone surface, the arrises are almost completely gone.*

Philadelphia Merchants' Exchange Conservation Strategy, 1992

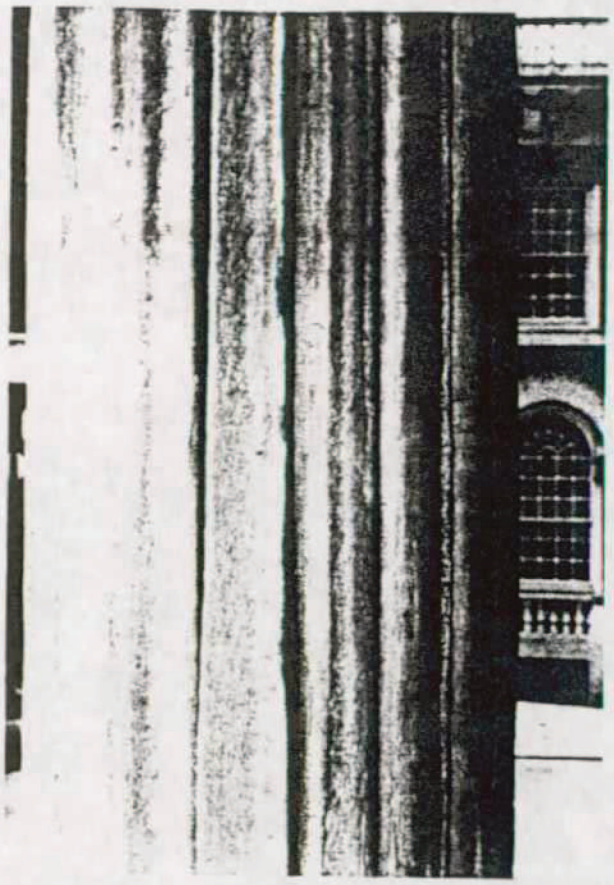


Figure 20. *Pennsylvania marble column shaft on the east facade shows a transition from exposed to sheltered areas marked by the accumulation of black alteration crusts in the sheltered area.*

In contrast to the other fully exposed stone at the Exchange, the condition of the lion statues is quite good. Carved details are softened but recognizable. The stone surface is slightly roughened but is not as markedly sugared as the columns. This apparent resistance to dissolution effects may be due to difference in stone characteristics; the stone from which the lions were carved has a tighter petrographic fabric than some of the other stone in the Exchange. In addition, the lions may also have had a more limited exposure to the elements.

Dentils and the upper sections of walls are partially sheltered by the roof overhang and thus show little evidence of dissolution deterioration. Dentils on the east facade, however, have slightly rounded edges and very rounded lower corners and have lost tooling marks in some cases. The walls show little impact from dissolution, except perhaps for a slight rounding of the original tool marks on the stone.

Alteration

Chemical alteration of the marbles at the Exchange is manifested by the blackening or discoloration of the surface. The alteration crusts vary in appearance from soft thin orange crusts (Figure 21) to thick, hard black crusts (Figure 22). Under the microscope, the thinnest crusts appear as an opaque orange glaze that obscures the underlying marble; randomly scattered fine black particles on the surface of the glaze are the only discernible feature. Black crusts appear as rough hummocky

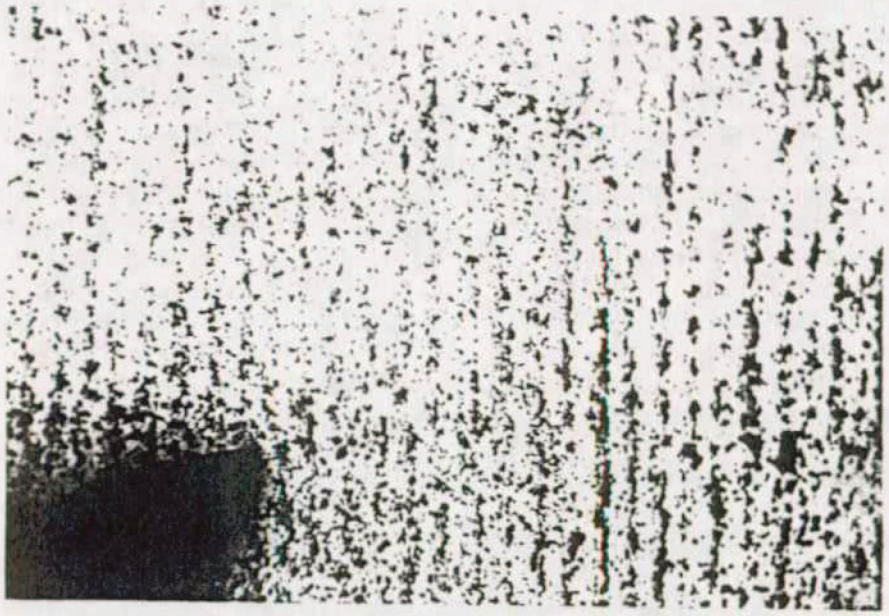


Figure 21. *Orange alteration crust on the east facade portico wall made from Pennsylvania marble partly obscures the original tool marks. Pen cap in lower left is for scale.*

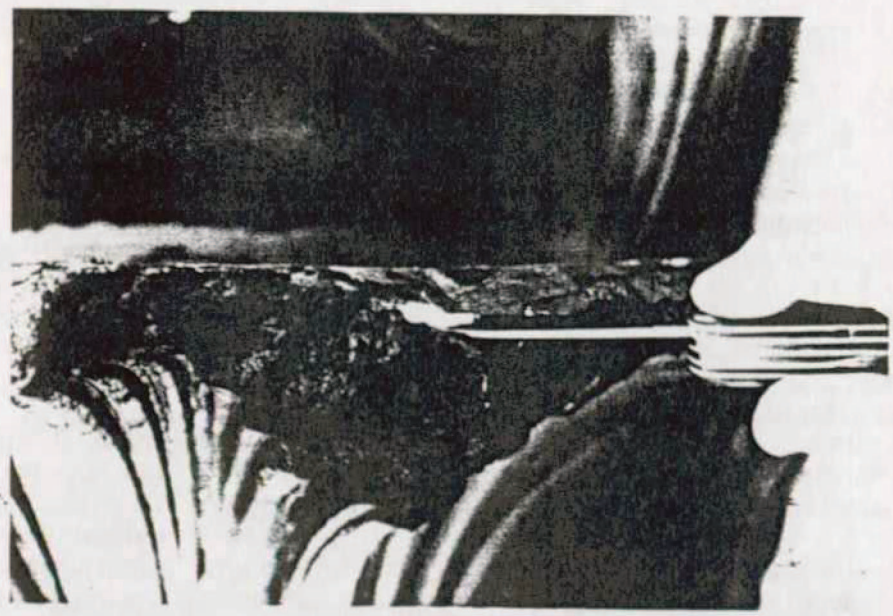


Figure 22. *Carrara marble underneath a black alteration crust on the east facade is completely disaggregated into loose grains, seen on a knife blade.*

surfaces covered by fine black particles; the marble is fully obscured by the dirt. X-ray diffraction and scanning electron microscopy with energy dispersive X-ray analysis show that both types of crusts are predominantly composed of gypsum (Appendix B). The gypsum in the alteration crusts consists of elongate crystals that range in shape from blocky, rectangular blades to thin needle-like crystals (Figure 23a). The elongate crystal habit and the random orientation of the gypsum crystals on the marble surface forms a mat that traps airborne particles (Figure 23b) giving a blackened appearance to the crust.

The major difference between the orange and black crusts is in the abundance and diversity of particles trapped in the network of gypsum crystals. X-ray diffraction analysis found gypsum, calcite, and fluorite in the orange crusts and gypsum, calcite, and quartz in the black crusts (Appendix B). Scanning electron microscopy reveals an abundance of mineral fragments, organic material (e.g., pollen), dirt, and pollutant particles trapped in the black crusts. There are fewer particles overall and less dirt in the orange crusts. The gypsum in orange and black crusts also differ. The gypsum crystals in the black crusts are 10 - 15 μm long and 1 - 2 μm wide, which have grown at random angles forming a crisscross network of openings. In orange alteration crusts, the gypsum crystals are generally shorter, broader, and poorly defined. Where they can be measured they are 8 - 10 μm long and ~5 μm wide. Many gypsum crystals in the light crusts are rounded and uneven or covered by a very fine-grained coating. The crystal structure suggests that the smaller, less defined crystals in the orange crusts have experienced repeated cycles of dissolution and precipitation.

The black crusts at the Exchange are located on the inward facing sides of the columns and capitals. The lighter crusts on the Pennsylvania marble have accumulated on the walls which may reflect differences in sheltering rather than variations in the stone. The thickness of the gypsum crusts vary with their location on the building; the thickest crusts are in areas that have probably never been washed, while similar but thinner crusts have accumulated where the stone is occasionally wet. The thickest alteration crusts have accumulated on the inside of column capitals. Slightly thinner, less pronounced darkened crusts on the sides of the capitals that receive occasional washing from rain appear as a gradual zone of transition from exposed to sheltered stone and unaltered to greatly altered surfaces.

The second floor portico column shafts also have tough black crusts on the inside. As before, the black crusts form in visible zones on the columns, prominent in the sheltered areas but becoming thinner where there is occasional rain washing (Figure 20). The crusts are particularly striking on the arrises of the column flutes. Some of these crusts are cracked and fractured parallel to the stone foliation, and while they appear fragile, pieces of the blackened layers are very difficult to remove. Thinner, orange crusts have accumulated on the sides of the arrises and in the flutes. The orange and black crust distribution on the column shafts reflect the presence of moisture, evaporation, and pollutant exposure. Because they are more protected, the troughs of the flutes probably retain surface moisture from condensation longer than the arrises, resulting in longer cycles between dissolution and reprecipitation of gypsum. The darker appearance of the arrises may reflect that the deposition is enhanced relative to the flutes.

Black crusts on the ground level columns are concentrated where the stone faces the building, but outward facing areas close to the street are also black. The impact of traffic is evident in the abundance and type of particles in the crusts. Particles from auto emission are common, as are salt (NaCl) crystals. These crusts are particularly notable because although they are thin (0.03 - 0.07 mm), the crusts on the originally smooth surface of the column

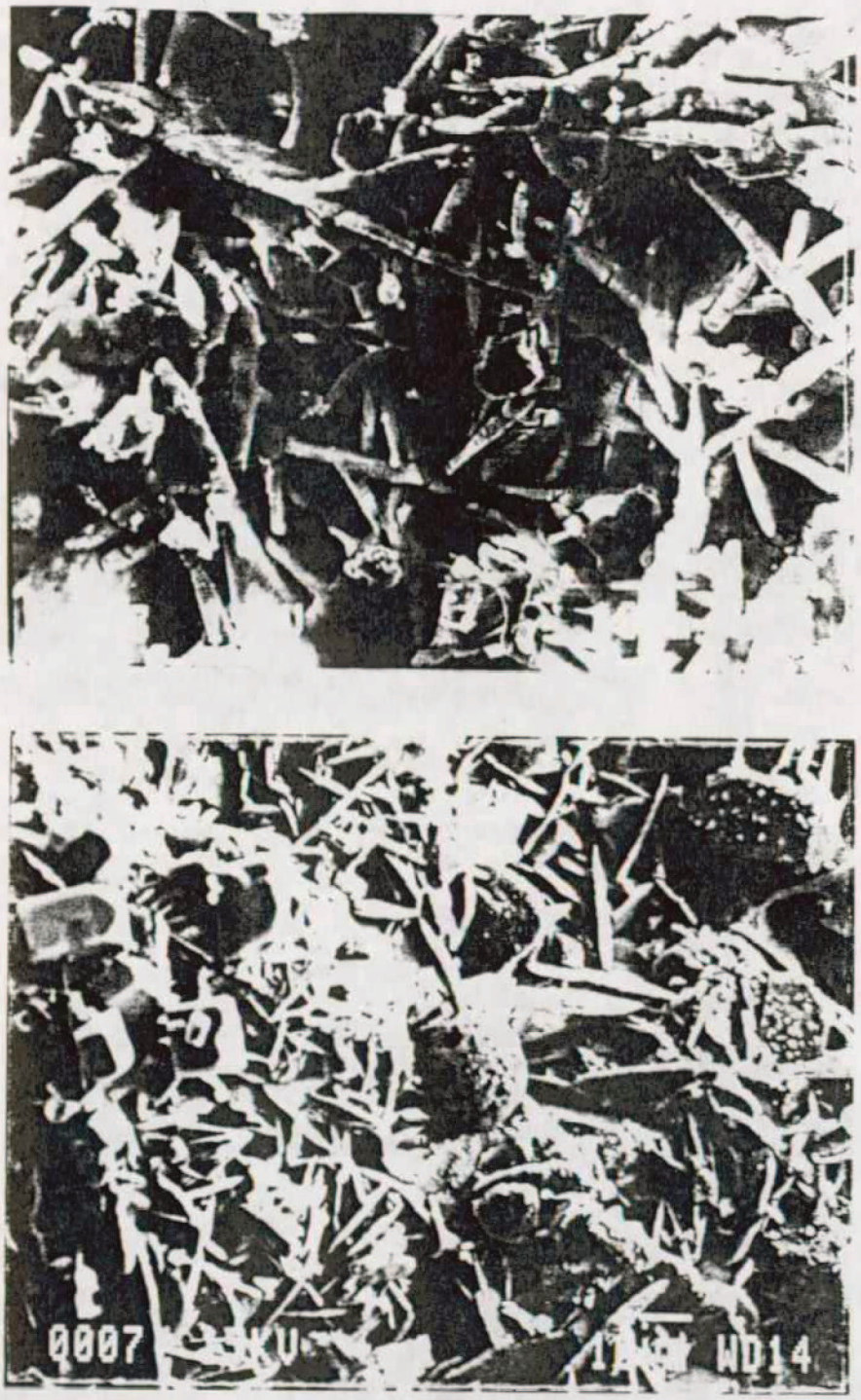


Figure 23. *Scanning electron micrograph of black alteration crusts on Pennsylvania marble of Column 14; a) bladed gypsum crystals form a network that covers the stone surface and b) pollutant particles (center), dirt, and salt crystals (cube, left-hand side) are readily trapped by the open network formed by the gypsum crystals.*

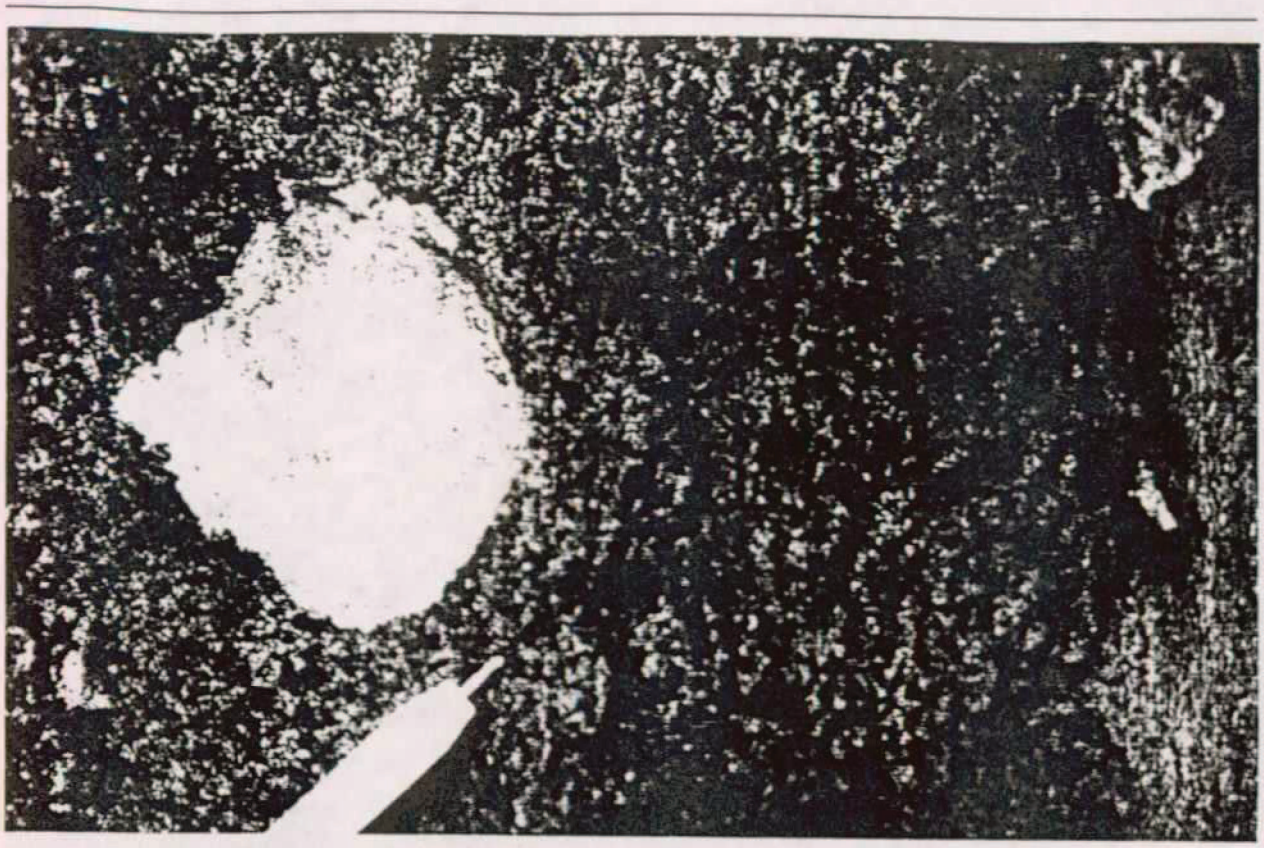


Figure 24. *The blackened alteration crust on a ground level column on the west facade has blistered off, exposing white, newly-revealed and disaggregated Pennsylvania marble underneath. Smooth area on right appears to be the original surface of the column.*

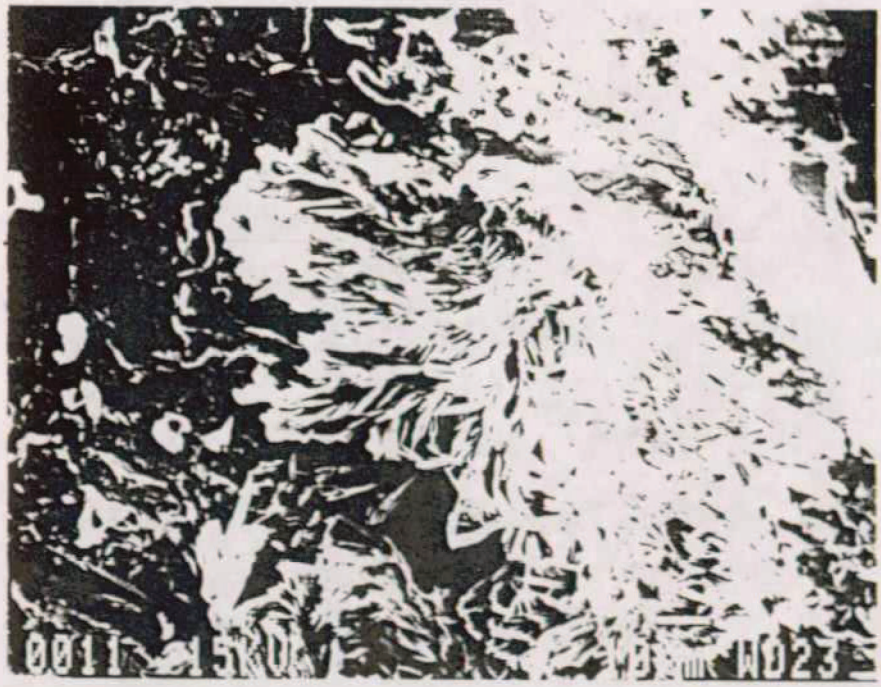


Figure 25. *New gypsum crystals (white, fine grains at center) have formed on a calcite grain (dark grain in background) that was underneath a black alteration crust on a Carrara marble capital on the east facade.*

shafts have blistered in patches (Figure 24) exposing newly revealed, crumbling stone underneath.

In contrast to the columns, the walls of the building have only minimal alteration crusts. Two light colored gypsum crusts have formed here; one is orange, soft, and easily scraped off the wall; the other crust is light yellow, tough, and tightly adhered to the stone surface. Both types of crusts are gypsum with trapped particles. Some of the light colored crusts, particularly on the north side of the east facade, contain fluorite as well as gypsum. Systematic sampling and analysis of these alteration crusts on the second level east facade wall (Appendix B), indicates that the abundance of the three mineral phases varies around the facade. The presence and distribution of fluorite in the crusts was unexpected, and may reflect an early attempt at cleaning the building. In contrast to the dark crusts, the stone underneath the thinner crusts is intact and does not show signs of beginning disaggregation. These light crusts may represent an early stage of decay, with disaggregation beginning when the crusts reach a certain thickness or density. Alternatively, the light colored crusts may reflect an undocumented treatment.

Disaggregation

While the colored alteration crusts appear to preserve the original detailed features of the carved stone, the marble can be severely disaggregated underneath (Figure 22). The black crusts on the Carrara marble consist of a distinct black outer layer (about 0.1 mm thick) underlain by a dense light-colored transition zone (up to 0.6 mm thick) under which the marble is disaggregated. Some new gypsum crystals are found in the disaggregated zone (Figure 25), but it is not clear whether these small intergranular gypsum crystals formed before or after the disaggregated marble was exposed. The black crusts on the Pennsylvania marble are thinner and consist of a black layer (0.03 mm to 0.07 mm thick) with no discernible transition layer. The marble appears more intact under these thinner black crusts. While it appears that the Carrara marble is more susceptible to disaggregation beneath the alteration crusts than the Pennsylvania marble, the integrity of the underlying marble may in part reflect their relative exposure, rather than the original petrographic character.

Although it appears that the Carrara marble is more susceptible to disaggregation under the alteration crusts than the Pennsylvania marble; the crusts on these marbles have developed in areas of slightly different exposure to water, so the integrity of the underlying marble may in part reflect their relative exposure. Where the Carrara marble is more sheltered, slow evaporation of surficial moisture and the relatively tight texture of the Carrara marble may trap water that later disaggregates the stone. Possibly, the foliation of the Pennsylvania marble permits greater movement of moisture in the stone, and thus helps to minimize disaggregation of the stone under the alteration crusts. If little water is trapped in intergranular spaces prior to the accumulation of an impenetrable alteration crust, then the effect of temperature cycles or salts precipitating in intergranular areas would be reduced, resulting in less disaggregation of the encrusted marble.

COMPARISON OF THE WEATHERING OF THE MARBLES

Variations in inclusions, texture, and grain characteristics are the most striking difference between the Pennsylvania and Carrara marbles. The disaggregated grains of the two marbles are visibly different in color; Carrara marble grains are yellow to beige, while Pennsylvania marble grains are blue to gray in color. The composition of the calcite from both marbles, however, is very similar (Table 1). Although the grains in the Pennsylvania marble sample appear smaller than those in the Carrara marble sample, grain measurements indicate that their size ranges overlap (Figure 14). Calcite grains from the Carrara marble are mostly rounded to slightly angular (Figure 15b); in rare cases a minor inclusion phase

may be attached to the calcite grain. Calcite grains from the Pennsylvania marble are also rounded to slightly angular, but many individual grains have abundant inclusions of muscovite and apatite (Figure 4).

Many of the Pennsylvania marble calcite grains have a rough, dog-toothed surface suggestive of an etched surface which contrasts with the smooth surfaces of the inclusion minerals dominating the grains in the Carrara sample. Amorphous looking "plates" that contain calcium and phosphorous cover the surface of many Pennsylvania marble grains that were taken from the partially sheltered wall on the east facade portico. Although the plates look like a precipitate that has formed on the grain surface, their source is unknown. A significant number of Carrara calcite grains collected from under a thick black alteration crust have surficial gypsum crystals (Figure 25). It is unclear, however, whether this intergranular gypsum developed after the stone was significantly disaggregated, or whether early growth of the gypsum was the mechanism that caused the disaggregation. It is possible that the intergranular crystals are an artifact, because accumulation of gypsum crystals is predominantly a surficial phenomenon. Analysis and examination of limestone from an older building has shown that although elevated levels of sulfate are detected for some distance into the stone, gypsum in crystal form is restricted to the near surface area (McGee and Mossotti, 1992).

Texture differences are reflected on a visible and a microscopic scale. In contrast to the Carrara marble, the pronounced foliation of the Pennsylvania marble is a major weakness that has been visibly accentuated by exposure. But on a microscopic scale, within the planes of foliation, intergranular gaps are narrower in the Pennsylvania marble than in the Carrara marble. Polished thin sections of poorly consolidated samples of Carrara and Pennsylvania marble allow a comparison to be made of the grain boundary and pore structure characteristics of these two marbles (Figure 15).

The grain boundaries of the Pennsylvania marble sample are fairly thin, typically 5µm wide, with some boundaries at about 10 µm. In contrast, the Carrara marble grain boundaries are fairly wide; typically 20 to 30 µm, ranging from 5 µm to 60 µm. Further, the area occupied by stone versus pore space differs and may be significant in choosing treatment actions. On average, for a 1.8 x 1.7 mm area in a SEM photograph, 2.9% of the Pennsylvania marble sample is pore space (92.9% is calcite grains) compared to 12.2% pore space in the Carrara marble (83% calcite grains).

SUMMARY

In general, the Pennsylvania marble has suffered more from dissolution deterioration whereas the Carrara marble shows more pronounced effects from alteration. The abundant inclusions and foliated texture of the Pennsylvania marble may make it more susceptible to dissolution deterioration because water can readily penetrate along inclusion-calcite boundaries and along the pronounced foliation planes in the marble. The Carrara marble may be particularly susceptible to alteration deterioration because thin films of surficial moisture cannot readily be absorbed by the relatively impervious stone, and thus remain on the stone surface longer, enhancing sulfur deposition and promoting growth of surficial gypsum.

PHOTOGRAMMETRIC DESCRIPTION OF MARBLE DECAY

Victor G. Mossotti and A. Raouf Eldeeb

PHOTOGRAMMETRIC DOCUMENTATION

In 1987, baseline stereophotogrammetric recording of the Exchange was undertaken, including east and west elevations (Plate 1) and close-range recording of selected architectural elements (Plates 2-5; Appendix B). Close-up stereopairs were taken at a distance of about 1.25 m both in 1987 and in 1991 with the same Wild C40 camera system (Oehrlein and Associates, 1987). A map of the close-range stereopair locations is found in Figure B-1. It is the long-term intent to repeat the close-up stereorecording at 5-10 year intervals to evaluate changes in the condition of the marble. In order to relate any changes to environmental exposure, the marble decay needs to be quantified as accurately as possible. For this purpose, extreme care was taken to establish a consistent procedure with adequate controls that would permit precise comparisons between stereopairs taken at different periods.

Glass-plate negatives were selected to maximize the dimensional stability of the imagery over time. Permanent reference points (or micro-benchmarks) were used in addition to traditional temporary paper targets. The precise locations of the micro-benchmarks were mapped in three dimensions with calipers and 1 mm scales as input for the image processing. Synthetic sapphire was chosen for the micro-benchmarks because it is manufactured under strict quality control standards, dimensionally stable regardless of temperature and humidity, highly resistant to weathering, and clear in color. The micro-benchmarks were set 1/2 - 1 inches above the stone surface in 1/8-inch holes, secured with a clear cyanoacrylate adhesive. An acrylic adhesive was chosen because it will cure under moist conditions. The durability of the adhesive is perhaps the weakest link in the long-term measurement protocol. (Oehrlein and Associates, 1987).

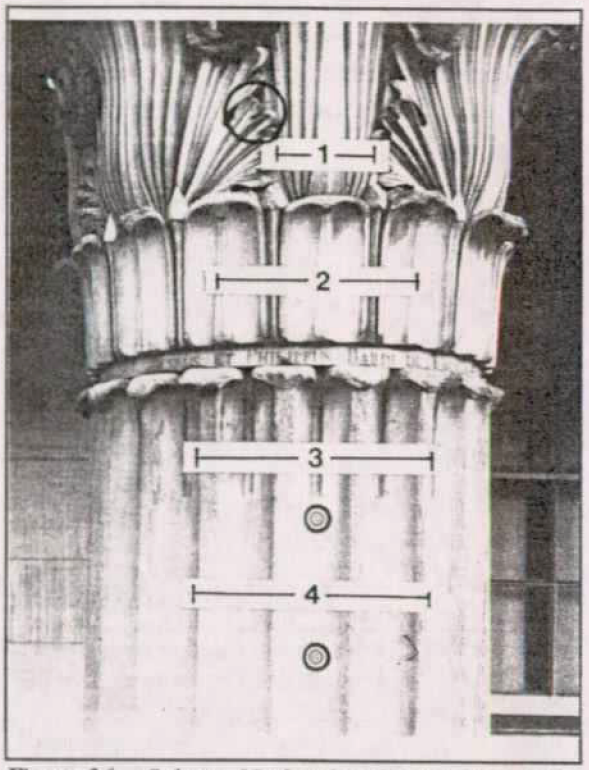


Figure 26. Column 12 showing the various profiles or scan lines.

The glass-plate images were analyzed by the U.S. Geological Survey (USGS) Photogrammetric Plotter Lab, Denver (Coe et al., 1992) (Plates 2 and 3). In each set of images, three-dimensional profiles were collected, plotted, analyzed, and archived for future reference. The location of the profiles scanned on the upper column/lower capital images is indicated in Figure 26. Profiles 1 and 2 traverse Carrara marble, while profiles 3-4 trace Pennsylvania marble surfaces. Additional data were taken for the dentil friezes, also Pennsylvania marble. Data files

of the profiles (or scan lines) and in a few cases, digital terrain models (DTM), were provided to USGS-Menlo Park for quantitative statistical interpretation. A description of the number of data files for each feature is found in Appendix B, Table B-1.

In part, the precision of measurement depends on the registration of the pairs of images and on the reproducibility of the scan lines. Figure 27 plots two replicate profiles from the 1987 image of a flute arris on the outside of Column 3, indicating that great attention must be paid in the photogrammetric analysis and interpretation in order to detect marble erosion.

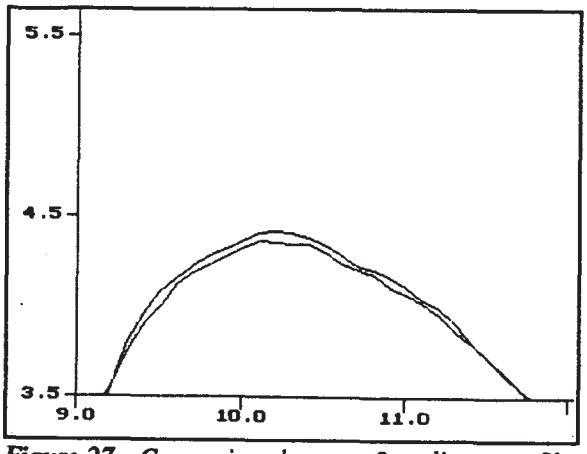


Figure 27. Comparison between 2 replicate profiles in 1987 image of Column 3 - scan line 4.

IMAGE ANALYSIS

Interpretive Approach

Studies of marble erosion using close-range photogrammetric methods are based on the comparison of reference points and stone surfaces taken at two or more different times. When sets of images are identical in scale and content, then the photogrammeteric profiles can be rigorously compared and can be used to identify micro-scale morphological changes on the order of 10s of μm over the period of study. In this study, ideal photogrammetric controls were not achieved, resulting in detection limits ranging from 150 μm and 8 mm. This degree of measurement sensitivity is probably sufficient for most historic preservation purposes. There are several methods of comparison that can be used, depending on the degree of photogrammetric control available and on the relative erosion rate of the material.

Differential Recession Method (▲-Recession)

This technique measures absolute changes in the depth dimension (or z-coordinate) of the stone surface. When the photo plane is parallel to the primary stone surface, this appears as surface recession.

Differential Texture Method (▲-Texture)

This procedure measures changes in the depth dimension relative to neighboring surfaces on either side; usually this appears as change in the surface texture.

These approaches can measure changes in marble condition at the Exchange between 1987 and 1991, as well as in future photogrammetric recordings. Recent short-term erosion rates, however, may not be representative of the entire history of stone decay at the Exchange. Since the question of whether marble decay rates have changed over time is important to decisions relative to potential conservation treatments, it is important to make an estimate of erosion rates prior to 1987, even though these results may not be as accurate or as precise as the short-term measurements. In order to investigate marble decay prior to 1987, it is necessary to define a surrogate for unavailable baseline information on the condition of the marbles in the 19th century. For this study, it is assumed that the inside portions of the columns as recorded in 1987 are essentially unweathered, and thus represent a near

approximation of the original surface form and finish of the two marbles.

Differential morphology (▲-Morphology)

To obtain reference profiles of objects crafted 160 years ago, we assumed that the inside views represented the unweathered condition. The comparison graphically delineates craftsmanship irregularities between the two columns, on average about 8 mm (Figure 28). A "composite reference profile" was synthesized from Column 3 and Column 10 inside views to represent an average original morphology of the unweathered surfaces. This is graphically displayed by an error-band two standard deviations wide ($\pm$ 1σ) on the profile trace (Figure 29). These composite reference profiles represent the best available approximation of the average original carved surface. In comparison with current profiles, an estimate of total loss over the life of the building is made. In the following discussion, we refer to any comparison of a profile with the corresponding composite reference profile as a "morphology audit."

The morphology audit can be conducted subjectively by visual comparison of the reference and current profiles, or it can be done quantitatively by computer integration of the difference between the profiles. In the visual interpretive mode, the shape of the object is contrasted with a standard reference profile and the amount of erosion described in specific linguistic terms: *undetected*, *slight*, *moderate*, *high*, and *radical*. See Table 2 for definitions these terms.

Analytical Limitations

The ability to quantify marble loss in a relative short time-frame requires close registration between sets of stereo imagery and the associated three dimensional data sets. This registration demands that tight control be maintained over a large number of measurement variables from the start of the photogrammetric procedure (benchmark location and photography) to the end. The limitations of the quantitative application of this analysis can be rigorously characterized and understood in terms of measurement detection limits. The magnitude of the detection limit determines the shortest time interval needed to observe surface recession, textural, or morphological changes.

▲-Recession method: The detection limit for recession or loss of relief gauges the ability of the method to detect changes in the depth dimension at the same location between different sets of imagery. The detection of changes in relief depends on the reproducibility of the absolute depth dimension (z-coordinate) of a given point on a profile in the pairs of images from 1987 and 1991. This requires that the before-and-after coordinate systems be in close registration. The detection limit varies dramatically depending on the steepness of the object in the depth or z-direction. The minimal detection limit was found to be 130 μm on the flattest regions of the profiles; detection limits on steeper regions were much greater.

▲-Texture method: The textural detection limit reflects the extent to which the method can detect relative changes in the topology of the surface from one point on the x-axis to the next. The textural detection limit is independent of setup calibrations and benchmarks. It is mainly the result of random errors associated with the measurement of relief as the surface is scanned. The textural detection limit, defined in terms of the reproducibility of the textural index of a standard surface, was found to be 210 μm (see Appendix B for detailed description).

▲-Morphology method: The detection limit of the quantitative method for assessing changes in morphology is critically dependent on variations in craftsmanship from one similar object to the next. This limitation, represented by the error-band on the composite reference profiles, was found to be 8 mm.

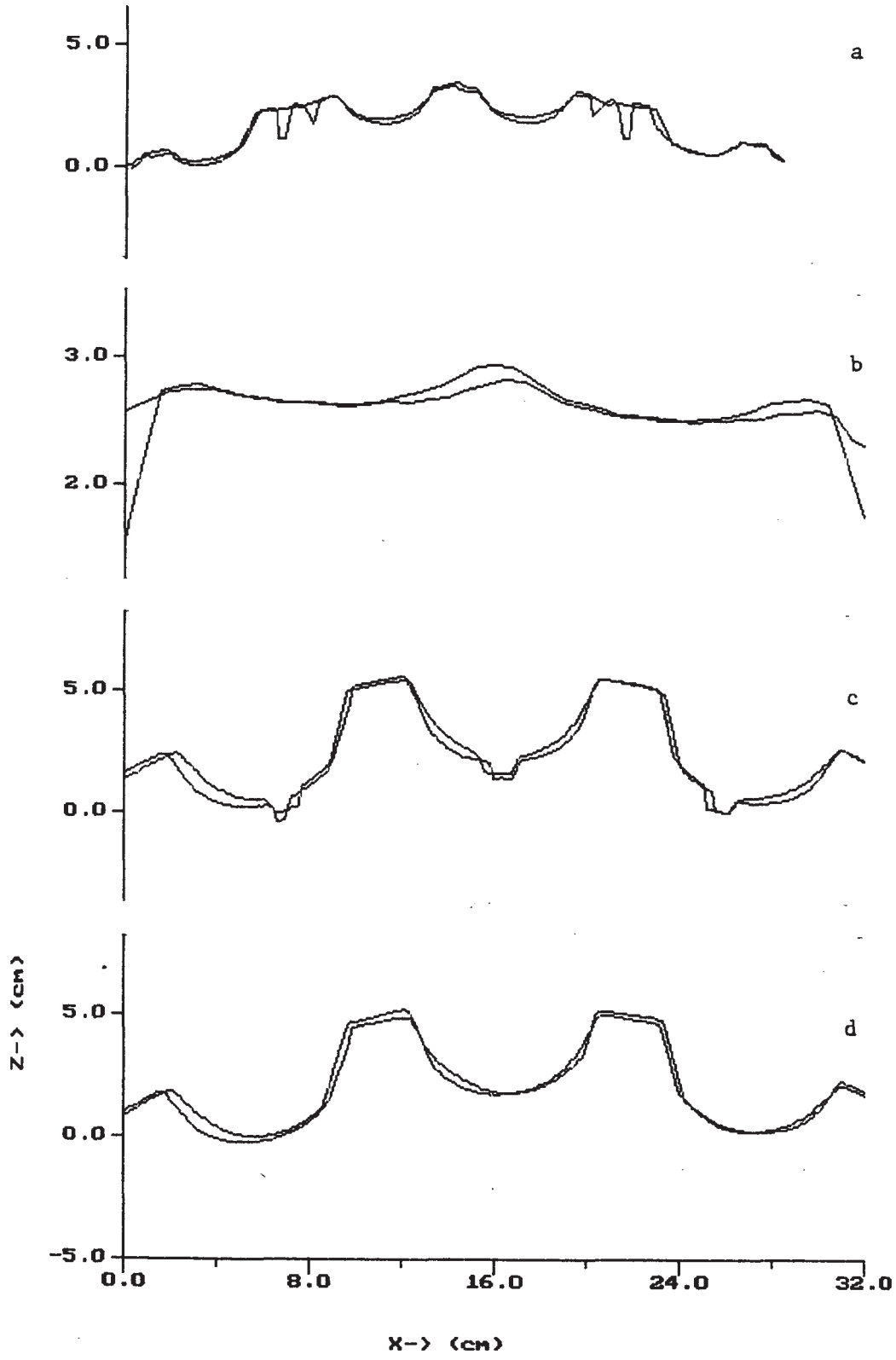


Figure 28. *Comparison of inside Column 3 and inside Column 10 for each scan line; a) acanthus stalk - scan line 1, b) lower capital -scan line 2, c) upper flute with 'slot' - scan line 3, d) lower flute - scan line 4.*

Analysis of Upper Column/Lower Capital Stereoimagery

Three basic features, acanthus stalk (scan 1), acanthus leaf (within the circle) and lower capital (scan 2), were selected for close investigation of the Carrara marble; dentils and flutes (scans 3 and 4) were studied on the Pennsylvania marble (Figure 26). Each type of profile was examined for evidence of short-term and long-term erosion by checking for textural changes and recession between 1987 and 1991, and for long-term losses by morphological comparisons. Data processing details for each type of feature are expanded in an USGS open file report in preparation (Mossotti, et al.).

Pennsylvania marble

Dentils on the west facade of the building are in better condition than those on the east facade (Plate 5). On the west side the edges and corners are sharp and the original tool marks are visible on the faces. In contrast, on the east facade the dentils have rounded edges, the lower corners are nearly all rounded, and only a faint suggestion of tool marks remains on some of the dentil faces. Originally sharp edges and corners of the Corinthian column capitals are more rounded on the south facing portion of the east facade, than on identical features on the north facing side. Dentil profiles were used to develop and refine the image analysis procedures for both long-term and short-term weathering.

Two traverses across the flutes were taken, 13 cm and 32 cm from the top edge of the column drum. The lower profile contains the simplest geometries, and the most weathering of all the features examined. The upper profile was selected to include the "slots" found in the base of the flutes, in order to provide additional sharp edges against which weathering might be detected (Plates 2 -3).

Figure 29 shows morphology audits for the lower flute profiles of the inside and the outside of Column 10. It shows that there is virtually no long-term weathering on the inside, and clear evidence for long-term weathering on the outside of Column 10 (Plate 2). Figure 30 shows morphology audits for lower flute profiles of Columns 10, 12, 15 and 16 (Plate 3). The average short-term recession rate for slots and flutes in the east portico was found to be 72 $\pm$ 33 μm/year.

It is evident that long-term weathering of the flutes and arrises are substantial on the outside of all of the columns and is directionally dependent. Similar deductions can be made from the morphology audits for upper flute profiles of Columns 10, 12, 15 and 16 shown in Figure 31. Comparison of upper and lower flute profiles indicate that the columns are weathering at a faster rate near the top of the column.

A computer program was developed to quantitatively compare the flute profiles to the composite reference profiles. The difference between the profiles was integrated, and converted to units of mass-of-flute eroded per unit length-of-column. The results are shown in Table 3 and are summarized by erosion roses for upper and lower flute profiles in Figure 32.

	Flutes		Slots	
	gms per cm length	μm/yr	gms per cm length	μm/yr
Col. 3	0	0	0	0
Col. 10	10.4	62	12.2	73
Col. 12	15.3	91	15.8	94
Col. 15	8.0	47	9.6	57
Col. 16	16.0	95	11.9	71
Mean	12.4	74	12.4	74
Error	$\pm$ 3.4 g		+_ 20 μm/yr	

Table 2. Flute/arris loss per flute in 160 years.

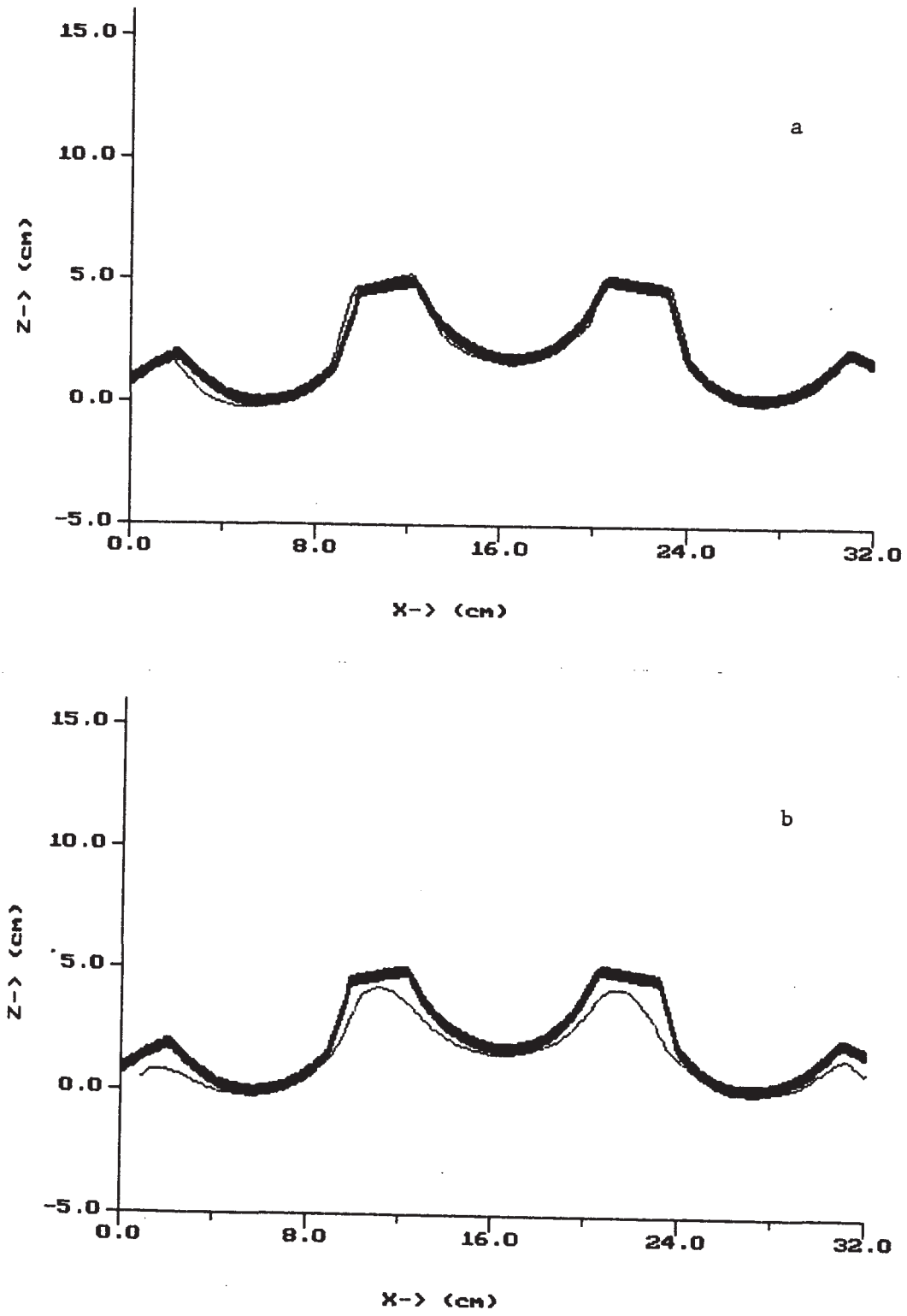


Figure 29. Morphology audits; comparison with lower flute profiles, a) inside Column 10; and b) outside Column 10. The broad line is a plot of the composite reference profile.

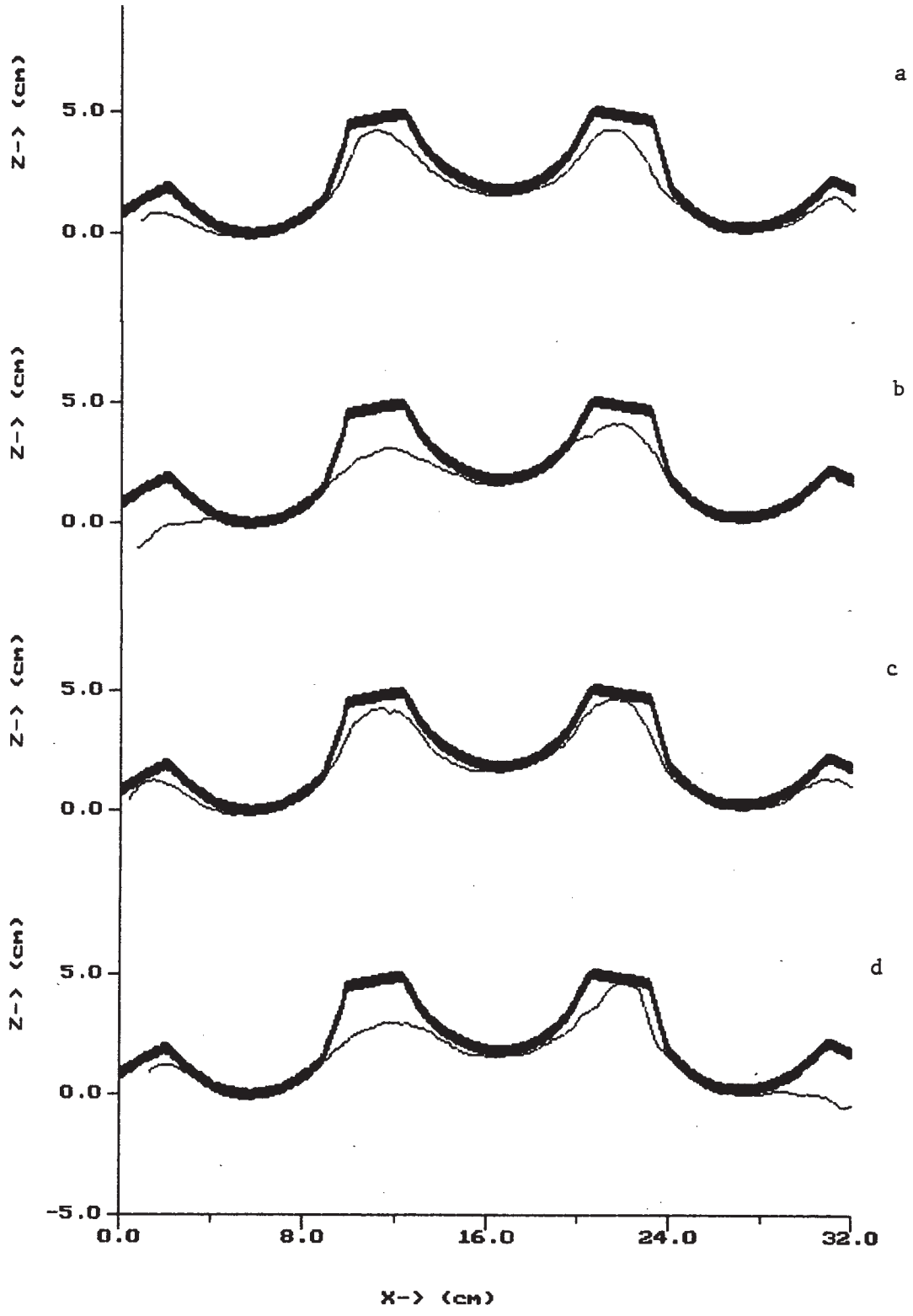


Figure 30. Morphology audits; lower flute profiles, outside Columns a)10, b)12, c)15, and d)16.

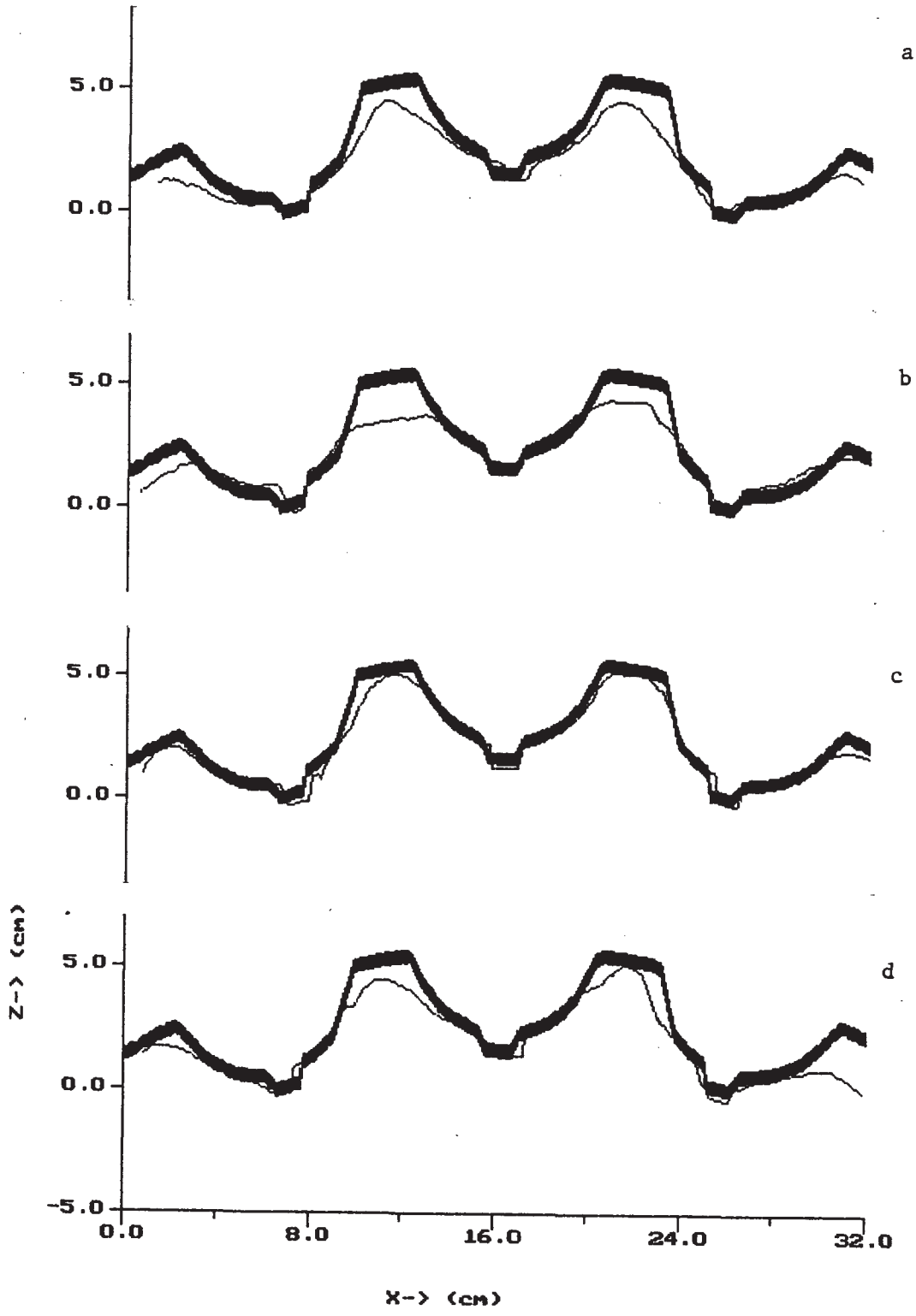


Figure 31. Morphology audits; upper flute profiles, outside Columns a)10, b)12, c)15, and d)16.

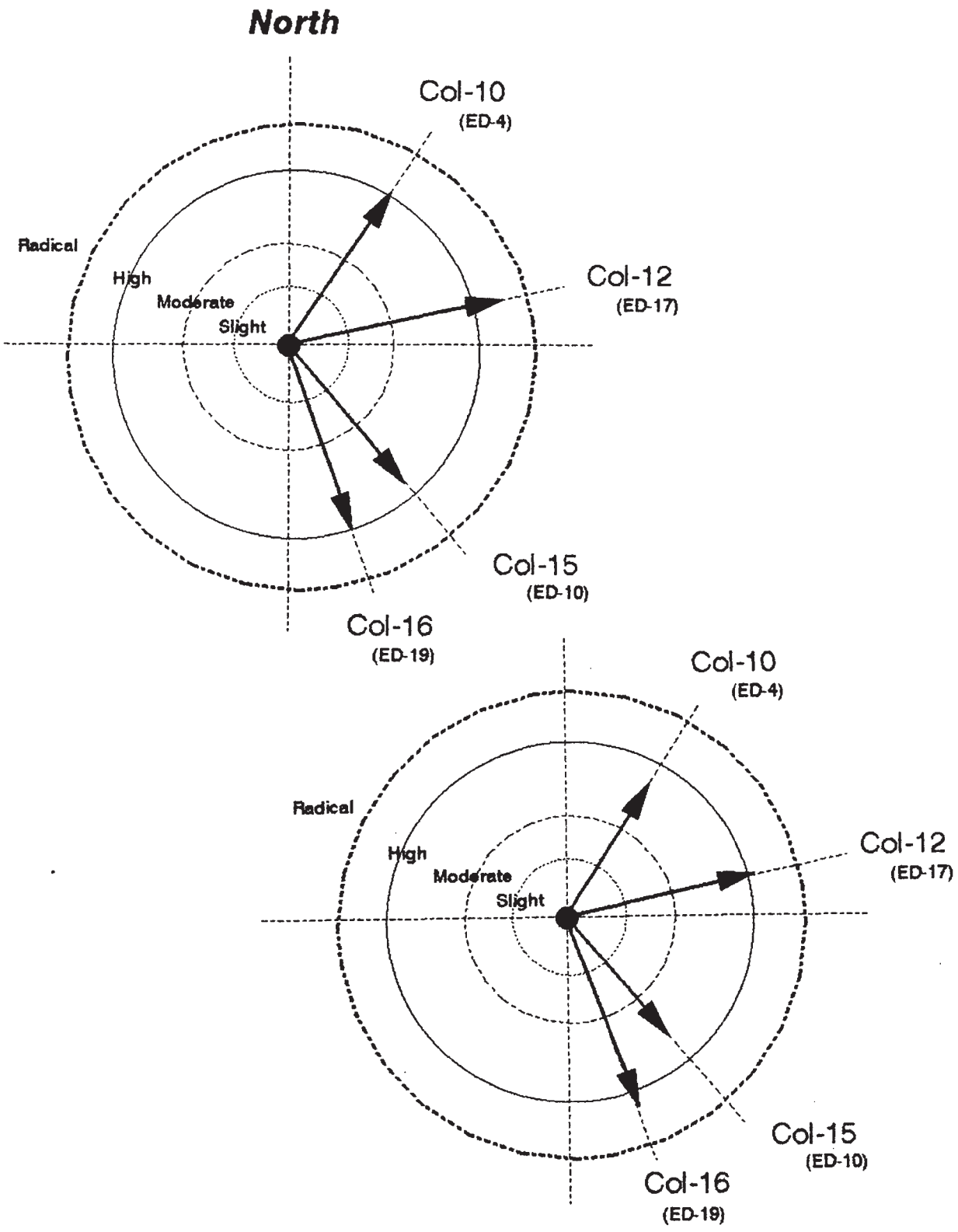


Figure 32. Long-term directional erosion pattern for Pennsylvania marble upper flute (top) and lower flute (below) profiles.

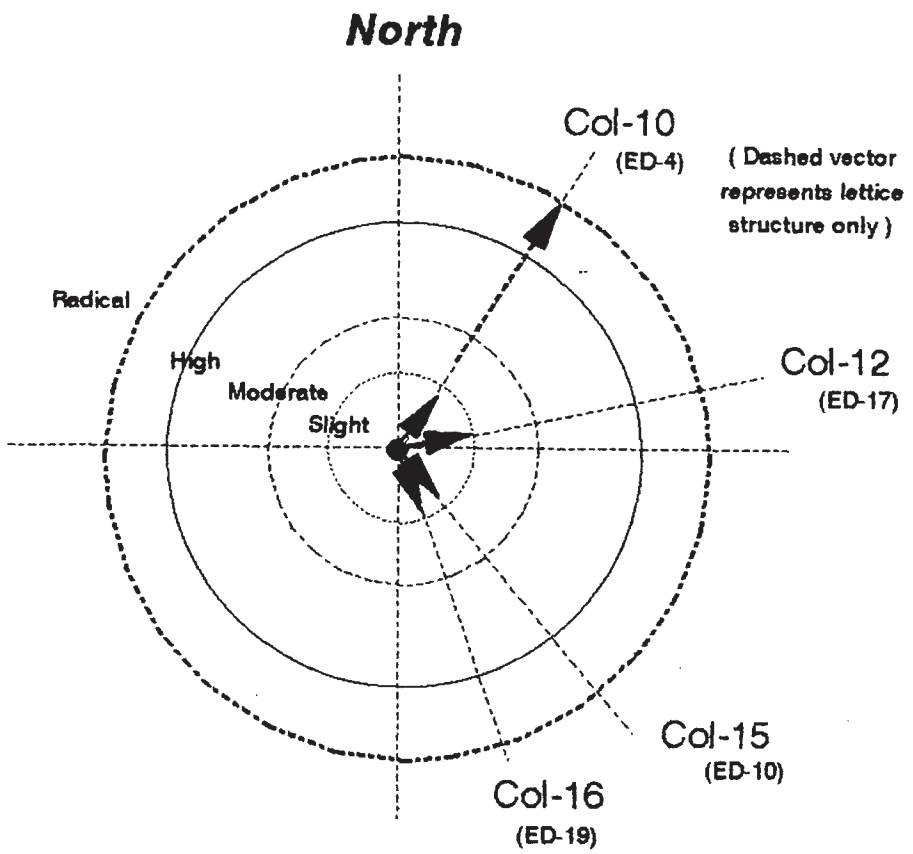


Figure 33. The long-term erosion pattern for Carrara marble is represented by the collection of solid vectors bunched together in the center of the erosion-rose. The dashed vector indicates catastrophic weathering on the acanthus leaf on Column 10, the only direction for which acanthus leaf data were available.

The values in Table 3 also can be represented in terms of average recession of the region studied. The average long-term recession rate was found to be 74 ± 150 μm/year; erosion rates as high as 224 μm/year were observed along the edges of the flutes and arrises.

The findings for Pennsylvania marble erosion can be summarized as follows:

- All exposed areas show pronounced long-term weathering.
- Columns 10 & 15 show slight short-term weathering.
- Both long-term and short-term average recession rates were in the range 60-100 μm/yr.
- Erosion immediately below the capital is faster than erosion 20 cm below on the column.
- Columns facing the east and southeast (Columns 12 & 16) are weathering faster over the long-term than are the columns facing other directions.
- The shortest time intervals needed to observe erosion of Pennsylvania marble by the various techniques are:

▲-Recession:	2 yr
▲-Texture:	5 yr
▲-Morphology:	36 yr

Similar estimates of time intervals for measuring Carrara marble loss cannot be made, since the erosion rate is significantly slower.

Carrara marble

Short-term textural changes in the Carrara marble is not detectable. The textural index of the Carrara marble near the peak of the second scan line on the lower capitals was measured to be 160 μm; however this is below the detection limit of the method of 210 μm. Long-term erosion was not detected along the second scan line, although a slight amount of long-term erosion was detected in the first scan line across the acanthus stack.

Spalling of the edges of the acanthus leaves can be measured using a three dimensional plots (or digital terrain model (DTM)) as described in Appendix B. Three dimensional plots of DTMs on the ends of acanthus leaves observed on west Column 3 and on east Column 10 (Appendix B). Comparison of the general shape of the surfaces depicted in the figures reveals spalling of the east relative to the west over the last 160 years. A small amount of short-term weathering near the edges was indicated. Analysis of the upper capital imagery, which documents the dramatic loss of marble volutes, would prove to be useful. Volutes may be particularly amenable to DTM analysis.

For the Carrara marble, the rate of erosion appears to increase from the lower part of the capital up to the area of the acanthus leaves. The difference between the apparent erosion rates may be due to the generally increasing relief of the carving from bottom to top of the capital. Virtually no long-term erosion was detected on the lower capital while spalling was identified on the edges of the acanthus leafs. The Carrara marble exposed on the outside of Column 10 on the east side of the building is weathering at a slightly greater rate than is the marble on the inside of the column. This is an indication of the role of rain and wet deposition play in the decay of dense marble that is substantially sheltered. As there is little erosion, there is little or no directional dependence of the weathering (Figure 33).

ENVIRONMENTAL EXPOSURE

Donald A. Dolske and Susan I. Sherwood

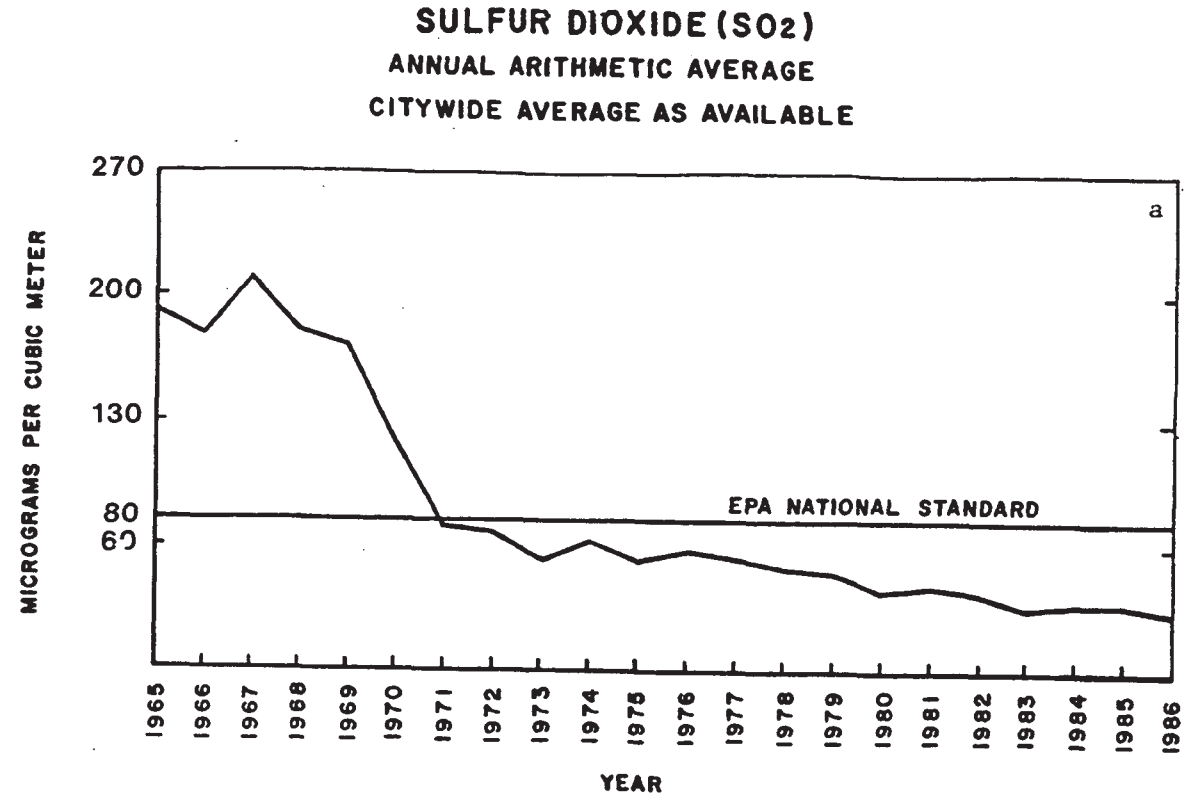
The purpose of this aspect of the project is to determine if the relative exposure to weathering agents (rain, pollutants, moisture, and temperature cycles) can explain the observed variations in marble deterioration at the Exchange. There are two kinds of applications for this knowledge. First, a detailed understanding of the microclimate and pollutant deposition regimes would serve as a basis for selecting appropriate stone conservation and maintenance options. Second, a detailed study of pollutant deposition to a weathered marble building in an urban area presents the potential to expand the technical understanding of marble decay. This goal is to achieve a sufficient understanding so that we can predict marble decay to the Exchange under other exposure conditions (e.g., under different traffic patterns); can predict decay of other materials at the Exchange site (e.g., proposed substitute or treated materials); or can predict decay of marble in other buildings or monuments for use in site-specific or regional development planning decisions.

Building facades inherently include a variety of environmental exposures that affect wet and dry deposition of pollutants to its surfaces. The general physical and chemical processes of marble weathering and deterioration are relatively well-known (Amoroso and Fassina, 1983; Winkler, 1975). It has been observed (McGee, 1989; Camuffo, 1982) that deterioration occurs by different processes and at greatly differing rates on various parts of a building. Performance of the stone in a building facade is more complex and is affected by highly variable deposition and exposure patterns. The design of the individual building, the neighboring structures, and the location within a city are all important determinants of a facade's exposure (Sherwood, et al., 1990). Variations in the magnitude and timing of temperature, insolation, moisture, and other exposure cycles determine pollutant deposition to the historic marble. As a result, facade deterioration may vary greatly in rate and in process. Similarly, substitute or treated material will undergo the same cyclic exposures to weathering agents. Therefore, understanding the microclimate of the Exchange is a key element in formulating a plan to manage the historic fabric.

This chapter discusses monitoring results for the range of microclimate and pollutant deposition conditions that the Exchange experiences in the present environment. In addition to microclimate and deposition, continuous measurements are made of meteorological conditions at the roof of the Exchange, including precipitation amount and chemical composition. Predicted deposition of sulfur is tested against collections of soluble surface deposits on the columns and capitals. Philadelphia pollution data from other sources is presented in attempt to place weathering at the Exchange in its urban and historical context.

POLLUTION IN PHILADELPHIA

As in most American cities, the current levels of pollution in Philadelphia are significantly less since the implementation of the Clean Air Act in the 1970s as shown in Figure 34. Measurements of SO_2 concentrations in U.S. cities before the 1960s are rare (Lipfert, 1987). Estimates of historical levels of pollutants are useful in order to consider the change in condition of a structure since its original construction. In theory, such information can provide insight into questions of timing of deterioration (does most of the marble decay stem from the 19th or the 20th century?) and to gauge future decay rates based on contemporary atmospheres, which tend to have more acidic rain and



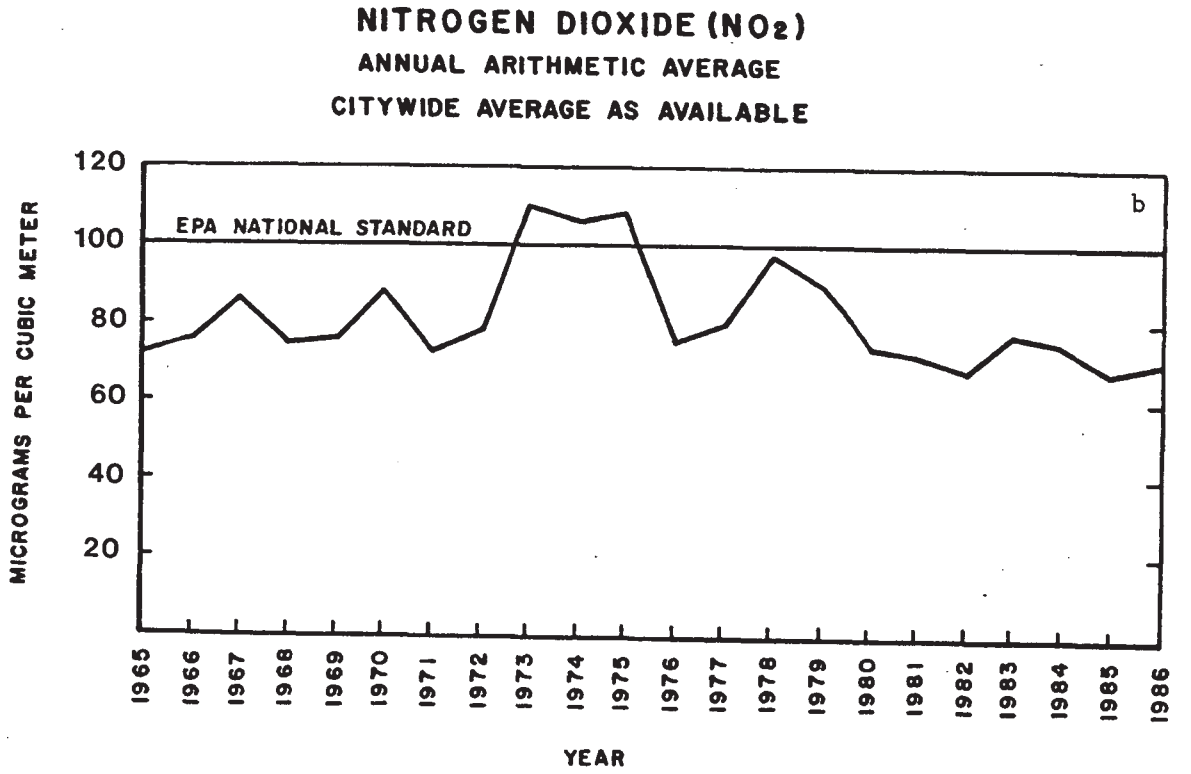


Figure 34a. Annual citywide average sulfur dioxide levels for Philadelphia 1965 through 1986.
Figure 34b. Annual citywide average nitrogen oxide levels for Philadelphia 1965 through 1986.

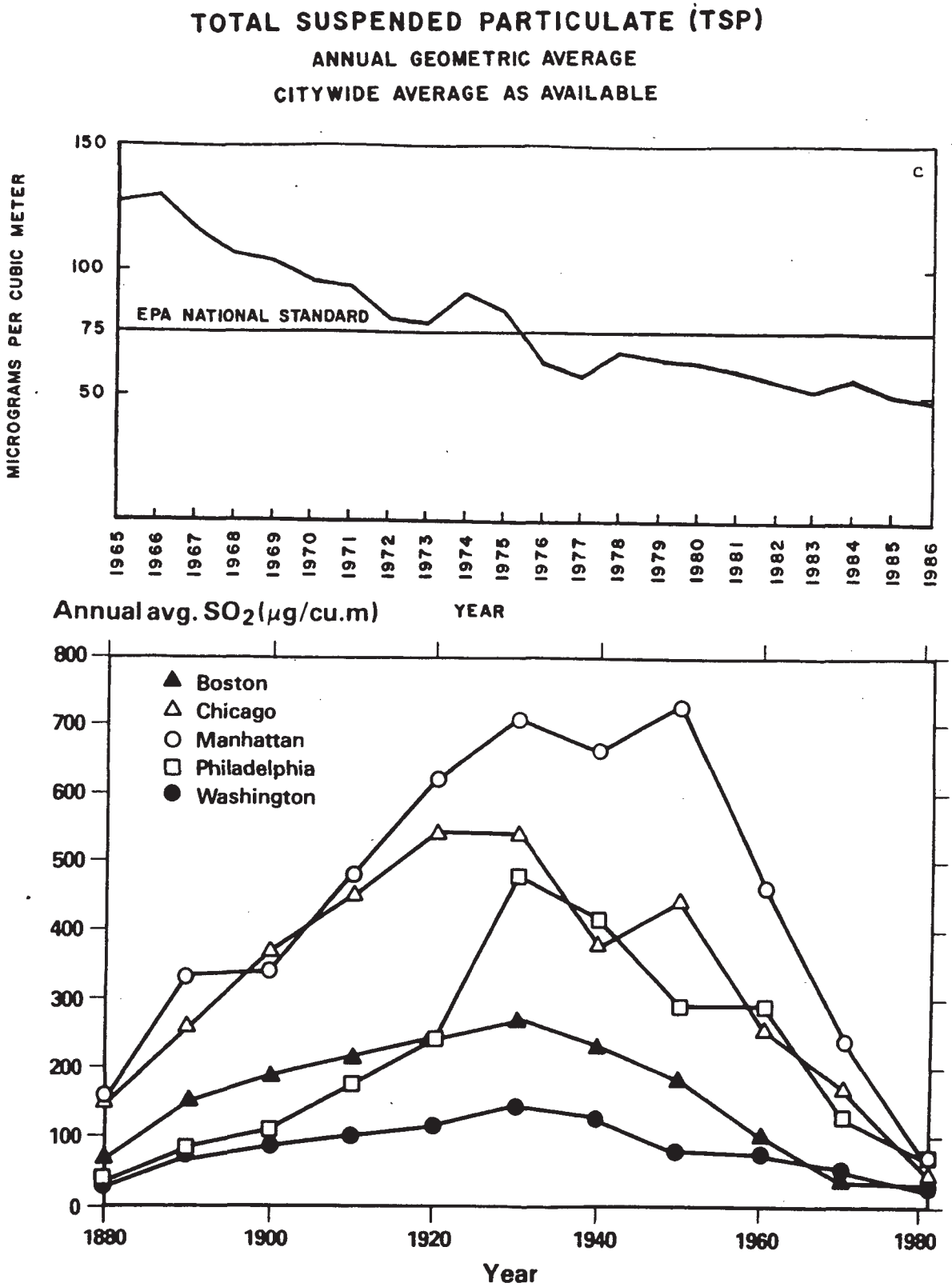


Figure 34c. Annual citywide average particulate matter levels for Philadelphia 1965 through 1986.
Figure 35. Estimates of historic SO_2 levels (μg/m3) (Lipfert, 1987).

less polluted air. Figure 35 presents estimates of SO_2 concentrations from 1880 to 1980 for Philadelphia and other major cities in the Northeast. These estimates are based primarily on population statistics and fuel use trends.

It was possible to construct a highly detailed 1880s emissions inventory for central Philadelphia and, to a lesser extent, western Camden because of the availability of detailed insurance maps for Philadelphia beginning in the 1850s (Figure 36). The purpose was to determine if pollutant emissions varied significantly with compass orientation, such that the observed variations in stone deterioration could be explained by the relative exposure to pollutants. Given changes in industry over time, both in type and in location, it is not reasonable to assume that present spatial patterns of emissions would be similar to 19th-century patterns. Historic exposure conditions may have been radically different than today, because of the spatial redistribution of industry and change in transportation systems. Figure 37 plots the estimated levels of SO_2 in lbs/hour from non-stack industry and residential heating, assuming bituminous coal. See Appendix C for anthracite coal use and other pollutants levels.

Preliminary estimates of pollution from the pwer production that fueled Philadelphia's smokestack industries indicate that the North and West facades of the Exchange were exposed to 3-5 times higher concentrations of sulfur and particles than the East and South facades. In part, this reflects the absence of data from Camden's industries due east of the Exchange and, in part, our inability to estimate sulfur emissions associated with industrial processes, e.g., smelting, paper pulping, and ink production. The total exposure from industrial power is estimated at about 25 $\mu g/m^3$ annual average.

The units of the 19th-century pollution estimates should be considered relative, rather than absolute, given the nature of the data sources and estimation methods (Appendix C). At this point, the analysis is incomplete; the contribution of trains (which are certainly the closest emitter) and industrial emissions from smoke stacks within 5 km are not available; these emissions are expected to be highly significant.

Precipitation Chemistry

A comprehensive record of urban precipitation chemistry, including pH for each rainstorm and all major ions for a selected subset, was collected by the City of Philadelphia Air Management Services Laboratory since 1978. The rooftop site is located in a mixed residential and light industrial area in north central Philadelphia. A quasi-wet-only collector was designed with a rotating semicircular plexiglass shield over the funnel, in order to exclude large debris from the rain sample. Preliminary audits indicate a bias in the pH and/or chemical concentration measurements; however, internal consistency within the data allows time-trend and directional-source attribution analyses. The consistent use of the same collection and analytical methods for over a decade makes this a unique record of precipitation quality in the U.S. The composite monthly average pHs are shown in Figure 38.

For the twelve year period, monthly volume-weighted mean pH ranged from 3.77 to 4.91 with a mean and median of 4.31 and 4.32, respectively. A slightly decreasing trend in pH from the early to mid-1980s is indicated, with a slight increase overall at the end of the 1990s. For the period 1982 through 1988, Lynch (1991) and Lynch, et al. (1985) report mean pH for the Philadelphia region of 4.21, based on non-urban sampling sites such as Valley Forge. Rains from the east-southeast exhibit significantly higher sodium and chloride concentrations, as expected in storms occurring when winds are from the Atlantic Ocean. Finally, event volume-weighted mean pH is shown to be fairly uniformly pH 4.0

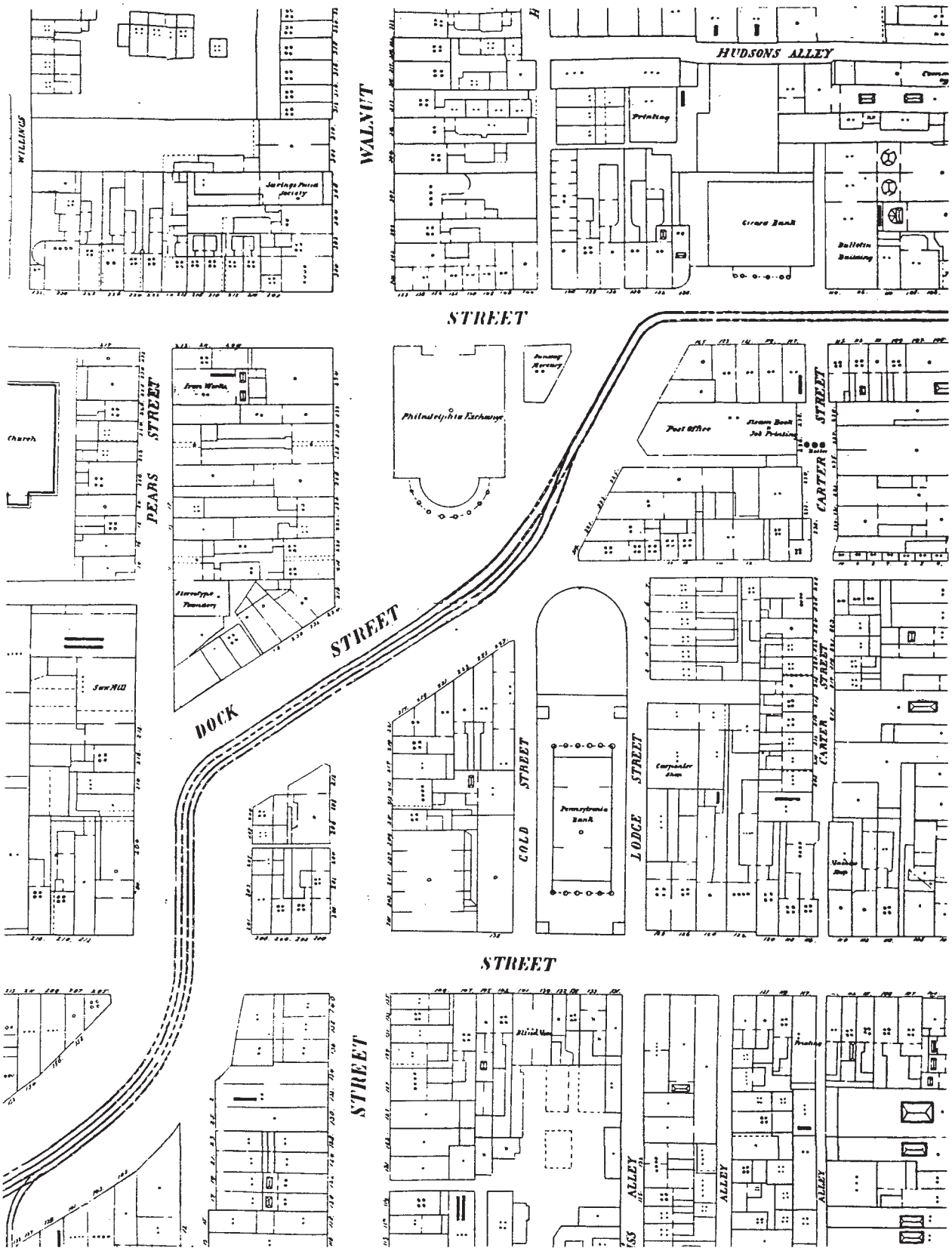


Figure 36. Hexamer Insurance Map excerpt, Vol. 1, 1865.

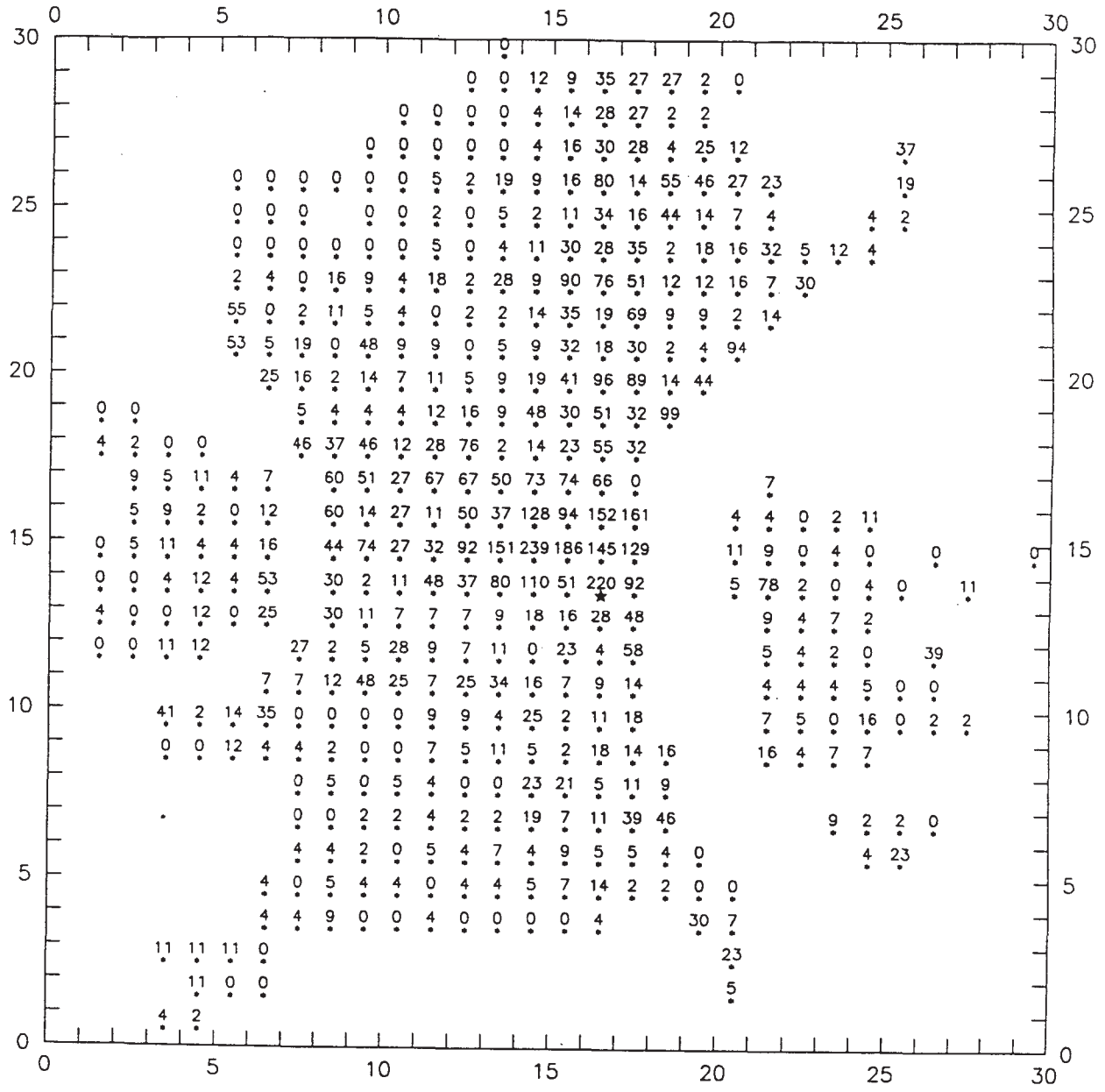


Figure 37. SO_2 emissions (lbs/hr) density map for 1890s. Based on Hexamer specially hazardous industries (assumes all bituminous coal used) and port of Philadelphia traffic statistics. No trains or point sources included.

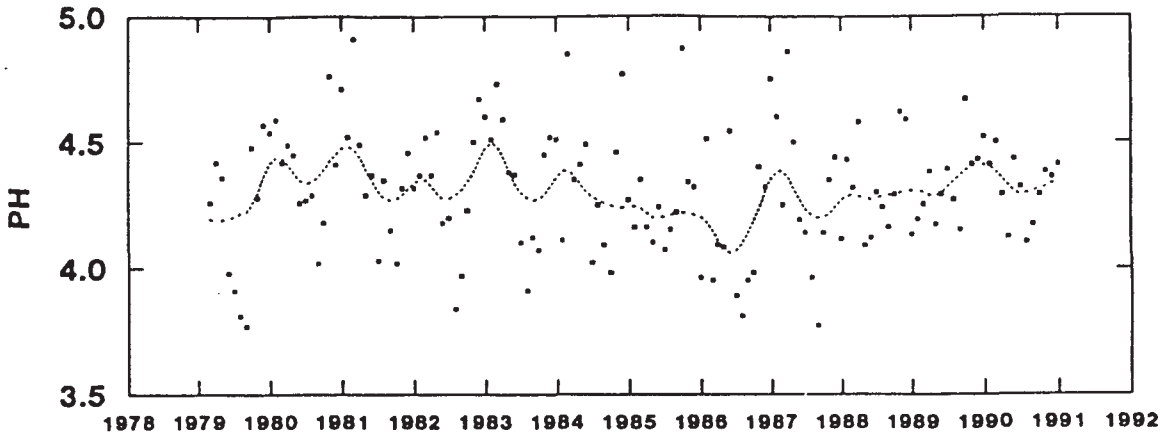


Figure 38. Precipitation pH for Philadelphia. Curve shows trend smoothed by a four-month moving-average filter.

from all westerly directions, with some variation and higher levels for all easterly directions. The maximum pH sector coincides with the marine influence, as indicated by sodium and chloride levels. These results correlate well with expectations based the geography of Philadelphia, tending to confirm further the general internal consistency of the data.

A wet-only semi-automatic rain chemistry sampler (Vermette, 1988) is located on the roof of the Exchange. Over 100 rainstorms have been collected since its installation in 1989.

The distribution of rain acidity and volume as a function of wind direction during the storm is shown in Figure 39. Rain volume is significantly greater from the south-east than from any other direction. The acidity of incident rain is quite consistent around the compass, except for storms from the southwest and northwest, which are about .5 pH unit (more than five times) more acidic than the rest. Nitrate concentrations are fairly evenly distributed by direction, but sulfate in rain (which usually exceeds nitrate by 2:1 in concentration) is much greater when the wind is out of the south-west. The sulfate:nitrate ratio is typical of rain chemistry east of the Mississippi. The average acidity and ion balance, however, is akin to more neutral rains west of the Mississippi.

Urban Meteorology

Philadelphia has a moist temperate climate, with wet springs and summers. A meteorological station was established on the roof of the Exchange to provide a general characterization of conditions at the site, relatively unaffected by the near field effects of the building itself. Equipment installed atop a mast includes a set of sensors for temperature and humidity, wind velocity and direction, and precipitation rate (tipping bucket gauge), all recorded as hourly means. Annual precipitation totals 130 to 150 cm; it rains 12% of the time, on average. The prevailing winds are from the southwest, except when it is raining. Air temperature during the study period has ranged from -7 to +33 °C. In general, the central city location of the Exchange seems to moderate the wind velocities observed at the building, which are relatively low at 1-3 m/second on average.

Measurements at the East Portico of the Exchange

Pollutant and microclimate instrumentation are attached to two columns on the north and

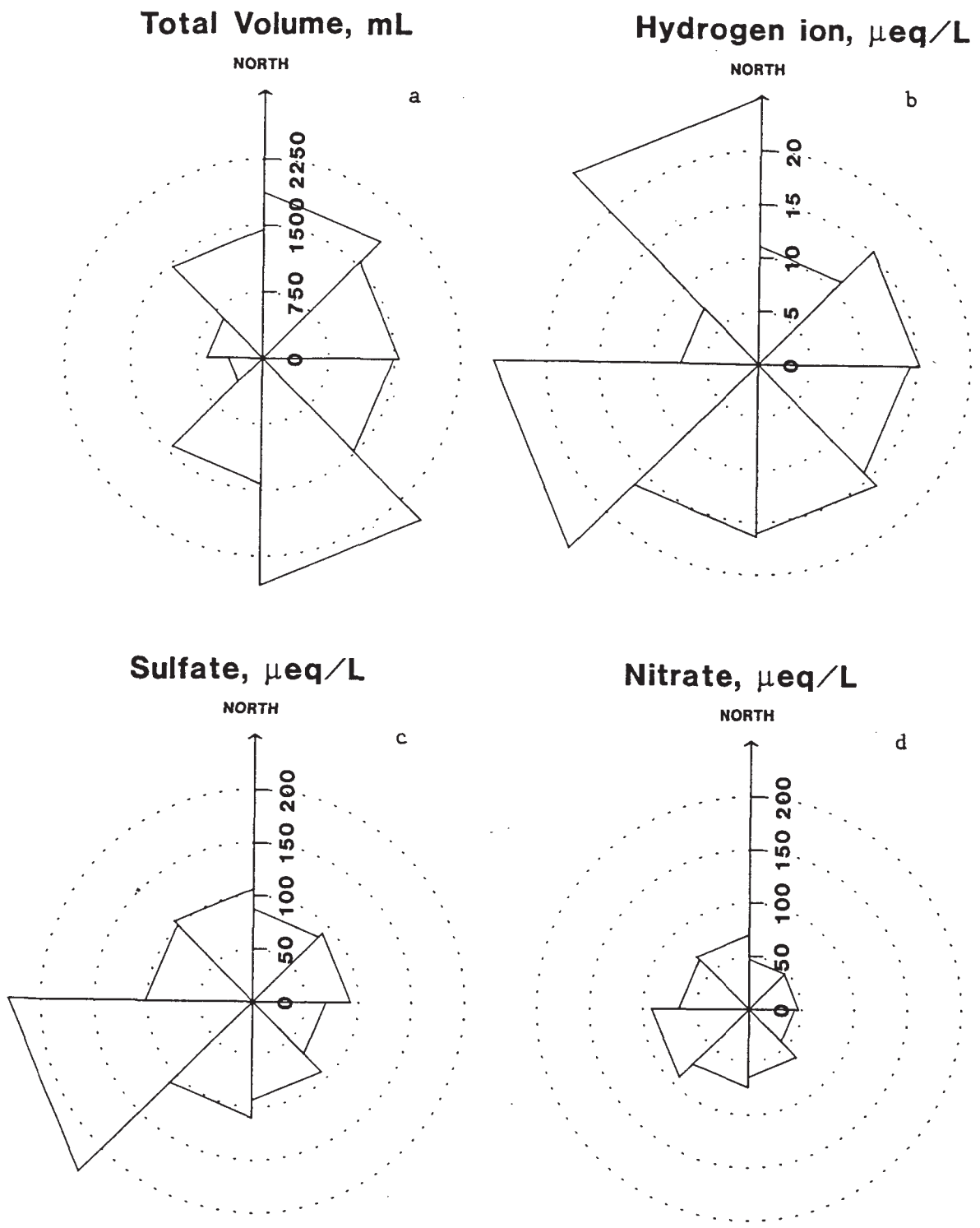


Figure 39. a) Rain rose for the Exchange rain collections in 1989-1991; b) Rain chemistry (H+) rose for the Exchange rain collections; c) Rain chemistry (sulfate) rose for the Exchange rain collections d) Rain chemistry (nitrate) rose for the Exchange rain collections.

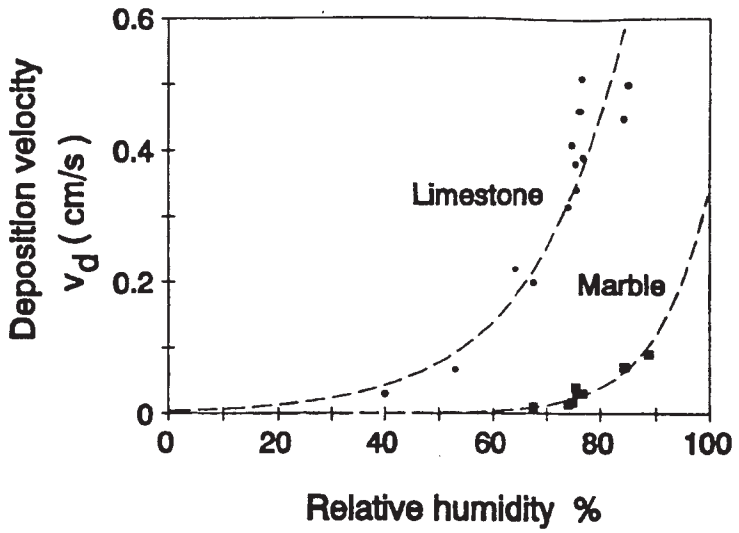


Figure 40. SO_2 flux to marble and limestone as a function of ambient relative humidity (Spiker, 1990; Spiker et al., 1992) These data are derived from a wind tunnel exposure of smooth, quarry fresh stone samples. Sulfur fluxes to stone in buildings are much more variable, since they depend on aerodynamics at specific locations.

A four-stage filterpack method is used to measure the airborne concentrations of particulate $SO_4^=$ and NO_3^- as well as gaseous HNO_3 and SO_2. Each sampler controls two filterpacks, one of which is connected to the sampling air stream when the surface is wet; the other is in line when the surface is dry. Thus, for each week, two measurements of pollutant concentration are made at each location: a "wet" period average concentration and a "dry" period average concentration. Using surface wetness to control collection of the pollutant concentration data allows a more accurate computation of dry deposition to the marbles. This is particularly important for sulfur dioxide since SO_2 deposition rate to a wet marble surface is an order of magnitude or more greater than deposition to a dry surface under otherwise comparable circumstances (Figure 40).

Microclimate Results

A two month scoping study was undertaken in late May 1987 to early July 1987 (Dolske, 1987; Table D-1) to estimate the surface moisture condition as a function of position within the building. Electronic moisture sensing grids were glued to the stone surface at ten locations and were read approximately every two hours. These preliminary data clearly indicated variability in spatial and temporal patterns of surface moisture on the building. Although these sensors and display units were carefully matched and calibrated at the beginning of the study period, differences appeared during the course of the study, perhaps as a result of atmospheric corrosion. Data from three sensors were not considered in this analysis.

The west capital appears to be consistently dryer than are all of the east locations in this calibration group. During the no-rain period, the range of east-west wetness disparity can be 30-60% (Figure 41a). The inside of the south capital tends to be about 27% wetter during the no-rain period than is the outside of the south capital (Figure 41b). The outside of the capital dries more quickly both in the early morning and at midday. There appears to be a slight general drying pattern during the daytime at all of the locations monitored. There is no discernable difference between the inside of the north capital and the inside of the south capital (Figure 41c). Apparently, there is a fairly uniform microclimate at the same height in all directions inside the east portico.

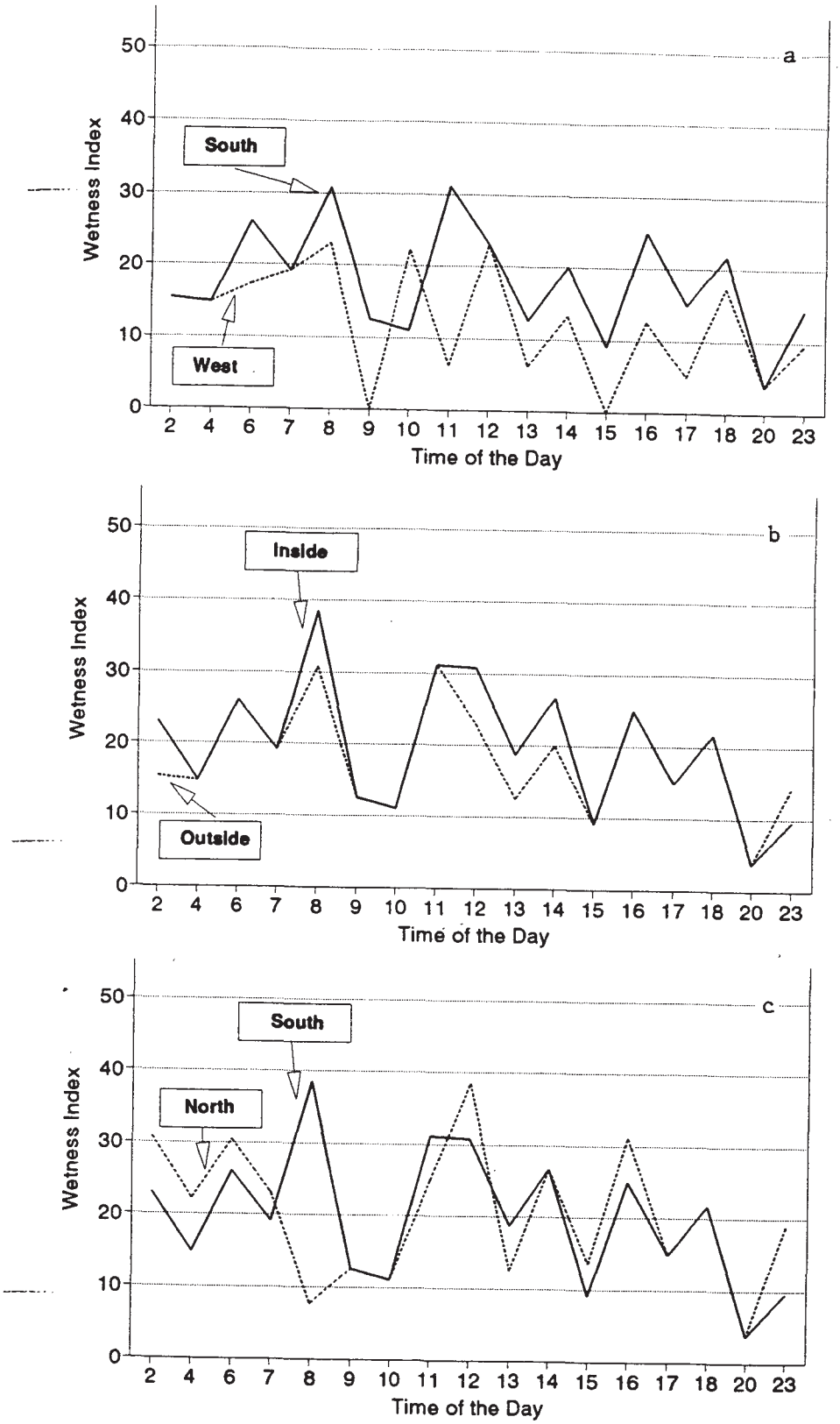


Figure 41. Diurnal wetness patterns May and July 1987, non-rainy days only; a) capitals west versus east; b) Capital 16 inside versus outside; c) Inside capitals north versus south.

south sides of the semi-circular colonnade on the east facade, approximately 12.5 m above the ground (Appendix D). Identical arrays of microclimate sensors are glued to each of the marble column shafts about 2.7 m below the cornice. These include: visible solar radiation intensity, stone surface temperature, and stone surface wetness. Air temperature, relative humidity, horizontal wind velocity instruments are mounted about 20 cm radially away from the column at the same level. A digital datalogger scans all sensors every 10 seconds, computing and storing the mean values on magnetic tape once each hour. See Appendix D for details of equipment and procedures. For the most part, these observations are understandable in terms of the expected amount of solar radiation at the various locations. Clearly, the probability of detecting moisture on the stone is inversely related to sunlight exposure.

Despite some concerns about failures of sensors facing east and southeast, comparison of the diurnal wetness patterns suggests a degree of consistency in the wetness patterns of the antefixes. The north-north-east antefix appears to run about 15% drier than the east-south-east antefix, particularly between midnight and dawn. There is a general drying of all antefixes throughout the day reaching a minimum at approximately 2 p.m. Thereafter, the moisture content on the antefixes seems to remain constant until just before dawn. Apparently, the dew-point of the air around the antefixes increases as the humidity increases during the early hours of the morning. This results in a slight increase in moisture on the antefixes early in the day. Antefixes exhibit more pronounced wetness variations during the day than do capitals.

Differences in sky view, or the ability of a given point to radiate away heat at night, thereby cooling to the dew point. The more enclosed aspect of the columns compared to antefixes, and the presence of nearby buildings on the south side of the Exchange would yield the differences in radiational cooling needed to produce the observed differences. Thus, the open sky or horizon angle is an important factor determining the moisture cycle at any given point on the facade, both from the point of view of solar input (heating) and longwave radiation (cooling).

Three years of microclimate data collected on the north and south sides of the east portico are presented in Figures 42 and 43. In Figure 42, each vector represents a three-year average of the values for that hour. In Figure 43, the vectors represent a similar seasonal average based on three years of data. The white band plots data from the south column; the gray, data from the north. In almost every instance, the north value exceeds the south valued. When the south value exceeds the north, the latter can be seen as a ray across the sector.

The microclimate measurements shown in Figures 42 and 43 illustrate the overall seasonal trends and differences within the building facade. Figure 43a plots solar radiation, which is a "forcing function" variable, as it measures the external energy input that controls temperature and moisture regimes most strongly. The north side receives scattered / reflected / sky light, except in the very early morning in the summer, where the sun is rising a bit north of due east. Seasonal variation in overall average cloudiness is shown by mid-afternoon magnitude of solar at the north side. South side, seasonally minimum values of solar radiation during daylight hours are observed because the sun is highest in the sky, and strikes the vertical column surface at a relatively lower angle. Winter should be the maximum for the midafternoon values, but is not because of increased winter cloudiness and shading by nearby buildings. Fall values in the early afternoon are somewhat greater than for spring (similar in sun position), because of cloudiness.

There is not much seasonal variation in relative humidity (Figure 43b), except when

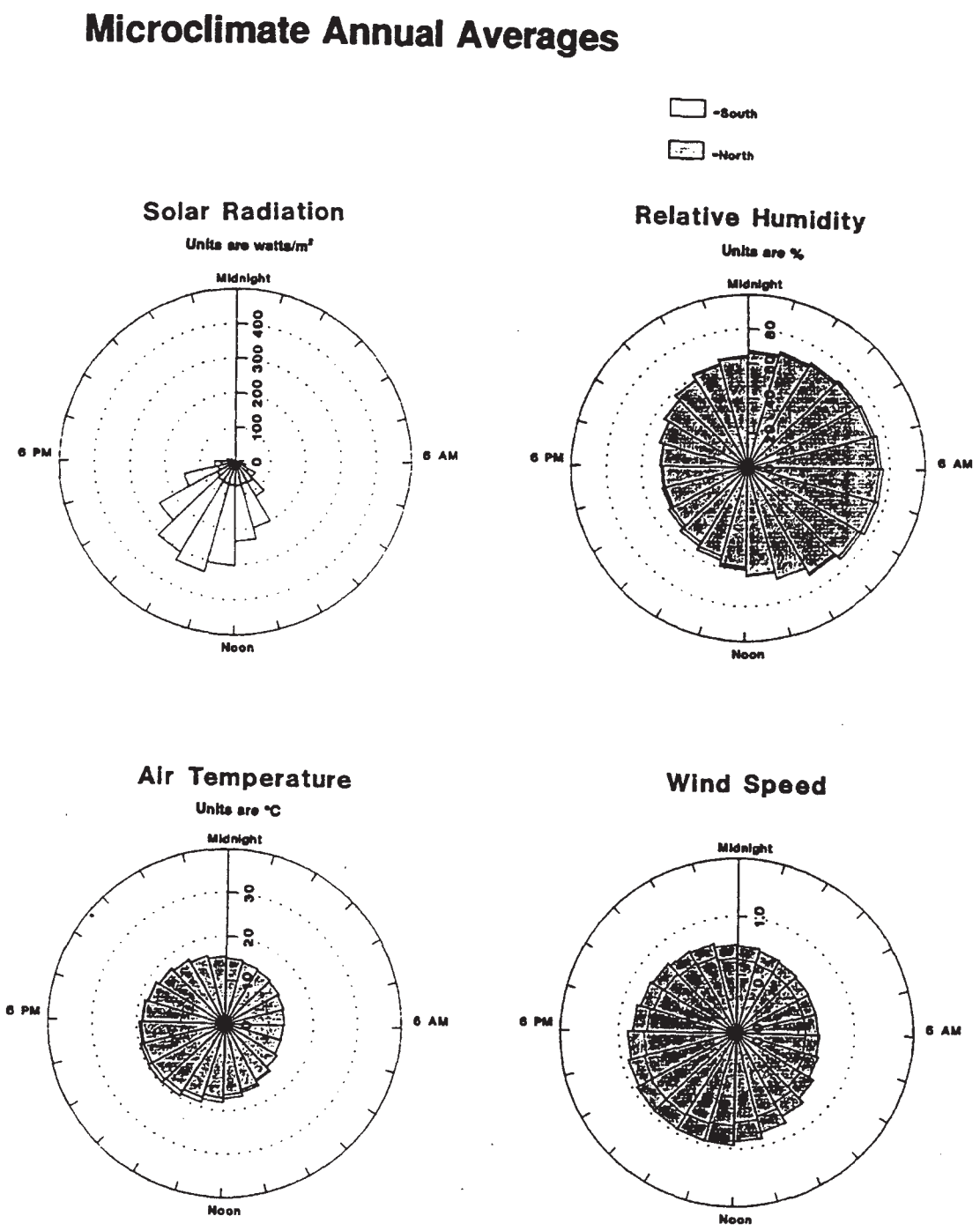
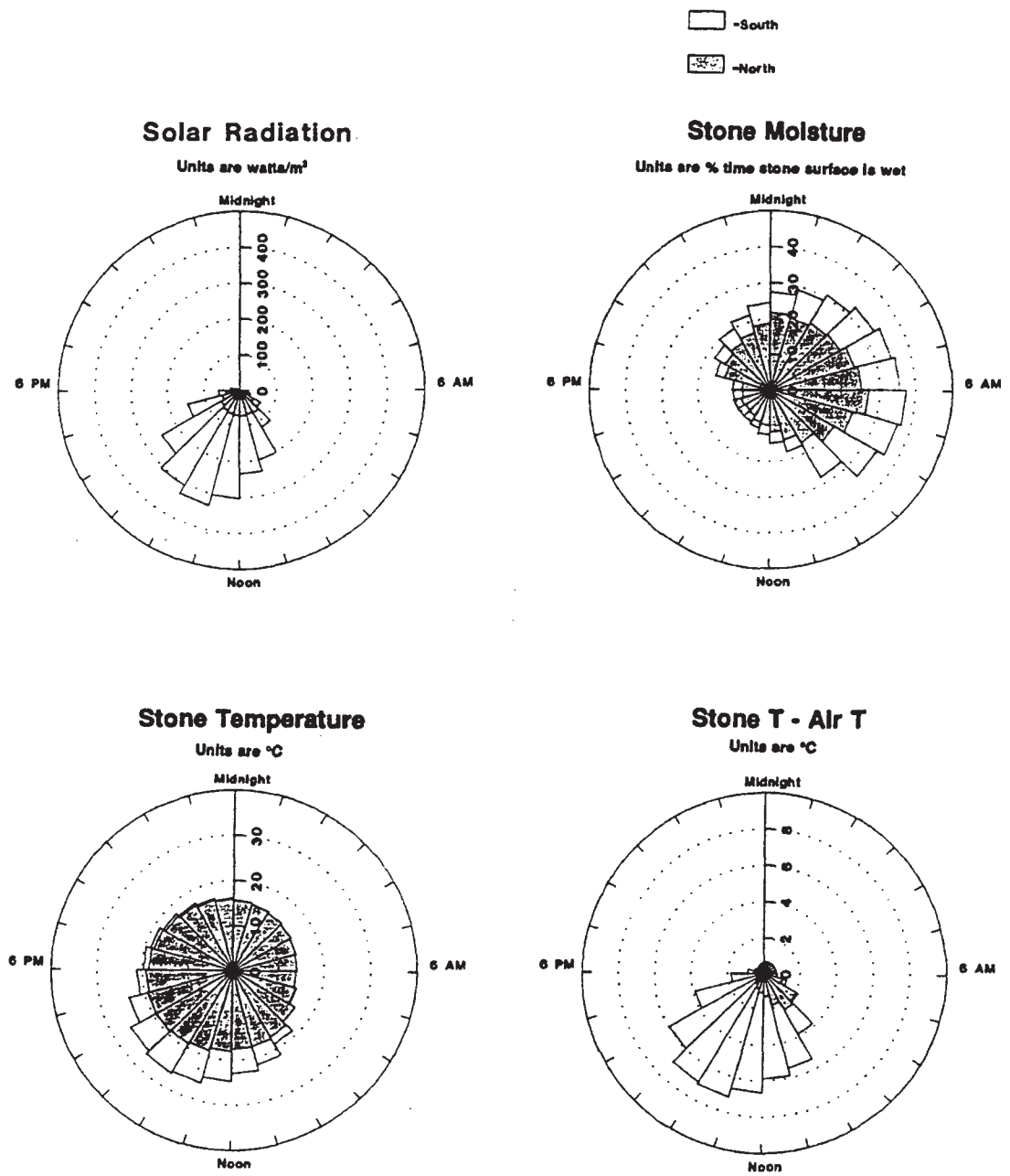


Figure 42. Microclimate data-annual averages for each hour; a) ambient parameters; b) stone parameters.

Microclimate Annual Averages



winter sub-freezing, arctic dry air brings down the average a bit. Insolation and related drying on the south side decreases building specific sources of moisture in the still night air, so south side values tend to exceed the north side in the morning and into the day. These tend to equalize by mid-afternoon. Air temperature values (Figure 43c) are very similar from one side of the building to the other, as expected. Such differences as there are demonstrate that the sensor array responds to near-surface conditions, such as humidity cycling and microscale heating of the air. Although the peak solar input to vertical surfaces are expected in winter (based on solar position), shading and cloudiness prevent maximum potential energy inputs. This does not entirely hold true for the stone temperature (Figure 43d).

The seasonality of the difference between air and stone temperature (Figure 43e) is very similar to solar radiation values. The difference between air and stone surface temperature is greatest for the north side in the summer, as compared with the south, where the maxima is in mid-winter. These differences relate to the seasonal pattern of solar radiation input to walls. The stone surface is cooler than the air more frequently on the north side than the south, where the temperature differences are much greater and more variable. Note that the north column experiences surface heating during summer mornings, in contrast to the very slight difference at other times of the year. The timing of the daily maximum heating changes during the year. In winter, it is 1 p.m. to 3 p.m.; in the summer, it is earliest, 11 a.m. to 2 p.m. It is apparent that surface temperature differences (especially surface temperature elevation above ambient air temperature) control the evaporative drying of building surfaces at differential rates.

The surface moisture (Figure 43f) represents the percent of time the ASTM wetness sensor reads "on." It is strictly speaking not a measure of the moisture content of the stone itself, which can retain moisture in the fabric for significantly longer periods of time. This measure of stone surface moisture is thought to be fairly representative of the moisture condition as seen by SO_2 gas, and should relate well to periods when sulfur deposition is enhanced. The probability of rain is equally distributed throughout the day and night, occurring some 12 percent of the time. Rain and post-rain stone surface moisture account for the observed 10 to 15 percent minima at any given hour. Reduction in relative humidity, occurrence of precipitation as snow, and sleet that does not wet the stone significantly, are some of the reasons that explain the minimum values in winter. Note that in the summer the highest absolute time of stone surface wetness occurs, but the greatest north-south differences occur in the fall. This phenomena results from interactions between solar radiation inputs and condensation and evaporation conditions that are beyond the scope of this report. The stone surface moisture data indicate that, in general, the south side tends to be somewhat wetter than the north side.

Pollution Concentration Results

An overview of the airborne pollutant concentration data for three species: total nitrate (particulate NO_3^- and HNO_3), particulate sulfate, and sulfur dioxide is shown in Figure 44. The open and filled symbols represent the mean values for the north and south columns, respectively, combining the wet and dry measurements at each sampling location. The curve traces a one-month moving average of an overall mean value for the building. These concentration data illustrate that the air quality at the Exchange is typical of large American cities, with significant week to week variability and some degree of seasonality evident. It is also noteworthy that there are at times significant differences between concentrations measured at the two locations on the same building. Differences on the order of 50% or more have

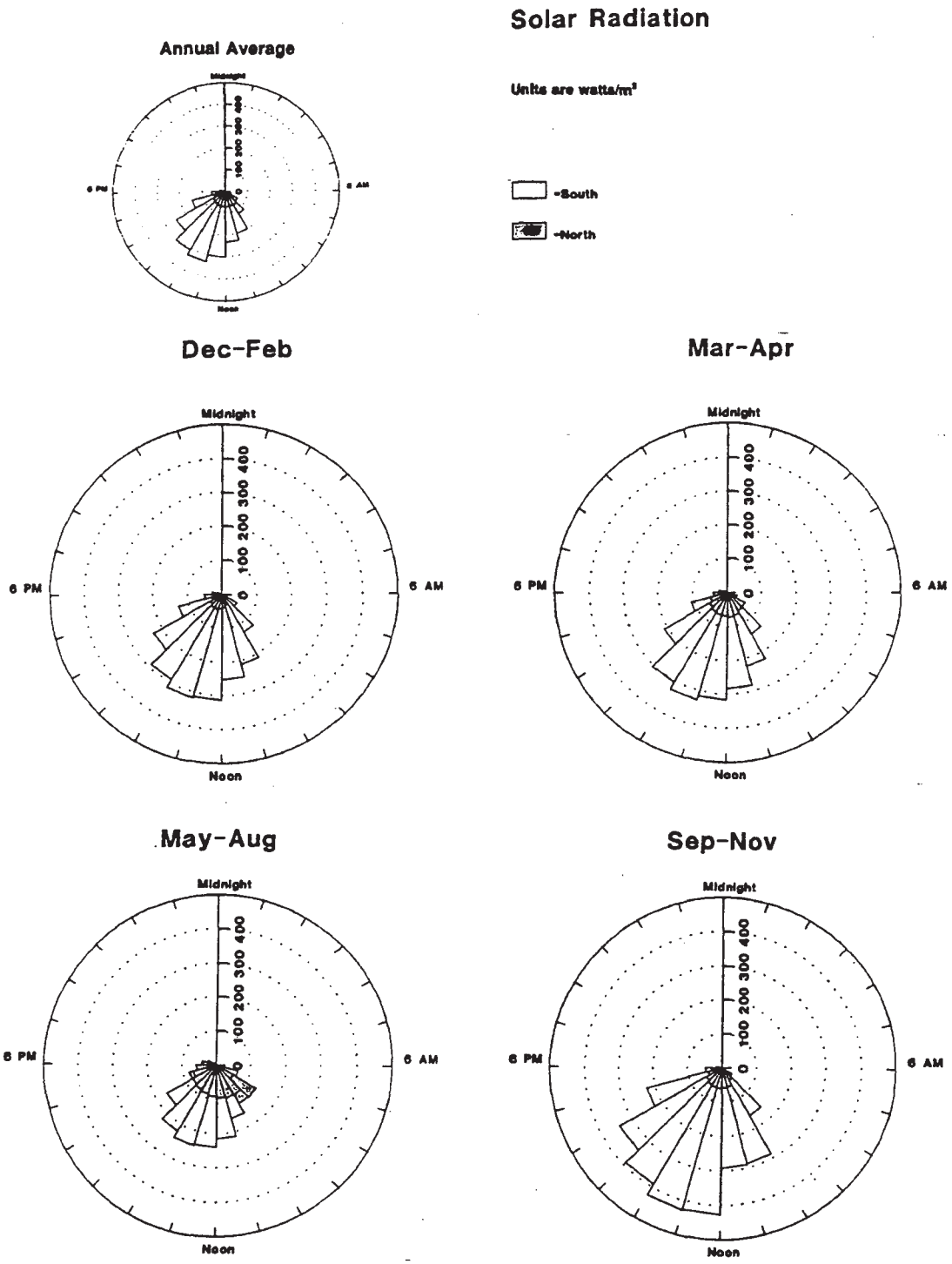


Figure 43a. Microclimate data-seasonal averages:solar radiation intensity (watts/m²).

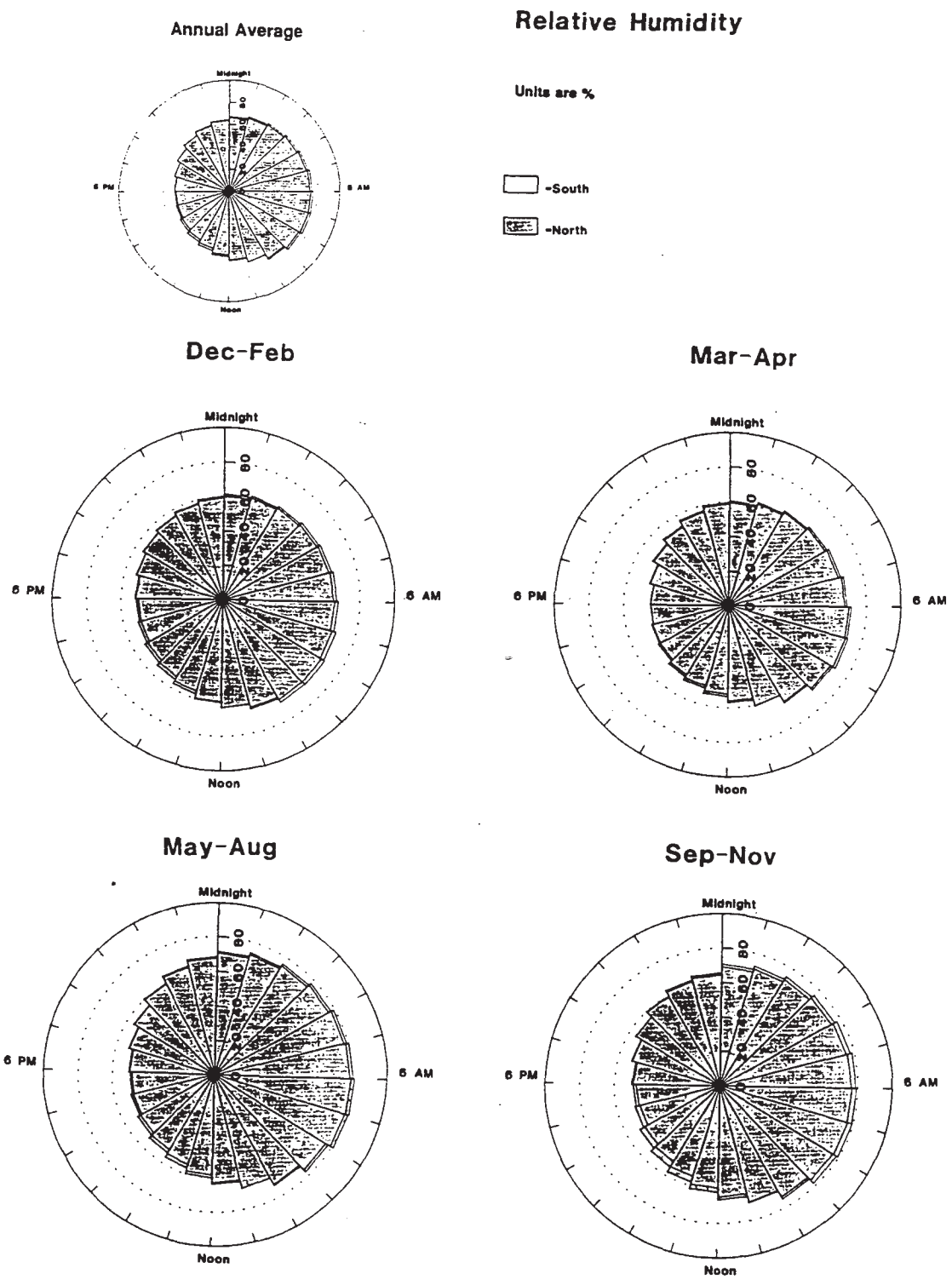


Figure 43b. Microclimate data-seasonal averages:relative humidity (%).

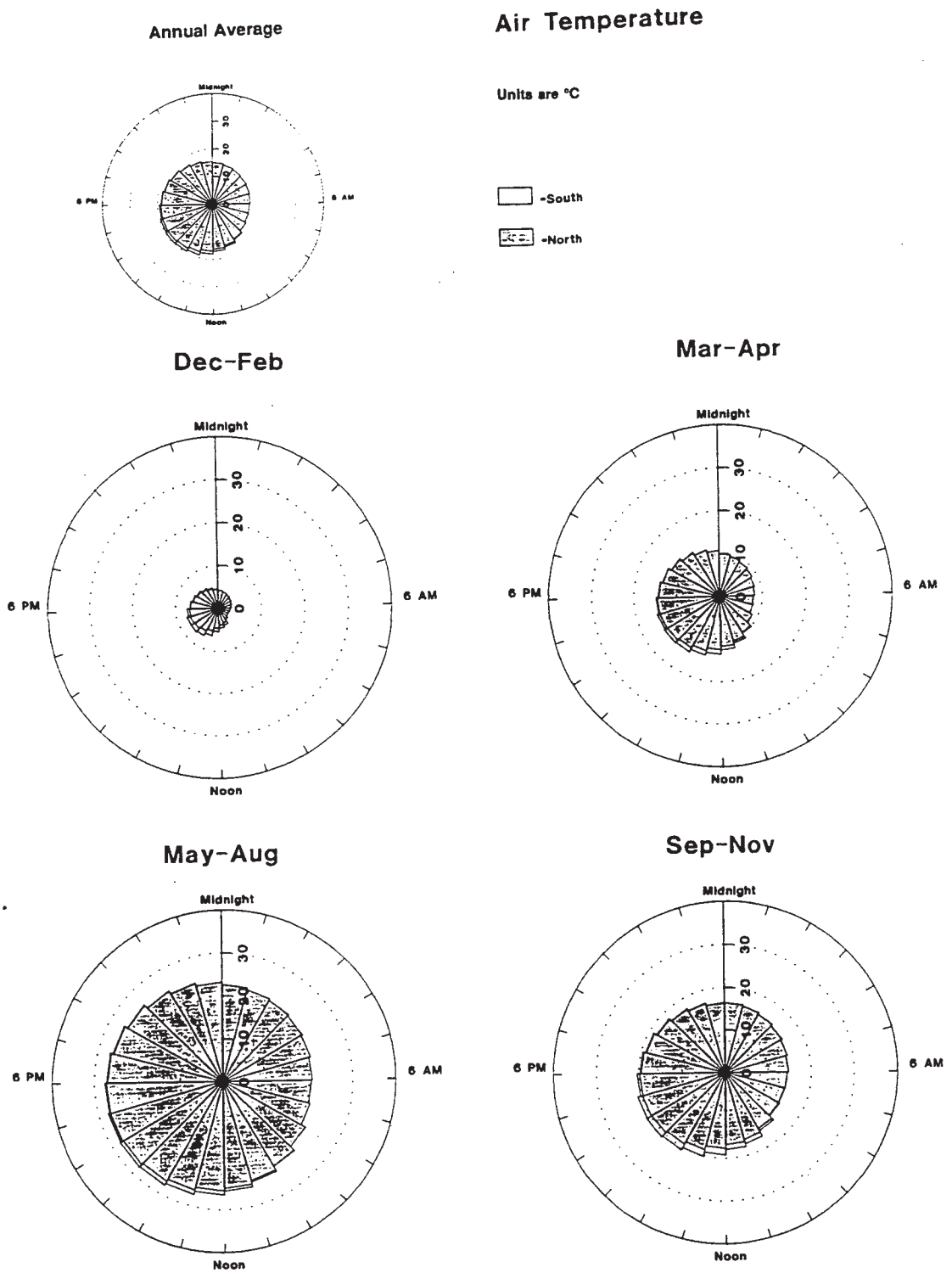


Figure 43c. Microclimate data-seasonal averages:air temperature (°C).

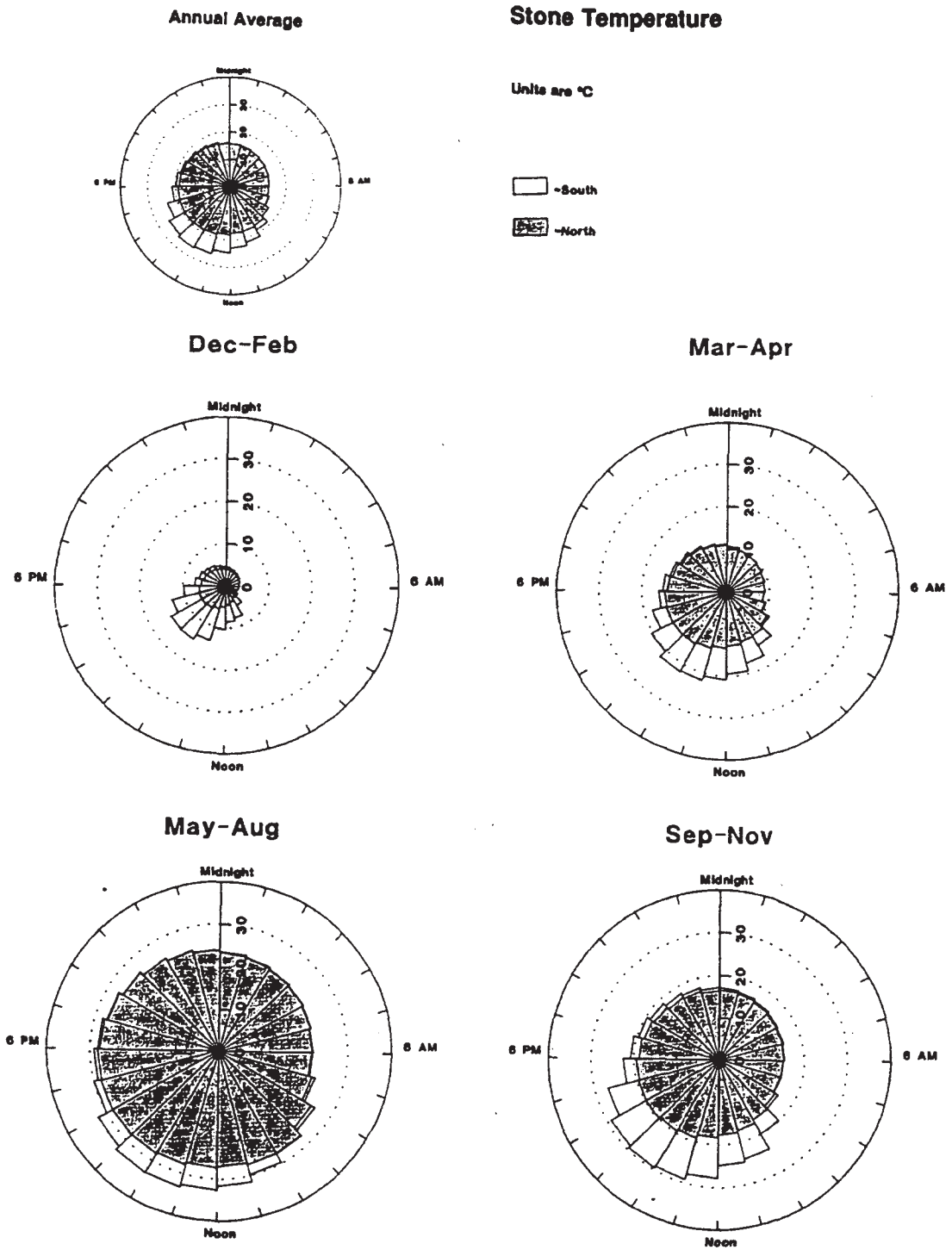


Figure 43d. Microclimate data-seasonal averages:stone temperature (°C).

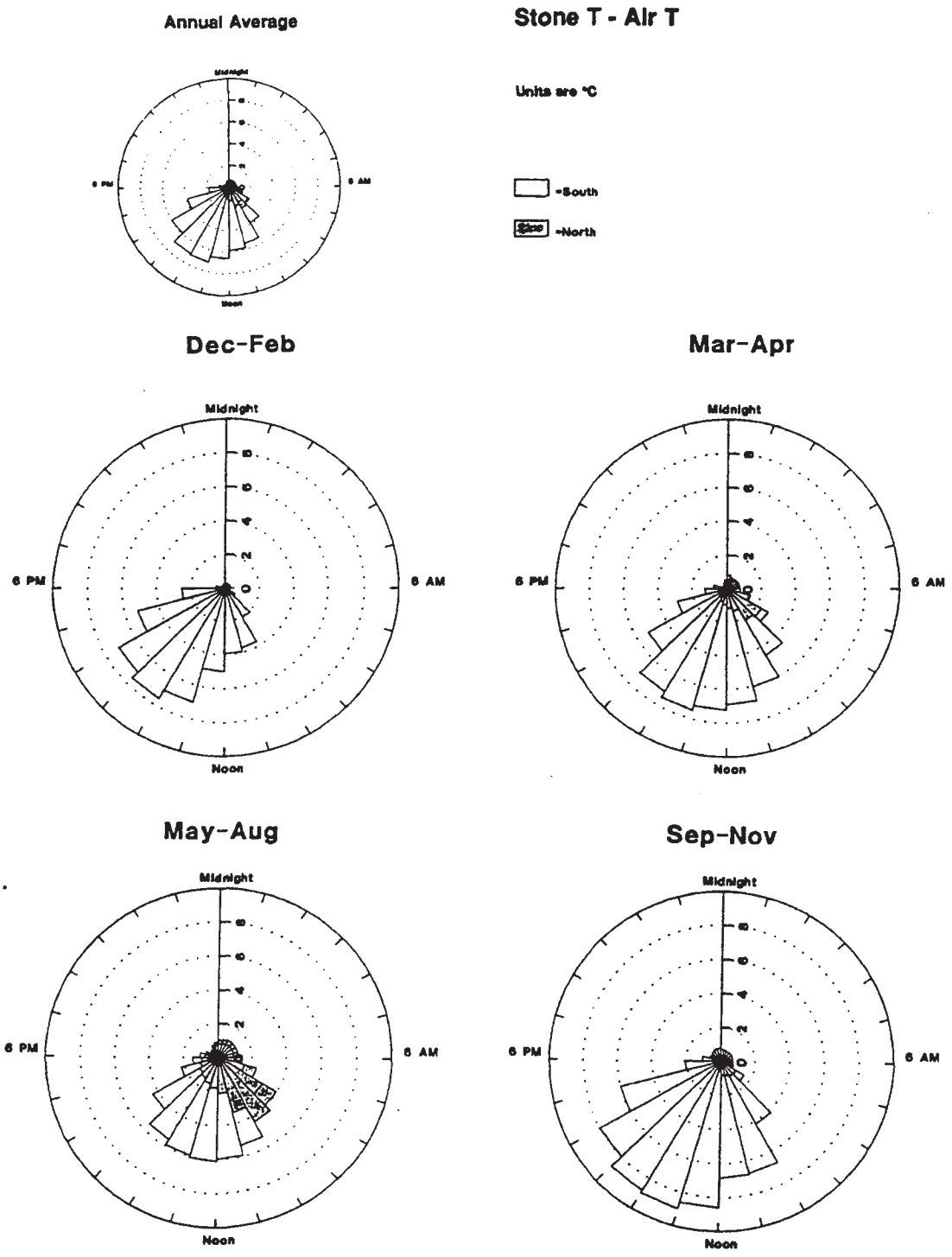


Figure 43e. Microclimate data-seasonal averages:air minus stone temperature (°C).

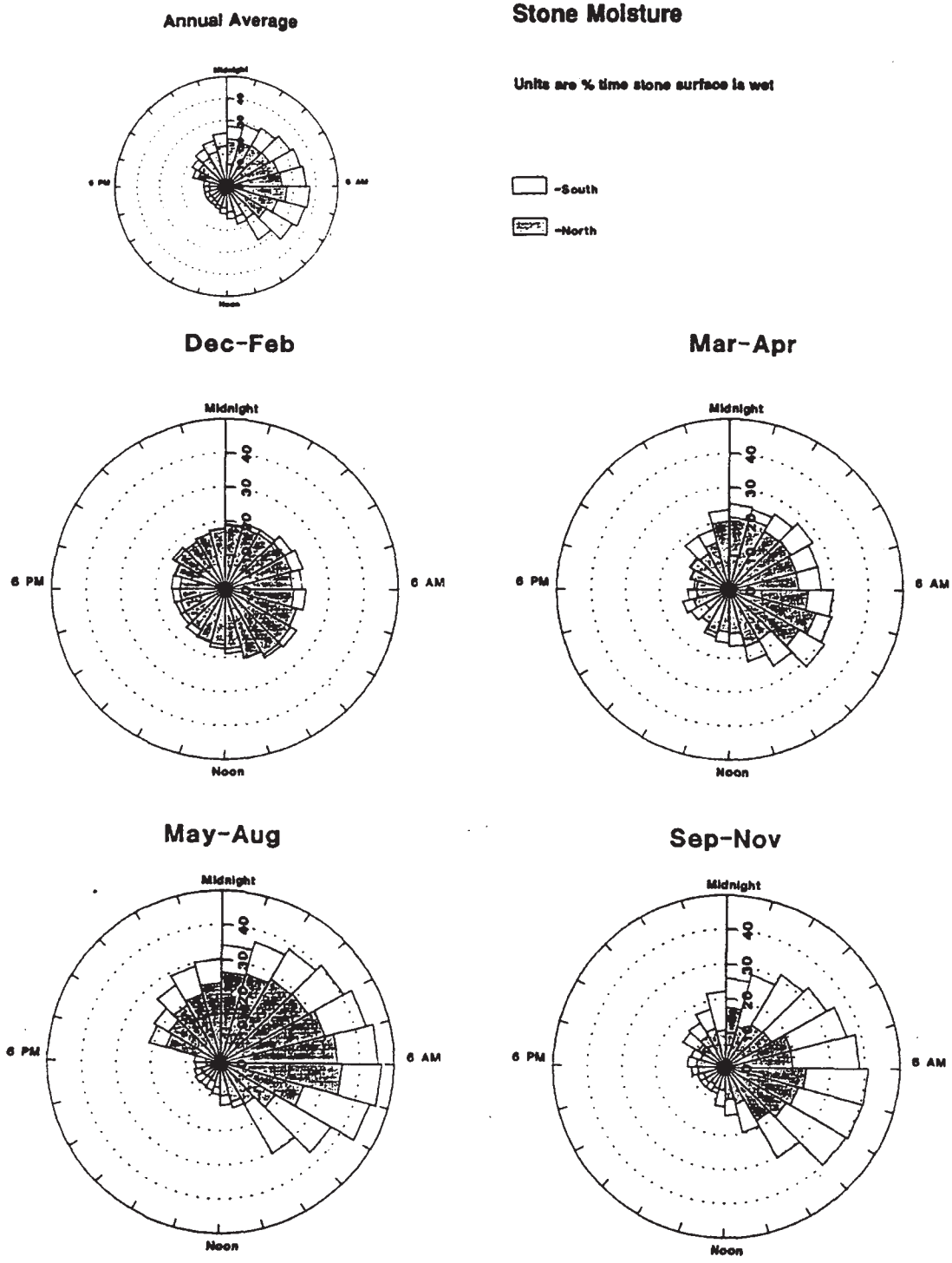


Figure 43f. Microclimate data-seasonal averages:stone surface moisture (% time wet).

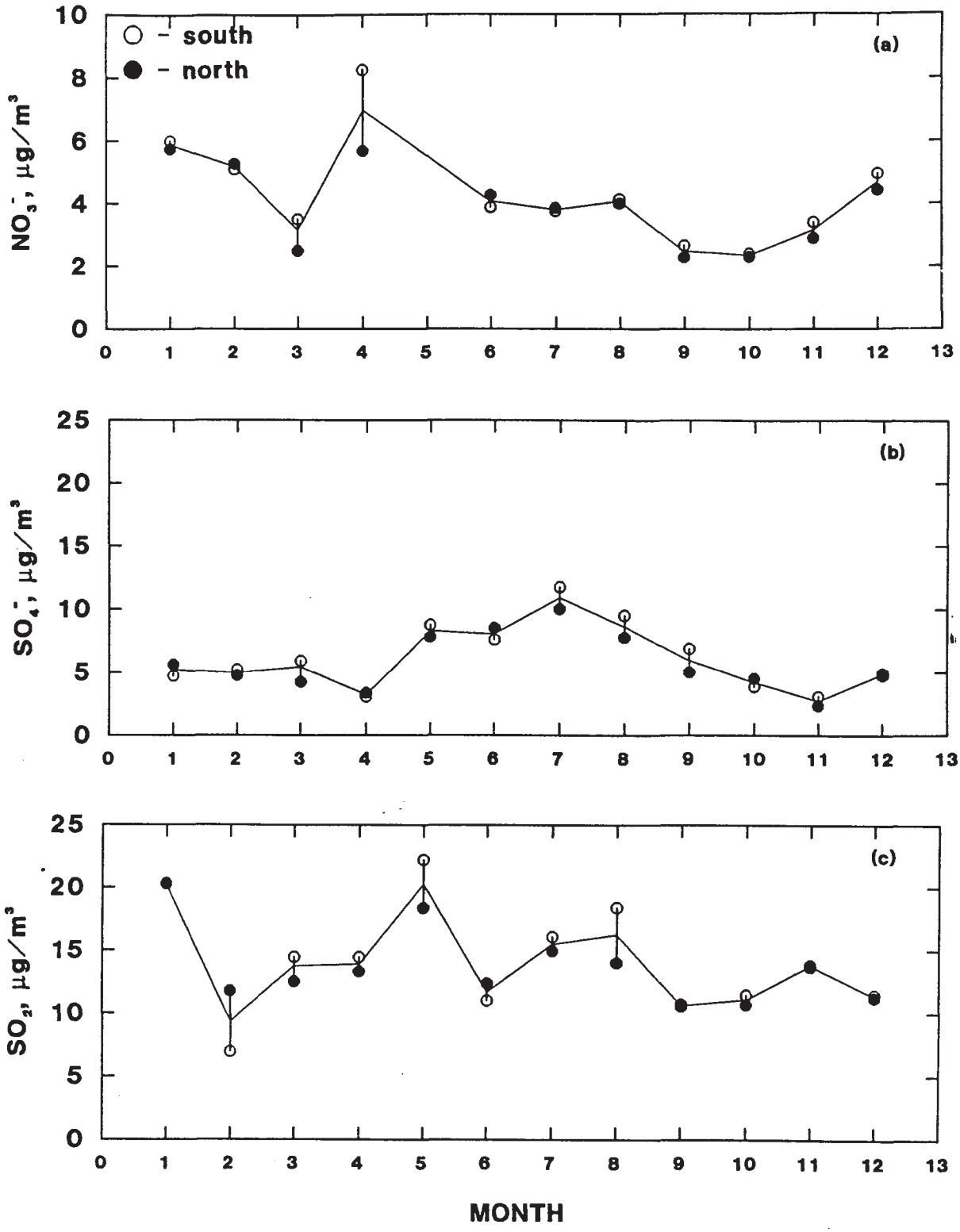


Figure 44. *Pollutant concentrations at the Exchange; monthly averages based on first three years of data; a) total nitrate b) particulate sulfate c) SO_2. Open circles indicate south side; closed circles indicate north side.*

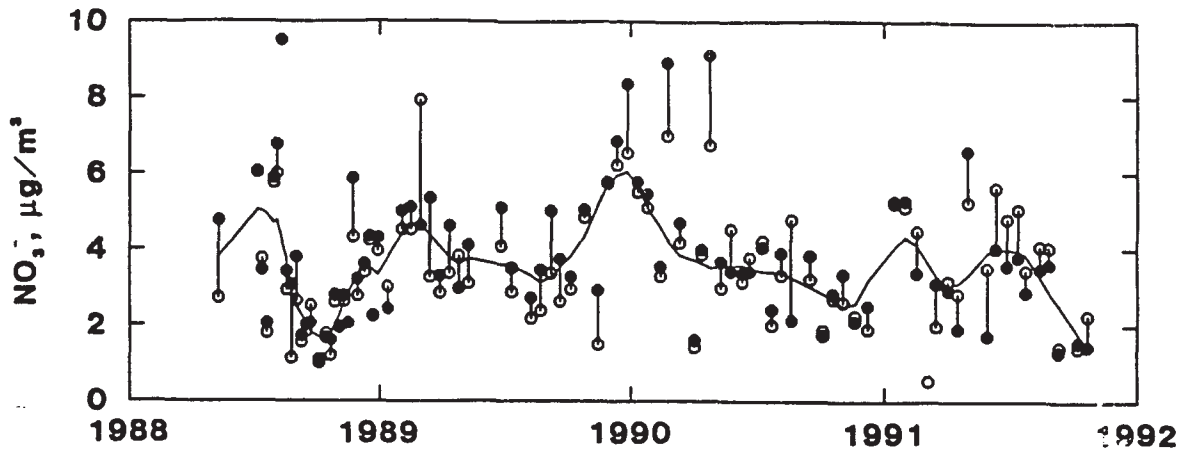


Figure 45. *NO_x concentrations from Spring 1988 to Fall 1991. Open circles indicate south side; closed circles indicate north side.*

been observed, although side by side operation of these sampling systems result in measured concentrations reproducible to about 5% (Dolske and Stensland, 1983). Thus, the observed differences are most likely explained by variation in pollutant exposure. The north column faces a pedestrian plaza approximately 300 m by 100 m, whereas the south column abuts Walnut Street, a busy thoroughfare and city bus route. Recently, buses have been permitted to idle on east side of the plaza, about 100 m from the north column sampling station. This may explain the increased tendency for the nitrate concentrations to be greater at the north sampling location in 1991 (Figure 45).

Pollutant Deposition and Accumulation on Marble Surfaces

The rates at which airborne pollutants are transferred to building surfaces by dry deposition are strongly affected by the presence of moisture, which enhances the rate of reaction of depositing chemicals. In trafficked urban locations, pollutant concentrations vary greatly during the course of a day. For example, an area of a building which remains wet when pollutant concentrations are higher would receive higher deposition than other part which dried prior to peaks in pollutant concentration. Over time, a far greater accumulation of deterioration accelerating pollutants could deposit in one area relative to another, perhaps only a few meters distant.

Washdown techniques provide a relative index of stone decay, based on the chemistry and porosity of the surface. Deionized water is used to rinse a defined area, removing accumulated soluble pollutant deposits. The architectural details of the Exchange provide two relatively similar, easily definable, concave areas on the vertical flutes of the coarse-grained column marble and on the lower foliage of the fine-grained Carrara capital. One column adjacent to each of the microclimate/pollution sensors was selected for bi-weekly or monthly collections during warm weather. The washdown locations were selected with reference to direct exposure to rain and differences in visible surface accumulation and discoloration.

Four faces or "exposures" at the two columns are sampled as shown in Appendix E. The protected face of the capitals are partially

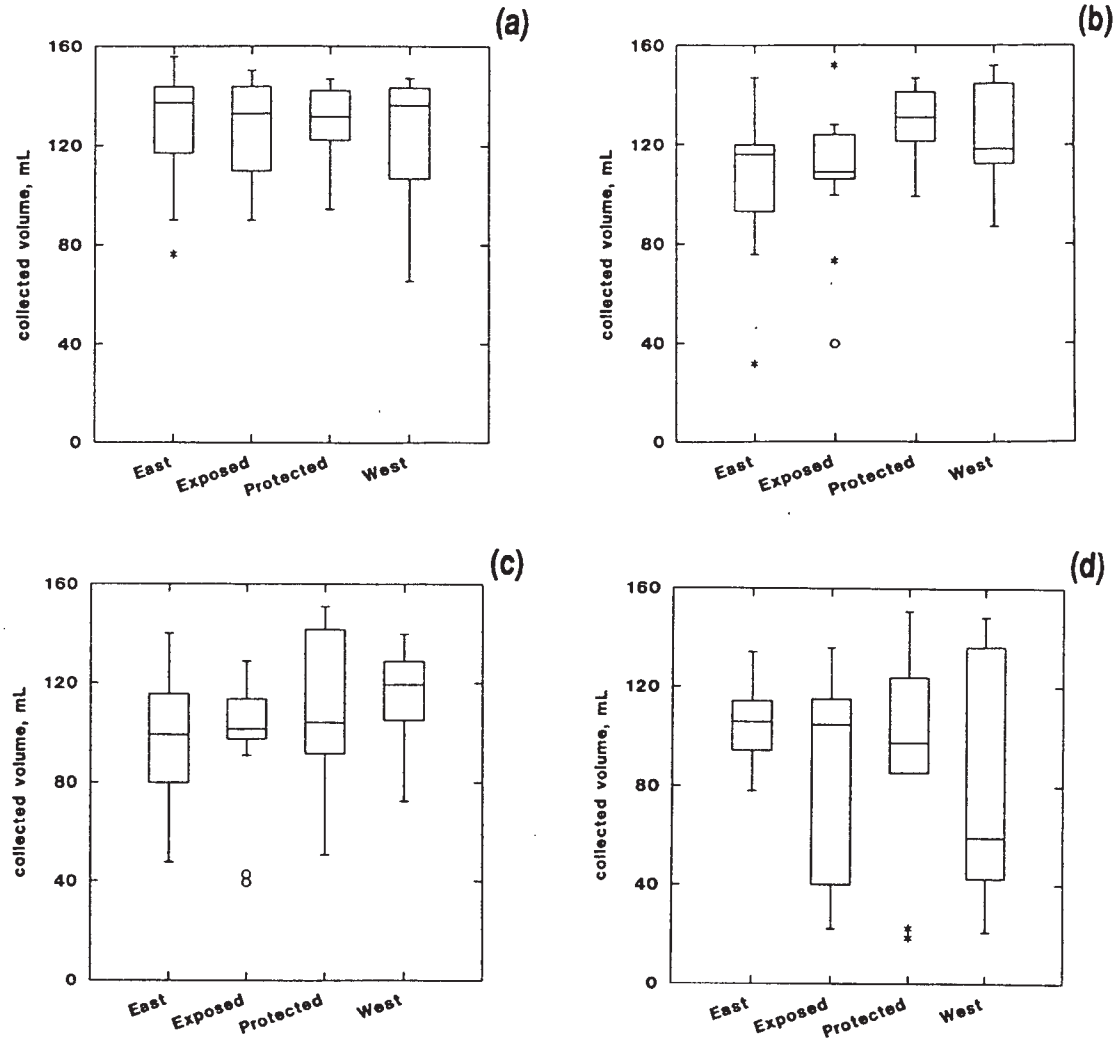


Figure 46. Volumes of solution recovered from the Exchange washdowns; a) North capital; b) South capital; c) North column; d) South column. Exposures are as indicated in Appendix F.

sheltered from rain by projections from the upper capital, while the exposed face of the columns are fully washed by rain. This distinction applies to a lesser degree to the east and west sample locations, where both columns and capitals can be partially exposed or sheltered by their position within the colonnade with respect to the incoming rain. The protected column and capital sample locations are both fully sheltered from rain.

To collect a washdown sample, a known volume (150 ml) of deionized water is used to flush the defined area of stone, approximately 100 cm^2. A narrow stream from a laboratory squeeze-wash bottle is applied for 60 seconds. The resulting runoff water is collected in a polyethylene and mylar funnel-and-bottle device, fitted with a flexible gasket at the stone-mylar junction to minimize loss of liquid. Washdown solutions are returned to the laboratory for ion chromatographic analyses of inorganic anions and cations.

	North Column Carrara	North Column Blue marble	South Column Carrara	South Column Blue marble
Sulfate in wash- down (median)				
protected, mg/L	22	18	32	16
exposed, mg/L	15	10	20	28
overall mean, 4 exposures, mg/L	19	14	26	22
predicted, mg/L	5.3	15.5	6.2	18.3

Table 3. *Sulfate concentrations in marble washdown solutions compared with estimates of sulfur flux to the Exchange marbles used in the Exchange.*

The volume of solution retrieved from the stone is a direct, if somewhat imprecise, measure of the porosity and to a certain extent, the integrity of the stone surface. If the surface is permeable, the washdown solution will be imbibed into the body of the stone. If the surface is dense, the water flows fairly efficiently over the 10 cm path and nearly all is retrieved. Volumes collected at the Exchange washdowns are shown in Figure 46. These data show a definite trend of decreasing volume returned with decreasing condition of the marble surface. Such data are perhaps useful to predict of the interaction between marble and consolidant (as well as an aid for estimating quantities of materials needed).

The chemistry of the washdown solutions indicate the relative accumulation of water-soluble pollutants at the various locations. The observed concentrations reflect both the amount of material deposited to the outermost layer and the relative solubility of the mineral salts into which the pollutants have been incorporated. Multiple collections at the same location show diminishing concentrations of sulfate and nitrate in the leachate, decreasing the nitrate value to 9% of the first washing, and the sulfate to 18% after 3 subsequent washings. This indicates that the technique removes some fraction of the soluble surface deposit, a fraction that cannot be determined at this time.

Table 3 presents average sulfate concentrations in the washdown solutions based on 14 collections for 16 different locations. The mean sulfate at all four exposures for both stone types at the south column is significantly greater than those observed at the north column, confirming the influence of the increased sulfur exposure on the street facade of the building. Further, sulfates are more concentrated in the Carrara leachate than in the comparable Pennsylvania marble solutions, except for the south exposed location.

The net sulfur flux to the fine grained Carrara marble is about one-third that to coarse-grained Pennsylvania blue marble. The sulfur flux estimates indicate that while deposition to wet marble is more efficient, the bulk of sulfur is deposited when marble is dry.

Table 3 also shows predicted washdown concentrations of sulfate in the washdown using the method described in Appendix E. A key simplifying assumption in the calculation is that the marble surface is washed by rain every five days, and that this washing removes all accumulated gypsum on the surface. The predicted sulfate values for the blue marble columns are within 20% of the observed

average overall, which is much closer than estimates for the Carrara marble capitals. The better agreement is explained in part because the simpler geometry of the columns is more similar to the obelisks from which the deposition velocities were derived than the capital geometry. More importantly, the columns are more fully washed by rain, fulfilling the assumption in the prediction algorithm that the surface is flushed clean by rain every five days. In contrast, sulfate leached from the Carrara marble is three to five times greater than predicted, with the largest underpredictions found for the protected sampling locations where sulfate readily accumulates. The difference between the predicted and observed sulfate concentrations for both marbles increases as the degree of protection from rain increases. In other words, the more the exposure situation deviates from the assumed situation, the less agreement there is between predicted and observed sulfate concentrations.

CONCLUSIONS

The air quality at the Exchange is typical of large American cities, with seasonal patterns, as well as week to week variability. There can be large differences in pollutant exposure at the two sides of the same building, as well. The West facade is consistently dryer than the East; within the East facade, the south side is wetter than the north. The pattern of rain volumes by direction appears to follow the marble erosion trend; the largest rains are from the east rather than the west, with the highest values in the southeast quadrant. While the rain is out of southwest less than 5% of the time, these rains are highly acidic, as are the rains from the north (12%). There is a seasonality to the stone surface wetness, and thus the deposition of sulfur pollutants. The largest differences between south and north occur in the autumn, while in the winter and spring, there is little difference. The relatively small increase in time of wetness (15%) on the south side of the building causes SO_2 deposition to wet marble be about 60% greater than to the north side. The sulfur flux calculations indicate that although deposition to wet marble is more efficient, under these exposure conditions, the bulk of the sulfur is deposited when the marble is dry. The net sulfur flux to Carrara marble is estimated to be about 30% of the flux to the Pennsylvania blue marble. Sulfate levels in leachate from the south column are greater than those observed for the north column, correlating with the measured increased time of wetness and exposure to atmospheric sulfur. The predicted values of sulfate in the Pennsylvania marble leachates fall within 20% of the observations for the overall average. In contrast, sulfate leached from the Carrara marble is three to five times greater than predicted, with the largest underpredictions found for the protected sampling locations, where sulfate readily accumulates.

ACKNOWLEDGMENTS

This research is conducted with support provided by the U.S. National Park Service, Cooperative Agreement CA 0424-6-8002, as part of the National Acid Precipitation Assessment Program. Laboratory support and additional analyses were provided by the Illinois State Water Survey Analytical Chemistry Unit. Special thanks are due to Bill Brookover and Frank Doyle at Independence National Historic Park for assistance in operating and maintaining the site. Raouf A. ElDeeb and Vic Mossotti of the U.S. Geological Survey contributed to marathon data-interpretation sessions that were very beneficial.

IMPLICATIONS OF BUILDING HISTORY, EXPOSURE, AND WEATHERING PATTERNS

Susan I. Sherwood

This is an introductory attempt to relate the historical and physical evidence to the current condition of the marbles, and to consider the implications of this evidence for the selection of conservation strategies. Preliminary information that speaks to particular conservation questions is presented to highlight the need for further discussion and interpretation. As is often the case, this draft interpretation will benefit significantly from review and discussions with co-authors, reviewers, and panel members. We expect this chapter to be substantially revised based on these additional insights.

CAUSE AND EFFECT RELATIONSHIPS

Table 4 outlines the broad range of effects and potential causes for the purpose of sparking discussion. Both qualitative and quantitative relationships can be developed in some cases; in others, descriptive observations can be ordered logically to describe the physical process. One approach is to classify observations by type of effect as discussed in Chapter 2 and 3. A second approach, the causal view, is presented in more detail below.

Observed Effect	**Relevant Architectural Elements**	**Possible Cause**
Patterns of erosion and increased permeability	Antefixes Dentils Column flutes Column bases Projecting moldings	Rain volume Perhaps rain sulfate Historical pollution Prior cleaning
Encrustation patterns	Black crust - capitals Black crust - columns Orange/light - walls Orange/light - columns	Solar radiation Wetness cycles Proximity to street Sulfur deposition Nitrogen concentration Particle concentration, especially carbon Historical pollution Prior cleaning/coating
Disaggregation	Loss of flutes/arrises Crumbling under black crusts Open ends of lost volutes	Moisture cycles Temperature cycles Penetration of acidic solutions Iron bands on columns - their installation, removal, patching
Cracking and spalling	Failure of volutes Chipping of carved relief Clutes, especially arrises	Moisture cycles Temperature cycles Removal of copper nets, Subsequent cleaning

Table 5. Relating marble decay at the Exchange to potential causes.

WEATHERING COMPARED TO EXPOSURE

Protected versus Sheltered

Within the context of a given facade, rain-washed versus rain-sheltered is an important distinction. By definition the volume of rain is much greater and thus the erosion is dramatically greater.

Rain washed areas have a much larger view of the sky, and more significant solar radiation input. The wetness cycles on fully exposed locations are longer because of the greater moisture input from rain and dew offset the increased evaporation rates at the outer surfaces. Protected locations are wet more frequently in the afternoons, and probably undergo fewer cycles of wet/dry and temperature extremes, although these factors have not been measured at the Exchange.

Sulfur deposition accumulates in protected areas, resulting in buildup of gypsum crusts. Washdown data demonstrate that, except for the Pennsylvania marble on the south side, twice as much sulfate can be leached from protected as from exposed locations. Figure 47 maps the encrustation at second floor level on the inside of east portico columns. Heavy black lines indicate black accumulation; dotted lines orange accumulation. The pattern of encrustation reflects the degree of rain sheltering for each column. Fewer flutes on the inside of east facing Columns 12 and 13 are encrusted than on Columns 9 and 16 at the ends of the colonnade, which are more rain sheltered. The specific location of crust rotates slightly around the columns, reflecting differences in exposure to rain and wind.

A few samples were taken of column crusts for composition analysis as shown in the pie charts in Figure 47. The light crusts on the inside of a northern column range from 5 to 50% gypsum, both contain fluorite like the neighboring walls. Two samples of black crusts on the inside of southern columns both contained 40% gypsum, while the calcite content ranged from 5 to 50%. Quartz was found in all but one of the crusts, but no pattern has been found. A more extensive crust sampling program is planned for the fall to develop a larger data set for interpretation of quartz occurences.

East versus West

The broadest comparison is between the west and east facade. The west experiences less rain volume, but that rain contains more acid. Historical information indicates that the Exchange is located within the densest concentration of emissions in the 1890s in the city. The relative pollution exposure is unclear because the information is incomplete. Current estimates (excluding train emissions) indicate that the west may have received more pollution in the 1890s than the east. The location of train tracks in the present Dock Street pedestrian plaza at the turn of the century, however, argues for greater particle and sulfur deposition to the east facade. In the absence of detailed microclimate measurements on the west, it is impossible to compare thermal cycles; the short-term survey indicated that the west is consistently dryer than the east.

The ground floor of both facades contain a fair amount of replacement material from various eras, so that except for the one-story columns, an exposure comparison is not valid. Above the ground floor, it is fairly well documented that the west facade has received less preservation maintenance over the life of the building, in part because of the inaccessibility of the west columns and walls, and in part because the changes in the cupola triggered more work on the east.

The east to west comparison shows the greatest difference in condition of the second story columns and capitals. There is minimal erosion on the west in contrast to centimeters of loss on the east. While crusts are present

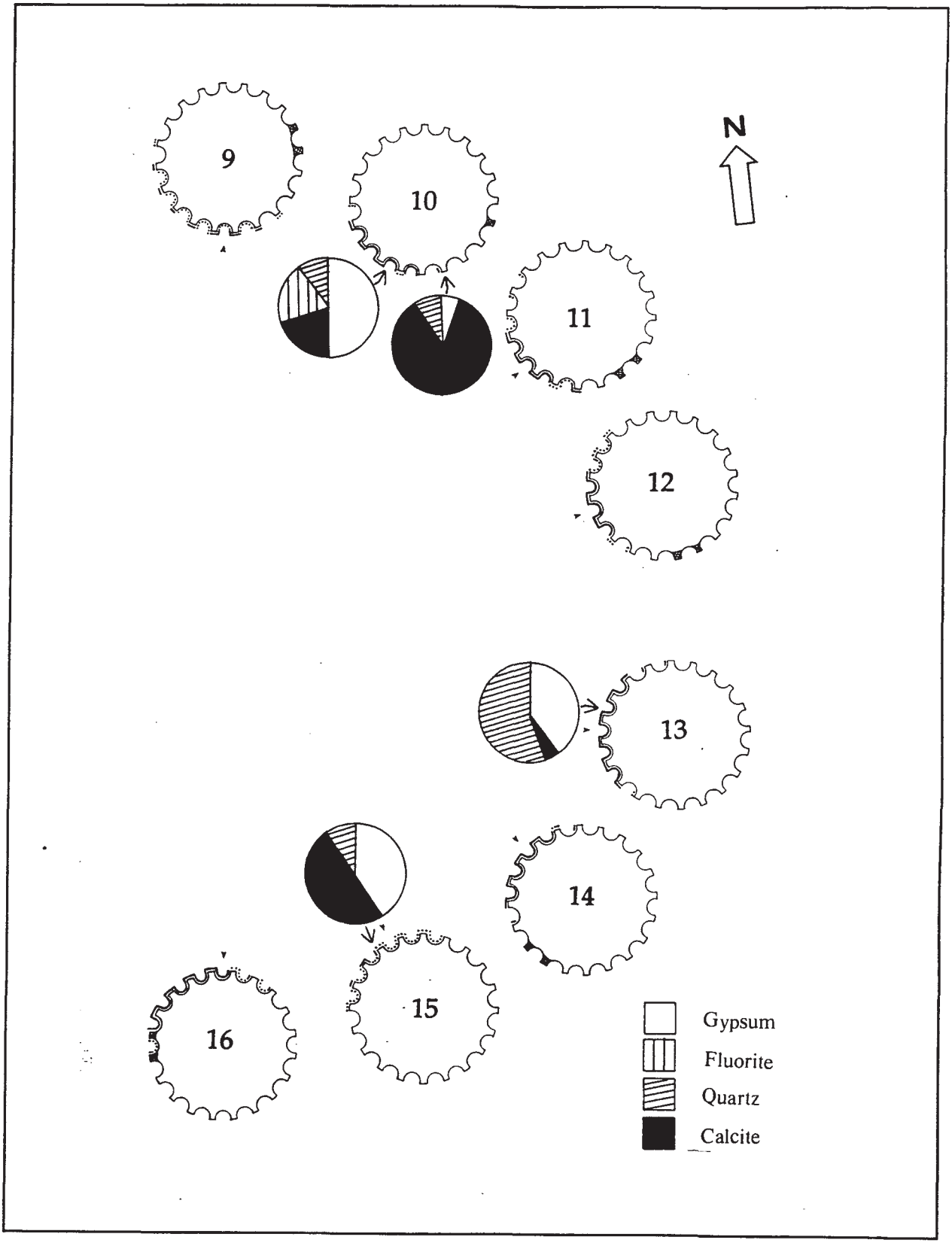


Figure 47. Encrustation on columns; distribution and composition.

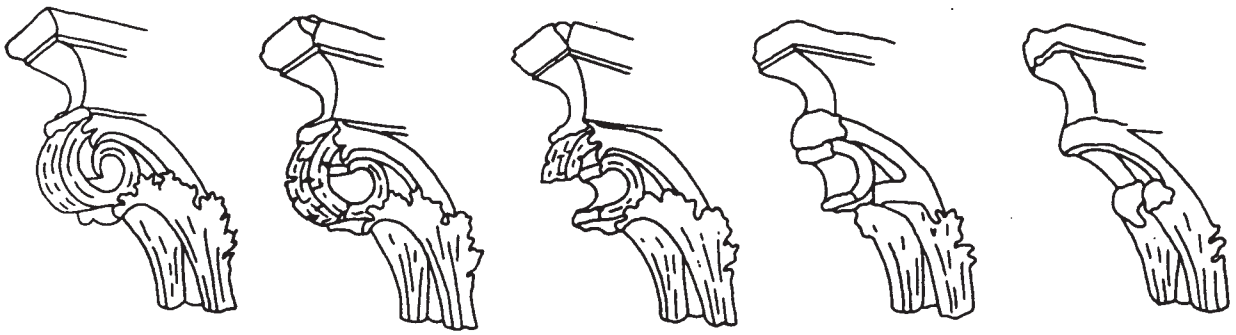


Figure 48. Progression of volute failure - cracking - radical loss - erosion.

on both facades, the buildup appears to be greater on the east. Marble on the east is very friable; similar observations are not available for the west. Cracking of volutes is more prevalent on the east. A schematic view of the progressive deterioration (cracking - radical loss - erosion) of the volutes in found in Figure 48. The drawing is based on observations of differing states of preservation of the extant capitals.

North versus South

One can compare the role of orientation at the north and south sides of the east portico. The north receives less direct rainfall of similar acidity than the south. Thermal and moisture cycles are more extreme and of longer duration on the south. The vehicle pollution is heaviest at the south side, although there may be a shift towards relatively more similar NO_x exposures since the change in city bus routes in 1991. The sulfur deposition is greater on the south because the surface is wet more frequently at this location. Historically, pollution levels are likely to have been greater on the north, because of the train traffic. Particles do not travel very far; the concentrations are an inverse square of the distance, as a rule of thumb. There appears to be no difference in treatment history for the various locations within the east facade, except for the possible indication of acid cleaning tests described below.

The contrast in condition between north and south is much less pronounced than between east and west. However, there seems to be a progression of increasing erosion (as estimated by dentils and exterior volute volume and flute loss measured photogrammetrically) as one moves from north to south. This may relate directly to the relatively greater volume of rain water that is delivered and/or to the increased sulfur deposition, which enhances the erosion through a gypsum intermediate.

Differences in surface encrustations are apparent in both quantity and composition. A preliminary survey (Figure 49, Appendix A) of light-colored crusts on the back walls of the east portico indicate a doubling of calcite content from northeasterly (20%) to north facing (40%), and a more dramatic decrease on south facing exposures (10 to 25%). The stippled wall sections were not encrusted at the second floor level. Enriched gypsum levels generally parallel depleted calcite content, except for the northern half of the portico. In these locations, 15 to 20% fluorite was found, which may indicate that this area was used as a test patch for cleaning with hydrofluoric acid which was not carried out.

Further, the north and south undergo very different thermal cycling. Figure 50 plots monthly averages of the temperature excursions for the outside of the north and south columns. The summer months are very similar, with the marble temperature crossing 30°C (black bar) about 40 to 50 times/month. The freezing cycles (white bar) are nearly identical between the two locations, except for December when the south freezes about 10 times more often. Between November and March the south column cycles through 10°C (hatched bar) at least twice as often as on the north. The significant difference between the north and south temperature cycles occurs in the fall, when the north side cycles between 20° C and 30°C once a day and the south side at least twice. The temperature cycles on the west facade have not been measured.

The temperature cycling may enhance the cracking and initial spalling of the fine-grained marble volutes. Calcite crystals deform when heated (Bloss, 1971), which tends to disrupt the interlocking mineral matrix, and can result in disaggregation. Crystalline marbles tend to suffer loss of strength as a result of temperature cycling; however a critical temperature threshold has not been established (Rosenholtz and Smith (1949), Skinner (1966), Biscontin (1966), Koehler (1988), Sage (1988)).

ADDITIONAL INFORMATION NEEDS

This attempt at synthesizing the physical and historical evidence indicates the need for additional information. The following is a preliminary list of additional studies that would address some of the unknowns and unresolved issues relative to the definition of an appropriate marble treatment strategy.

Examination of Stereopairs

Analysis of the upper capital photographs to evaluate the stability of remaining volutes, degree of surface cracking, (and perhaps to infer friability) would also help understand progression of the decay, and thus the causative factors. Analysis of the more distant facade views could provide insight into decay of more features, although with the associated decrease in resolution. Additionally, the remaining lower capital and antefix views could be interpreted as originally planned to provide a better measures of decay, as well as a more complete mapping of erosion roses.

Ultrasound Measurements of Carrara and Pennsylvania

Ultrasound can be used to evaluate the friability of the marble, particularly Carrara, and thus the need for stabilization. Further, this technique can provide some clues to the ability to endure cleaning, patching, repair. Similar methods can be used to evaluate the permeability of the Pennsylvania marble to determine the need for stabilization treatment.

West facade

Measuring microclimate ranges and evaluating permeability and friability of marble would provide a "control" for comparison with the east facade. Data from the west facade have the potential for being particularly useful in developing an understanding the role of thermal cycling in disaggregation and cracking of crystalline marble.

East Facade

Additional surveys of crust composition, and depth of erosion would help to understand how much protection is afforded by varying types of projection.

Measurement of Vehicle Emissions

Measurement of carbon and crustal particles, and other components of vehicle emissions can be used to assess soiling rate, as well as to identify the type of soiling and its

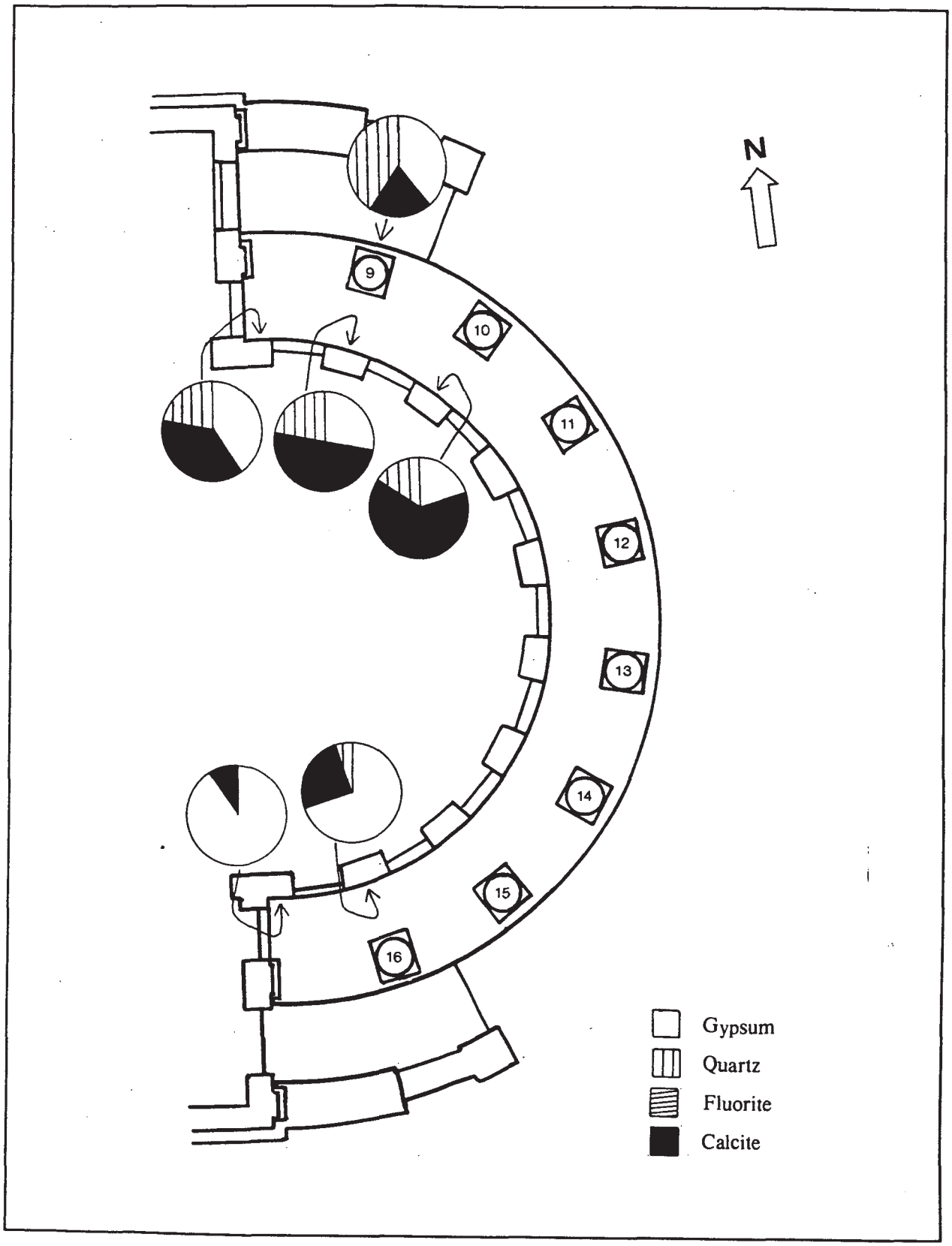


Figure 49. Composition of crusts on east portico walls.

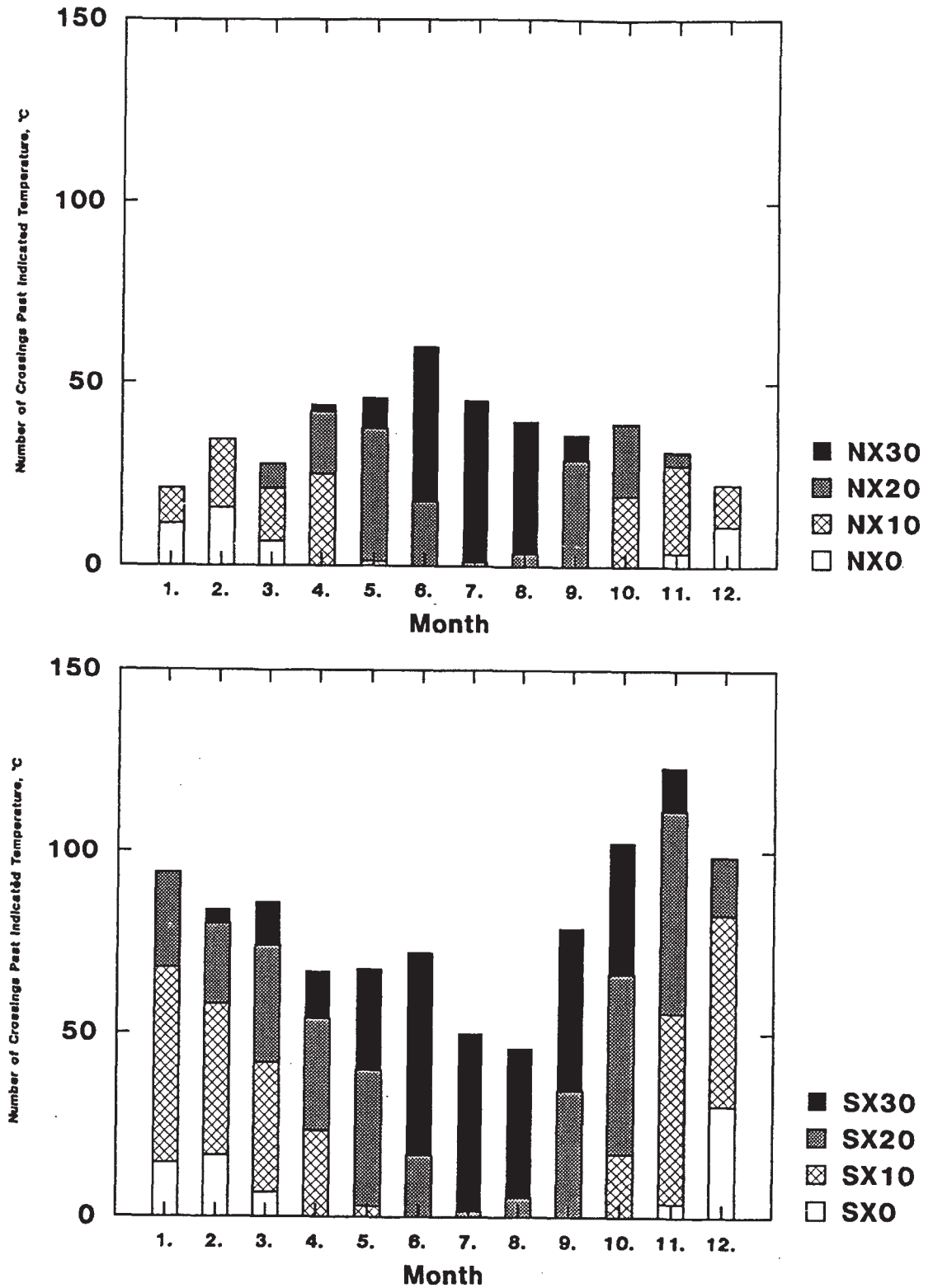


Figure 50. Monthly averages of temperature excursions; a) north; b) south.

susceptibility to cleaning. Further, such measurements can identify the relative contribution for various types of vehicles and zones of emissions.

IMPLICATIONS FOR STONE CONSERVATION

In marble conservation as in life, several forces pull in opposite directions, introducing multiple dilemmas into the decision-making process. A brief outline of the weathering considerations that impact the conservation treatment decisions is presented for discussion and expansion.

One of the dilemmas of consolidation is the desirability to begin with a clean surface. In the case of the Exchange marbles, cleaning would probably remove much of the original surface, and with it the carved features of interest, further exposing disaggregated, friable material directly to weathering agents.

Generally, permeable stone is rougher than dense stone, which increases the soiling rate, and thus the desire for more frequent cleaning. Weak stone will not tolerate cleaning as well, thus decreasing probability of a successful soil removal.

As the friability and permeability of the stone increases, the need for stabilization increases. At the same time, the probability of effective consolidant penetration into the stone increases and the probability of effective mechanical repair of the stone matrix decreases.

On the other hand, the presence of a gypsum crust cuts down on the ability for consolidants to penetrate. Further, the crust may contain contaminants that might interfere with polymerization of some consolidants. In addition, as the crust increases in thickness, the friability of the stone beneath is probably greater, indicating a more serious need for stabilization.

ACKNOWLEDGEMENTS

Thanks are due to the co-authors who all have contributed ideas over the course of the project, and specifically to E. McGee for the data in Figures 47 and 49, D. Dolske for Figure 50, and A. Andersen for Figure 48.

Conservation Treatment Options

This section presents a summary of discussions held May 22, 1992, at Independence NHP. The group included architects, engineers, architectural conservators, conservation scientists, and NPS park and regional officials. It is intended that this issues raised be addressed in greater detail over the course of the next year, including acquiring input from preservation professionals at the 1992 APT conference. The discussions highlights and recommendations from the May meeting are grouped into five general categories, without reference to relative importance or priorities, as follows:

- Additional Documentation
- Further Monitoring
- Treatment Options
- Further Management Actions
- Other Buildings in INHP

Additional Documentation

1. Survey and record the extent and variety of cracks on the exterior stonework; in capitals, columns and the walls.

2. Photograph each column capital from all four sides.

3. Survey wetting patterns during rain storms for comparison with marble erosion data.

4. Interview Joe Petrak about previous treatments to the Second Bank of the United States and the Exchange, particularly about the cleaning tests with hydrofluoric acid.

5. Interview Hank Judd about the Decosit treatment on the Exchange.

6. Replicate the 1960s HABS photographs to identify recent stone failure.

7. Consider other options for stereophotogrammetric monitoring, including the HABS system (German), the Danish system, and using film negatives instead of glass plates.

8. Take new photogrammetric stereopairs at 10 year intervals.

Suggestions made by Lee Nelson, former Historical Architect, INHP, and former Chief, Preservation Assistance Division, WASO:

9. Remove the best preserved capital to serve as a record of the carving methods and the form. Exhibit the capital in the park.

10. Make full size casts of a capital and the marble lions for possible future replication.

Further Monitoring

1. Monitor the epoxy repair made to the capital of Column 10; check for shifting, staining, appearance or growth of cracks; install a tell-tale or strain gauge to record movement.

2. Continue with the environmental monitoring; add a third station for the west facade. Duplicate the sensors for error control and calibration.

3. Monitor carbon, other particles, and marble soiling on the west, southeast, and perhaps northeast facades at $5-10,000/yr/station.

4. Place the environmental monitoring at the Exchange in the context of results from the city and State monitoring networks.

Treatment Options

Treatment Testing:

1. Devise a testing program which will evaluate the effectiveness and impact of proposed cleaning and consolidant treatments. Any proposed treatments should be subject to peer review before the implementation.

2. Further tests should be carried out to determine the relative importance of the mineralogy and petrography in the weathering process. Small cores (1/8" diam) may be taken for analysis of the depth of the gypsum alteration crusts, grain size distribution, and mineralogy.

Cleaning:

1. Conduct preliminary tests to determine whether a single method will successfully remove both the soiling and the gypsum crusts from both the Carrara and the Pennsylvania marbles. Candidate cleaning options include nebulized water, water washing, and poulticing with AB57. Microabrasion and pelletized CO_2 are candidates for removal of the surface soiling, but may not be effective for gypsum removal. Chemical cleaning methods were not recommended as candidates because of VOC (volatile organic compound) regulations.

2. Consider limited spot cleaning to remove soiling and gypsum crusts on the ground floor columns along the south facade.

Consolidation:

1. Test consolidants on Pennsylvania marble, tests shall include compressive strength, abrasion resistance, vapor permeability, color change, and reactivity with SO_2. Sufficient test data is already available for most treatments on Carrara marble substrates, except for SO_2 reactivity.

2. Consider the limewater method as a candidate surface treatment/consolidant.

3. Concerns about the use of chemical consolidants include: short lifespan, color change, lack of data on the long-term performance of new generation materials, and the potential for retreatment after exposure. Selective use of a consolidant may be necessary and is preferred to an overall application.

Replacement and Repairs:

1. Stockpile Pennsylvania marble from available sources including salvage and demolition companies. Store the stone in a covered area on pallets, possibly at Valley Forge NMP.

2. If a capital is removed for reference and exhibition, consider replacement with new stone. Consider the selection of the replacement material as a test for potential replacements of other capitals.

3. Consider partial replacement of decorative elements only (attached to the original central drum), if the upper capitals are deemed unsafe.

4. Consider spot repairs such as pinning and filling cracks and voids in the columns and capitals to limit access by rain and snow.

Further Management Actions

1. Negotiate reduction or elimination of bus traffic and idling time on Walnut and Third Streets with SEPTA.

2. Conduct cost comparisons and value analysis on the treatment options to aid in the decision making process.

3. Produce a five-year preservation management plan which will include planning for the next phase of study and

treatment testing. The plan should address management options, the budget and personnel resources required for each of the options, and a set of criteria for evaluating in-house vs. contract work. The scope of the plan should include further documentation and monitoring, testing for cleaning and consolidation, spot repairs and limited consolidation as may be appropriate, the removal of a capital for documentation, and consideration of a potential stone replacement program.

Other Buildings in INHP

1. Photogrammetrically record the Second Bank of the United States, Congress Hall, and Old City Hall. Make multiple sets of glass plate negatives for the Library of Congress and other archives.

2. Visually monitor the epoxy consolidant treatment on the First Bank for color changes, stickiness, spalling, and soiling. Take core samples to test the characteristics of the treated material after 10+ years exposure.

3. Carry out a condition survey of the Second Bank noting cracks, alteration crusts, and potential structural problems in the columns. Conduct strain testing of the major cracks.

4. Evaluate the performance of the fiberglass replacement architectural elements in the Park (including portions of the Exchange tower), including physical and visual characteristics.

REFERENCES

Amoroso, G. and Fassina, V., 1983, Materials Science Monographs, No. 11, *Stone Decay and Conservation*, Elsevier, New York, 453p.

Bascom, F., Clark, W.B., Darton, N.H., Dummel, H.B., Salisbury, R.D., Miller, B.L., and Knapp, G.N., 1909, *Description of the Philadelphia area, Pennsylvania-New Jersey-Delaware*. Geologic Atlas of the United States, Philadelphia Folio No. 162, U.S. Geologic Survey, 35p.

Biscontin, G., L. Marchesini, S. Frascati, 1972, L'alteration dans les marbres saccharoidaux. In: *Proceedings of the First International Symposium on the Deterioration of Building Stones*, La Rochell, France, pp. 193-199.

Bloss, 1971, *Handbook of Crystallography*.

Burnham, S.M., 1883, *History and Uses of Limestones and Marbles*, S.E. Cassino and Company, Boston, 392p.

Camuffo, D., M. Del Monte, C. Sabbioni, and O. Vittori, 1982. Wetting, deterioration, and visual features of stone surfaces in an urban area. Atmos. Environ., 16, 2253-2259.

Census, 1884, *Report on The Building Stones of the United States, and Statistics of the Quarry Industry for 1880*, 410p.

Cleveland, W.S., 1979. Robust locally weighted regression and smoothing scatterplots. J. Amer. Stat. Assoc., 74, 829-836.

Cleveland, W.S., 1981. LOWESS: A program for smoothing scatterplots by robust locally weighted regression. The Amer. Statistician, 35, 54.

Dale, T.N., 1912, *The Commercial Marbles of Western Vermont*, U.S. Geological Survey Bulletin 521, 170p.

Dean, Nancy E., 1988, Geochemistry and Archaeological Geology of the Carrara Marble, Carrara, Italy, in: N. Herz and M. Waelkens (eds.), *Classical Marble: Geochemistry, Technology, Trade*, Kluwer Academic Publishers, p. 315-323.

Dolske, D. A., 1987. Preliminary Data Summary: Philadelphia Merchant's Exchange Surface Moisture Study. U.S. National Park Service / Preservation Assistance Division, Washington, DC. 18p.

Dugan, C.J. and D.A. Dolske, 1992: A Twelve-year study of precipitation chemistry at the Air Mangement Services Laboratory in Philadelphia, Pennsylvania. *APT Bulletin*, in press.

Fairmount Park Art Association, 1974, *Sculpture of a City: Philadelphia's Treasures in Bronze and Stone*. Walker Publishing Company, Inc., p. 60.

Gilchrist, A., 1953, The Philadelphia Exchange: William Strickland, Architect. Transactions of the American Philosophical Society, Vol. 43, pp. 86-95.

Julian, Alexis, A., 1884, The Durability of Building Stones in New York City and Vicinity, in: Census, 1884, *Report on The Building Stones of the United States, and Statistics of the Quarry Industry for 1880*, p. 364-393.

Kohler, W., 1988, Preservation Problems of Carrara Marble Sculptures Potsdam-San Souci ("Radical Structural Destruction" of Carrara Marble, In Proceedings of the VIth International Congress on Deterioration and Conservation of Stone, Torun, Poland, pp. 653-662.

McGee, Elaine S. and Mossotti, Victor G., 1992, Gypsum Accumulation on Carbonate Stone, Atmospheric Environment B, (in press).

McGee, E.S., 1989. Deterioration of limestone and marble buildings in urban exposures. In *Make no little plans: A handbook of abstracts for the 1989 conference of Association for Preservation Technology International*. APT, Chicago, IL. p163.

McLain, D.H. 1974. Drawing contours from arbitrary data points. The Computer J., 17, 318-324.

Merrill, George P., 1889, *The Collection of Building and Ornamental Stones in the U.S. National Museum: A Handbook and Catalogue, from: Report of the Smithsonian Institution, 1885-86, Part II*, p. 277-648.

Miller, Benjamin, L., 1934, *Limestones of Pennsylvania*, Pennsylvania Geological Survey, Fourth Series, Bulletin M 20, 729p.

National Park Service Weekly Field Reports - Eastern Office of Design and Construction, 1963-65, Archives of Independence National Historical Park.

Oehrlein and Associates, 1988. Contract Report to U.S. National Park Service: PX-0001-3-0894, "Estimates of the relative deterioration rates of imported and American marble".

Petrak, J., 1963; Historic Structures Report Part II Supplement I, Architectural Data Section, Restoration and Reconstruction on Merchants' Exchange. Independence National Historical Park, Philadelphia, November 1963.

Rosenholtz, J. L., and D. T. Smith, 1949, Linear thermal expanison of calcite, var. Iceland spar, and Yule marble. *The American Mineralogist*, 34, pp. 846-854.

Sage, J. D., 1988. Thermal microfracturing of marble. In: *The Engineering Geology of Ancient Works, Monuments and Historical Sites, Balkema, Rotterdam*, pp. 1013-1018.

Sherwood, S.I., D.F. Gatz, R.P. Hosker, Jr., C.I.Davidson, B.B. Hicks, R. Linzey, E.S. McGee, R.L. Schmiermund, D.A.Dolske, D.Langmuir, F.W. Lipfert, V.G. Mossotti, and E.C. Spiker, 1990. *State of Science & Technology, Report No. 20: Processes of deposition to structures*. National Acid Precipitation Assessment Program, Washington DC, 145p.

Simon, G., 1961, Report on the Preservation of the Exterior Masonry of the Buildings Forming a Part of the Independence National Historic Park in Philadelphia with Particular Reference to the First Bank, the Second Bank, and the Merchants' Exchange. Philadelphia.

Skinner, B. J., 1966, Thermal Expansion, In: *Handbook of Physical Constants*, Geol. Soc. America Memoir 97, 75-96.

Spiker, E.C., R.P Hosker, Jr., S.I. Sherwood, and V.J. Comer, 1990. Abstract. Chamber study of SO_2 deposition to stone. In: Int'l Conf. on Acidic Deposition: Its Nature and Impacts, 16-21 Sept., 1990, Glasgow, Scotland.

Stone, Ralph, W., 1932, *Building Stones of Pennsylvania*, Pennsylvania Geological Survey, Fourth Series, Bulletin M 15, 316p.

Webster, R., 1976, Philadelphia Exchange Company (Merchants' Exchange). *Philadelphia: Three Centuries of American Art*. Philadelphia Museum of Art, Philadelphia, pp. 290-291.

Winkler, Erhardt, M., 1975, *Stone: Properties, Durability in Man's Environment*. Second Edition. Springer-Verlag, New York, 230p.

APPENDIX A: X-ray and Scanning Electron Microscopic Study of Alteration Crusts

Elaine S. McGee and Mary E. Woodruff

We have begun a systematic examination sampling and analyzing the alteration crusts on the east facade of the Exchange. Although samples of alteration crusts have previously been collected and examined with scanning electron microscopy, there was not enough material available from those samples to perform X-ray diffraction analysis. We also sought to systematically observe both the distribution and characteristics of the various crusts around the facade, in order to document characteristics that might reflect exposure of the stone, or the nature of the crusts.

Samples were collected by scraping a small amount of the crust with a knife blade. Six samples of light colored crusts were collected from the east facade portico wall, and four samples were collected from column shafts on the east facade; locations of the samples are described in Table B-1, and shown in Figures 47 and 49. We described the appearance of the crust on the building, observed characteristics of the crust during the sampling (eg. how soft, how tightly adhered to the underlying stone), and the appearance of the resulting (powder) sample. A small portion of each sample was reserved for SEM examination and the remainder was ground in an agate mortar with acetone and mounted for powder X-ray diffraction. Major and minor peaks on the X-ray diffraction patterns were identified and visual estimates were made of the proportion of each mineral phase in the sample. Portions of each sample were examined using the scanning electron microscope to see how the mineral phases, that were detected with X-ray diffraction, occur in the sample.

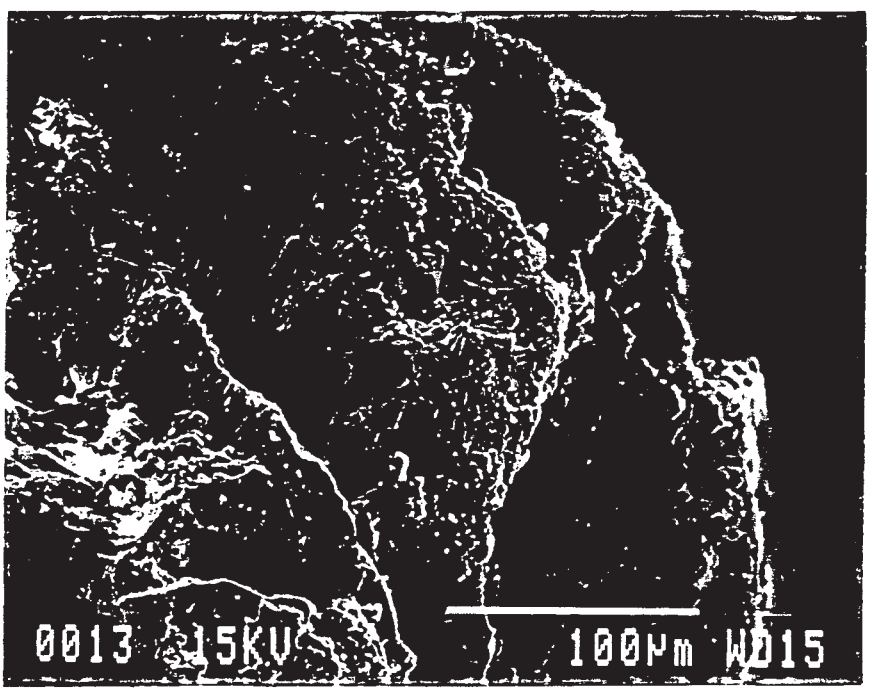


Figure A-1. *Scanning electron micrograph (SEM) of alteration crust sample 4/5. Gypsum crystals cover only a small portion of a calcite grain from the underlying marble; this relative proportion is reflected in the estimated abundance of these phases from the X-ray diffraction pattern.*

Using the SEM we are able to see many of the phases that are present in the sample, but it does not give us an adequate representation of the abundance of the phases. X-ray diffraction will detect phases with a crystalline structure that constitute at least 10% of the sample. Results of our observations, X-ray diffraction analysis, and scanning microscopic observations are summarized in Table B-1. Estimated proportions of the phases in the wall crusts are shown in Figure 49, and the proportions for the column crusts are shown in Figure 47.

The crusts consist of calcite, gypsum, fluorite, and quartz. The main constituent of the crusts is either calcite or gypsum. In some cases we suspect that part of the calcite that was detected is part of the underlying marble that came off when the alteration crust was sampled. The SEM images substantiated this explanation, and our estimates of the relative proportions of calcite and gypsum, such as with sample 4, where grains of calcite have thin crusts of gypsum crystals (Figure B-1).

Quartz is an accessory phase, present mainly in the black alteration crusts and seen in the SEM as individual grains sitting in the network of gypsum crystals (Figure B-2).

The presence of fluorite was a surprise, in part because it is not detectable with our present SEM X-ray analytical system, and in part because it seemed at first to be an unlikely alteration phase. However, the Historic Structures Report (Petrak 1963) recommended cleaning the stone with fluoride and water solution. Although we are not sure that the building was cleaned, some testing may have been done. The distribution and abundance of fluoride in our samples (Figure 47) suggests that treatment may have been concentrated in the north facing section of the east facade.

Our sampling and analysis of the light colored crusts around the east facade seems to be a good representation of the alteration crusts on the partially sheltered wall of the portico. There are no black alteration crusts on the wall, and our observations of the distribution

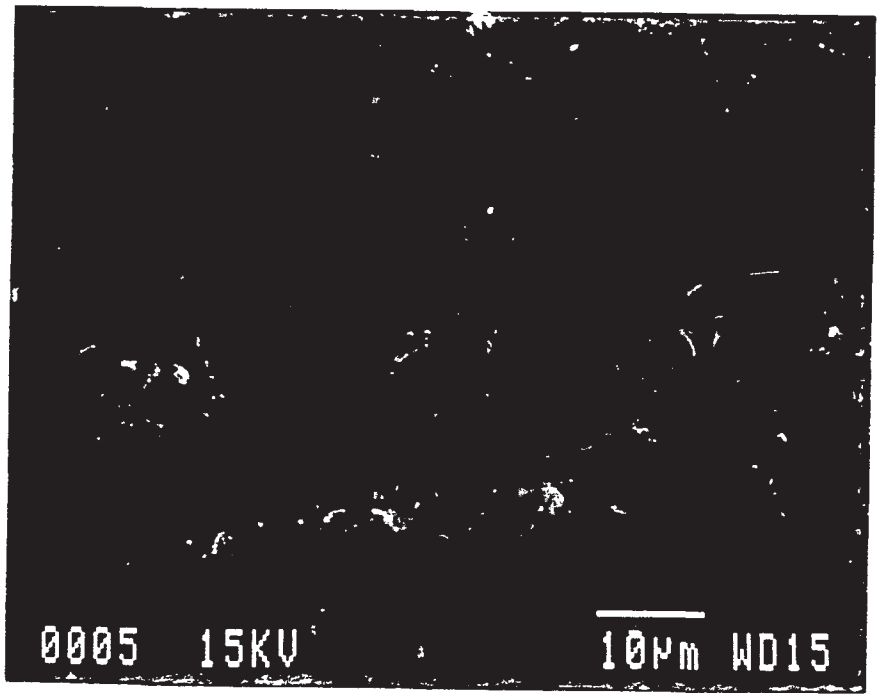


Figure A-2. SEM micrograph of a typical quartz particle in an alteration crust sample.

Sample	Location	Description	Phases
MXc10-A	Column capital	Black crust and underlying material	Gypsum 25% Calcite 65% Quartz 10%
MX210-1	Corner, across from Col. 8, 4 blks. from floor, east facade, north side	Orange wall crust, fine, white soft powder	Gypsum 40% Calcite 40% Fluorite 20%
MX210-2	Wall adjacent to Col. 9, 3rd block from floor	Yellow surface crust, very fine powder, texture like MX210-4, i.e., lacy, open network	Gypsum 30% Calcite 50% Fluorite 20%
MX210-3	Col. 10, inside flute, 4.5' from floor	Yellow crust, difficult to scrape, like MX210-1 in texture	Gypsum 50% Calcite 20% Fluorite 20% Quartz 10%
MX210-4	Col. 10, two "troughs" to right of MX210-3	Yellow crust, texture like sample MX210-2	Gypsum 5% Calcite 85% Fluorite 10%
MX210-5	Wall behind Col. 10, 4th block up, NE side of bldg.	Yellow crust, texture open, network like MX210-2	Gypsum 20% Calcite 65% Fluorite 15%
MX210-6	From wall behind Col. 16, 3rd block up SE side of bldg.	White crust, hard to remove	Gypsum 70% Calcite 25% Fluorite 5%
MX210-7	Corner, adjacent to Col. 16, 4 blks. from floor, east facade, south side	Yellow-orange wall crust, white underneath; hard to remove fine powder	Gypsum 90% Calcite 10%
MX210-8	Col. 15, SE side of bldg., inner ridge Flute, facing wall	Black crust, spalls off not sugary	Gypsum 40% Calcite 50% Quartz 10%
MX210-9	Col. 13, SE side of bldg., inner ridge	Black crust, spalls off	Gypsum 8% Calcite 90% Quartz 2%
		Black, scraped from surface sample	Gypsum 40% Calcite 5% Quartz 55%
MX210-10	Outside wall by steps under railing, NE side		Gypsum 40% Calcite 20% Fluorite 40%

Table A-1. Summary of the Exchange alteration crust samples.

of the light crusts look as though they fit in well with the environmental monitoring that has been done at the Exchange (Chapter 4). We have not yet done a systematic enough sampling of the column alteration crusts to interpret either their distribution or their composition. In part, the column shafts present a more complex exposure situation than the walls and that complexity is reflected in the significant variations of the few samples that we have collected and analyzed so far.

In addition to further sampling of the east facade column crusts, we plan to expand our sampling and analysis in two more areas: the second level portico on the west facade and the south west corner at ground level. Sampling along the west facade portico would give us a direct comparison with some of the areas and features that we have sampled on the east facade. By sampling the southwest corner of the building, particularly at different heights above ground level, we may be able to identify the area that has been most impacted by the corner's proximity to traffic. This combined sampling, X-ray, and SEM analytical approach will help increase our understanding of the nature and distribution of alteration crusts at the Exchange, and may provide a basis for selecting appropriate cleaning techniques.

Appendix B: Photogrammetric Project Methodology

Anett Andersen, Victor G. Mossotti, A. Raouf Eldeeb, Mary Oehrlein, Bob Ryan

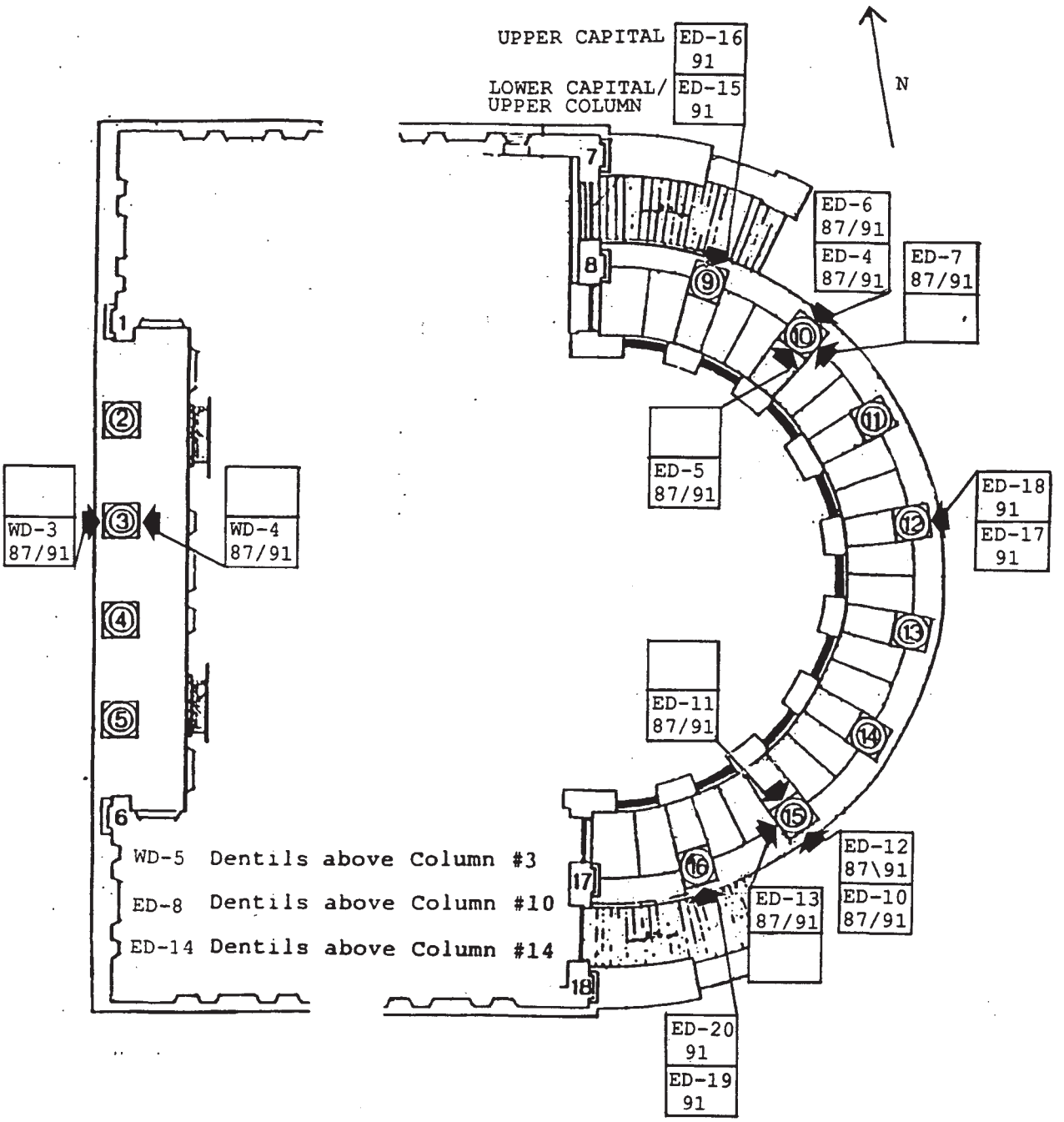


Figure B-1. *Location of the stereoimagery from 1987 and 1991. The codes in the labels indicate the identifier for the stereoimagery.*

Photogrammetric Control Points - Sapphire Microbenchmarks

In September 1987 and July 1991, synthetic sapphire studs were set into the stone of the Exchange to serve as permanent targets. The sapphire rod, produced by Saphikon, 51 Powers Street, Milford, NH 03055, was chosen because they are inert to reactions with the environment, and are dimensionally stable. The sapphire studs placed in 1987 measured .110 inches, or 2.8 mm, in diameter and .50 inches long. The adhesive used was Duro Quick Gel manufactured by Loctite Corporation. The targets were installed by partially filling the drilled hole with adhesive, inserting the rod until it was positioned 1/8 inch above the stone surface and the adhesive appeared at the face of the hole. If adhesive did not appear at the face of the hole when the target was in position, the target was removed and additional adhesive placed in the hole. The target was held until it was securely positioned in the center of the drilled hole and at the desired distance from the surface of the stone. Excess adhesive was cleaned from the face of the stone. In 1987, 51 targets were placed in column shafts and Capitals 3, 10, 15, and on the dentils above Columns 3, 10, 14, and also on two antefixae. An additional 89 targets were placed in 1991, in Columns 9, 12, and 16, as well as additional targets being placed on Columns 3, 10, 15 and on the dentils above Column 14 (Figure B-2). The studs set in 1991 were .110 inches, or 2.8mm, in diameter and 1 inch long. The targets were placed in holes 1/8 inch in diameter and 1/2 inch deep, using the same type of adhesive. The studs were installed using the same procedure used in 1987, although the targets were set approximately 1/2 inch above the surface of the surrounding stone to increase the control in the depth or dimension.

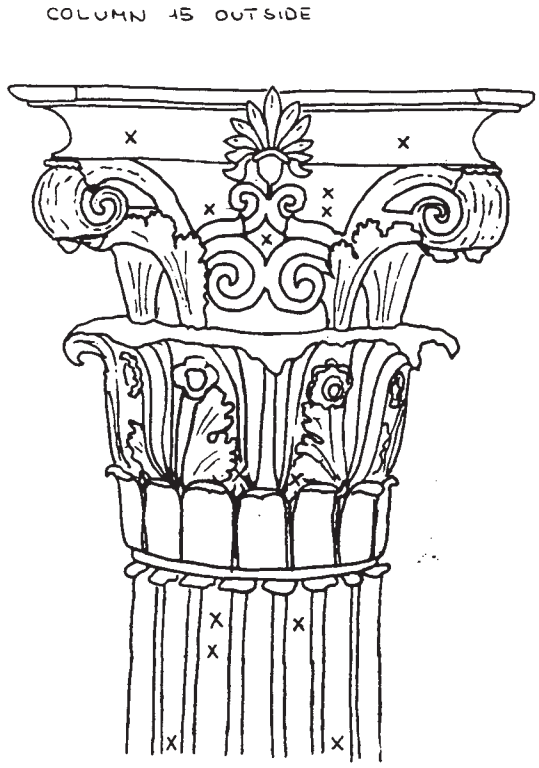


Figure B-2. Location of sapphire microbenchmarks in capitals and columns.

The following dimensions of all the microbenchmarks were measured with a millimeter scale, calipers, and depth gauge.

1. Height of the benchmarks above the stone surface, to give depth dimensions.

2. Distance between the benchmarks.

3. Height measurement of the drum (from the innermost corner of the intersection of the leaf with the drum to the end of the drum with top flat part).

4. Distance between the depths of two flutes equidistant from the centerline symmetry of the column.

5. Depth measurements giving relative distance between the leaves at the base of the Capital.

Photogrammetric Analysis

Figure B-1 indicates the locations of available close-up stereopairs, and the dates that they were taken. The stereo pairs were oriented using the coordinates of microbenchmarks (Figure B-2) as control points in a Kern DSR-15 analytical plotter using Multi-Model Stereo Restitution software (MMSRS). MMSRS was specifically designed for close-range photogrammetry in that the program will accept distances and azimuths as control and permits the simultaneous orientation of many small-frame photographs. The surveyed coordinate positions of the microbenchmarks were rotated before they were used to orient the photogrammetric models so that the x coordinate increased from left to right, the y coordinate increased from bottom to top and the z xoordinate increased toward the viewer. As the 1991 photographs contained more control points, they were oriented first. Then, image tie points were transferred to the 1987 photographs using digital stereoscopic point transfer techniques, avoiding the need to physically mark the glass plate negatives. Using this technique as well as the generic bundle adjustment module of MMSRS, the 1987 and 1991 images were tied together within a relative accuracy of .1mm. Once the stereoscopic models were set and oriented to the control, various kinds of measurements were made. In order to best show changes in surface detail, profile measurements were taken across 4 locations in each image of the lower capital/upper column, in increments of 1.0 mm. In addition, digital terrain models (DTM) or more simply, "grids" were placed over selected surfaces, with intervals of 1.0 mm in both directions (Figure B-3). DTM grids were measured over the surface of the dentil corners and end of the acanthus leaf, for the purpose of measuring volume changes.

Table B-1 notes in greater detail exactly which features were studied, the types of scans made over the features, and the columns for which data were available; the entries indicate the number of data files used in the study. Two data files indicates that scans were made from 1987 and 1991 imagery. Six indicates that three objects of the same type (e.g., dentils) were scanned in 1987 and 1991 imagery. Twelve files indicates that two different areas were repeatedly scanned in both 1987 and 1991 imagery.

Data processing and interpretation

The first line of inquiry in our data analysis concerned the assessment of the limitations of the overall photogrammetric procedure. Knowledge of the sensitivity of the method is critically important for discerning alteration of features on exposed surfaces. We found it useful to resolve the sensitivity of the overall procedure into two measurable components: textural sensitivity and detection limit for loss of relief.

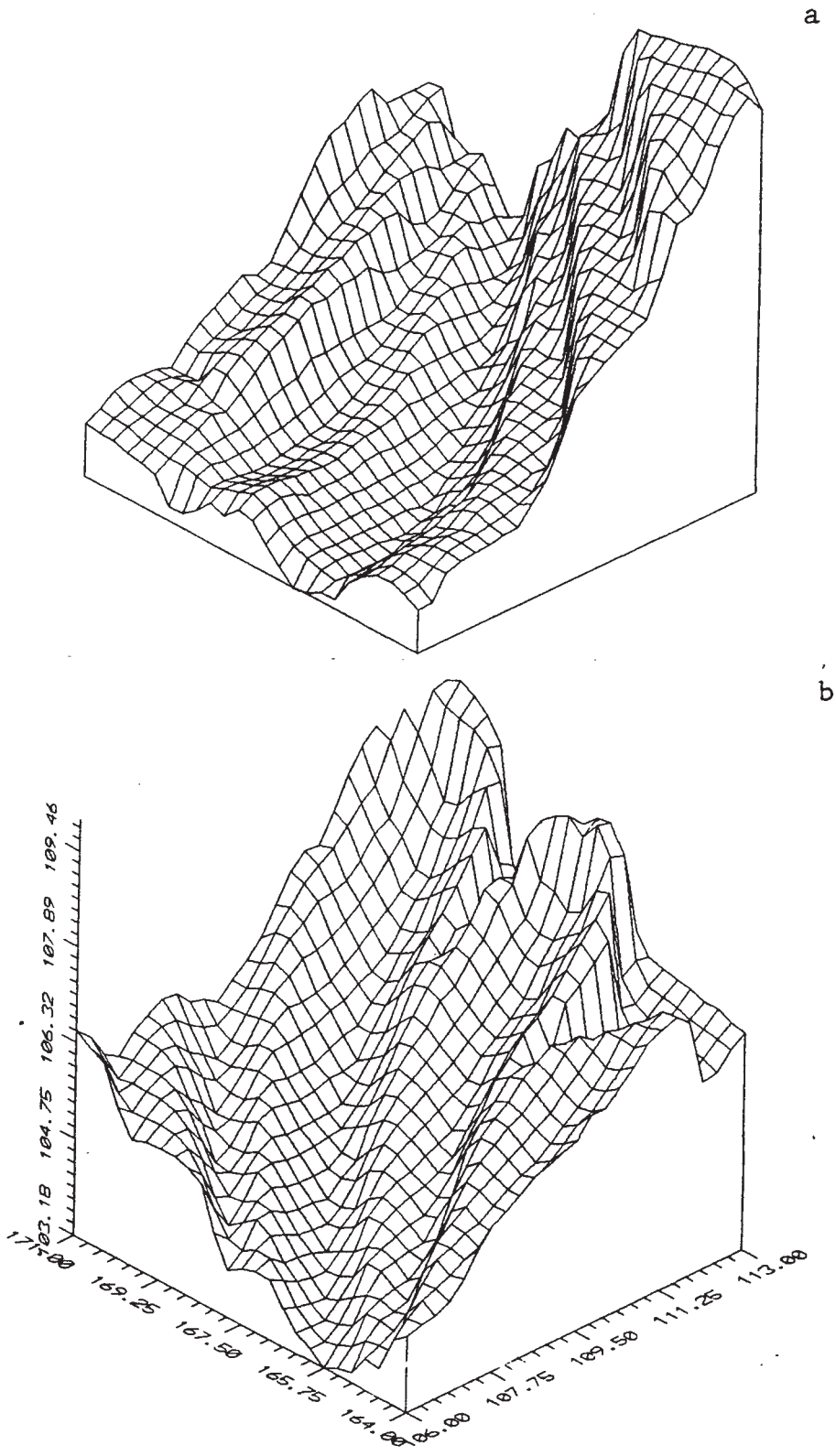
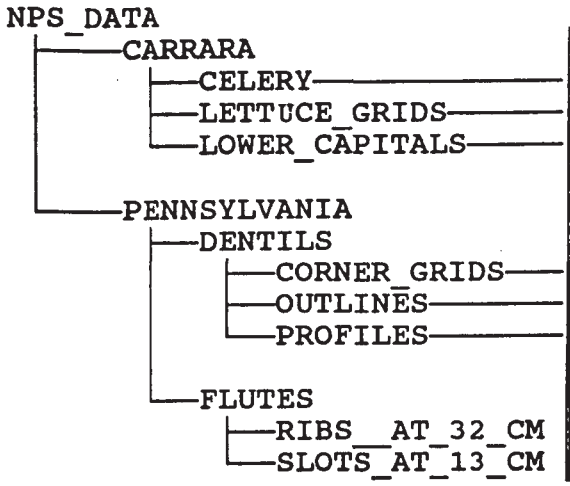


Figure B-3. *a) Digital terrain model of the end of an acanthus leaf on the inside of Column 3; b) Digital terrain model of the end of an acanthus leaf on the outside of Column 10.*



E-4	E-5	E-8	E-10	E-14	E-17	E-19	W-4	W-5
2	1		2		1	1	2	
2							1	
2	1		2		1	1	2	
1							1	
		6		6				6
		12		12			2	12
3	1		2		1	1	2	
2	1		2		1	1	2	

Table B-1. Data availability for stereoimage analysis.

Textural sensitivity

This quantity reflects the extent to which the method can detect relative changes in the topology of the object from one point on the x-axis to the next. The textural sensitivity is independent of setup calibrations and ground-truth references. It is mainly the result of random errors associated with the measurement of relief as an object is scanned in the lateral direction.

As a measure of the textural changes in a surface, we defined a quantity called the textural index that was based on an eight step procedure: (1) profiles are ordered so that the x-axes increase in the same direction, (2) profiles for each year are placed into tight x-axis registration, (3) data-gaps in the profiles are reconciled from YTY (year to year) (every data point in one year has a corresponding data point in the other year), (4) each profile is differentiated (dZ/dX), (5) a smoothing function is applied to the derivative profile, (6) the derivative profile from 1991 is subtracted point-for-point from the derivative of the 1987 profile, (7) the difference profile is segmented to isolate the regions where the errors in the CRP measurement are optimally low, and (8) the standard deviation in the YTY-difference-profile is calculated and taken as an index of the YTY changes in surface relief.

The determination of the textural sensitivity is estimated by measurement of the textural index from multiple profiles of an object in which the same stereo pair is repeatedly used. For example, multiple scans of the flute-ribs on the Pennsylvania marble reveals an error function that is critically sensitive to the shape of the profile. Specifically, the textural sensitivity explodes everywhere except over small zones at the flute-peaks and valleys. In particular, if measurements are confined to 3 cm intervals

centered at the flute-peaks or valleys, an error as small as σ=67 μm is typical. This translates into a minimal textural sensitivity of about 150 μm ($\pm\sigma$). A more detailed discussion of the procedure for estimating the textural sensitivity is given in an open file report in preparation (Mossotti et al.).

The determination of the textural index requires the availability of photogrammetric profiles of the specific surface under study at the start and at the end of the study period. Unfortunately, original close range stereoimagery are not available for the Exchange, a fact which precludes the calculation of the textural index over the long-term and limits its application only to short-term studies.

Detection Limits for Loss of Relief

This measure gauges the ability of the method to detect changes in the z-direction on a given column that are more or less uniform across the sample. This detection limit is given by the sum of all systematic errors and all random errors which introduce offset between two sets of images from different periods. Thus, the detection limit depends on the reproducibility of the absolute z-coordinate of a given point on the profile of an object between the two sets of images.

To define the detection limits, profiles of objects represented by stereo pairs from 1987 were statistically compared with those observed in 1991. The range was quite high; fom 800 μm for flute-ribs to 6,000 μm for dentils. This may reflect increasing experience with the technique, since the dentils were the first views to be analyzed. We note that while close-range photogrammetry indeed may be useful for the detection of short-term textural changes in objects, its usefulness as a tool for the measurement of short-term loss of relief is limited to mass loss rates on the order of 8 mm/measurement interval or greater.

Interpretation of Changing Morphologies and Erosion rates

Our use of interpretative photogrammetric analysis is based on the premise that measurements often are much more useful when they are stated in linguistic terms than when they are expressed to the fourth decimal place. We used interpretative analysis to simulate human thinking by quantifying subjective concepts such as hardly, somewhat, extremely, catastrophic, etc. In particular, by crafting a series of rules for assigning perceived levels of erosion into categories, in effect, we map an infinite spectrum of numbers into a few membership groups. The rigorous mathematical basis for such multi-modal logic, pioneered by Lofti Zadeh at Berkeley during the late '70s, recognizes that an object may have some degree of membership in more than one group.

More specifically, we reduced a plethora of statistics and profiles for each object into erosion patterns by mapping the results for each object into the five categories of erosion defined in Table B-2. Our judgments were based on the comparison of an object profile superimposed on a standard profile on our computer screen, on estimates of the short-term textural index, and when available, on estimates of erosion rates. The offset in the x, y, and z directions is arbitrary. Even visual comparison of the profiles, after mentally shifting one into juxtaposition with the other, shows that the general shapes are very similar, even after 160 years of exposure. We used a C-image DOS program, COMPARE.EXE, to preprocess profile data and to graphically contrast one profile with another on our computer monitor. We found that the morphology audit, implemented with the program COMPARE.EXE, to be an indispensable tool for cross-checking the relative morphologies of objects which may be separated in space or time and/or which may be nearly identical in shape. We also recognize that the original images can provide quantitative documentation of object

morphologies, documentation that can be archived for later use as an historical reference.

Erosion Category	Rule	
Undetected:	160 yr erosion:	Undetected
	Historical erosion rate:	Insignificant
	Long-term problem:	None
	4 yr erosion:	Undetected
	Recent erosion rate:	Insignificant
	Short-term problem:	None
Slight:	160 yr erosion:	Discernable
	Historical erosion rate:	Graceful aging
	Long-term problem:	Possible
	4 yr erosion:	Undetected
	Recent erosion rate:	Insignificant
	Short-term problem:	None
Moderate:	160 yr erosion:	Distinct
	Historical erosion rate:	Significant
	Long-term problem:	Definite
	4 yr erosion:	Undetected
	Recent erosion rate:	Insignificant
	Short-term problem:	Possible
High:	160 yr erosion:	Acute
	Historical erosion rate:	High
	Long-term problem:	Definite
	4 yr erosion:	Detectable
	Recent erosion rate:	Significant
	Short-term problem:	Definite
Radical:	160 yr erosion:	Structural failure
	Historical erosion rate:	Very high
	Long-term problem:	Critical
	4 yr erosion:	Definite
	Recent erosion rate:	Significant
	Short-term problem:	Critical

Table B-2. Classification of erosion rates.

Appendix C: 19th Century Pollution Estimates for Philadelphia

Anett Andersen, Susan Sherwood, Kathryn Sather
NPS Preservation Assistance Division

Mark Scruggs, John Bunyak, John Notar, John Vimont, David Joseph
NPS Air Quality Division

Estimates of pollution in 19th century Philadelphia in the vicinity of the Exchange are being developed to understand the history of environmental exposure of the marbles. Of primary interest is to discern the cause of extreme marble decay on the east facade in contrast with the west facade marble is relatively intact. The quality of the design and the expense of the marble use in the Exchange reflect the prosperity of the Port of Philadelphia as the "Workshop of the World" (Oliver Evans Chapter, SIA, 1990). The Dock Street location was at the same time convenient to the wharves and to the source of wealth as well as in close proximity to the densest sources of pollution.

Industrial emissions have been derived from insurance data, marine emissions from Port traffic statistics; and train emissions are to be based on fuel use by the Delaware Avenue Beltline and the Dock Street spur (not yet available). The 1890s was selected as a time period for which data are available for all three important types of emissions. Further, it may include the peak pollution exposure of the marble at the Exchange, which may highlight any inter-facade differences. In principle, a 100-150 year time trend could be developed using similar archival sources and analytical tools. In practice, the dearth of data to be collected and organized exceeds the scope of the project resources.

Insurance Surveys

The Hexamer Insurance Surveys of Philadelphia and the Sanborn Insurance Surveys of Camden provide detailed information about industries beginning in the 1850s and 1880s, respectively. The Hexamer maps were updated routinely every 10-15 years, depending on the intensity of development, so for some sections of the city a history of industry, and thus a history industrial pollutants, could be developed. Fortunately for pollution historians, combustion is a significant fire hazard as well as a source of pollution. High insurance risk industries tended to be those involving more combustion, and thus greater emissions. For this report, volumes in the 1890s were selected where available (Figure C-1). Industrial emissions within a 5 km radius of the Exchange were plotted on a grid of cells 350 m by 350 m, using information from the insurance surveys in two distinctly different ways.

When pollutants are emitted from a tall stack, the emissions tend to travel as a discrete plume. The travel characteristics of this plume depends to a large extent on the height of the stack, temperature of emission, and stability of the air mass into which it is injected. In pollution control terminology, these are known as point sources. In contrast, pollutants that are emitted from low stacks (less than 25 m) tend not to travel far, but rather contribute to the airflow that recirculates within the vicinity of the emission. These kinds of pollution emissions are known as area sources.

Emission density of area sources

The Hexamer insurance atlases classify buildings based upon the use of the building, and most industrial processes fall under the category of "specially hazardous" (Table C-1). The insurance atlases map the locations and numbers of boilers and smokestacks within each building, as well as noting the specific type of industry in some cases (Figure 36). The Sanborn insurance atlases of Camden

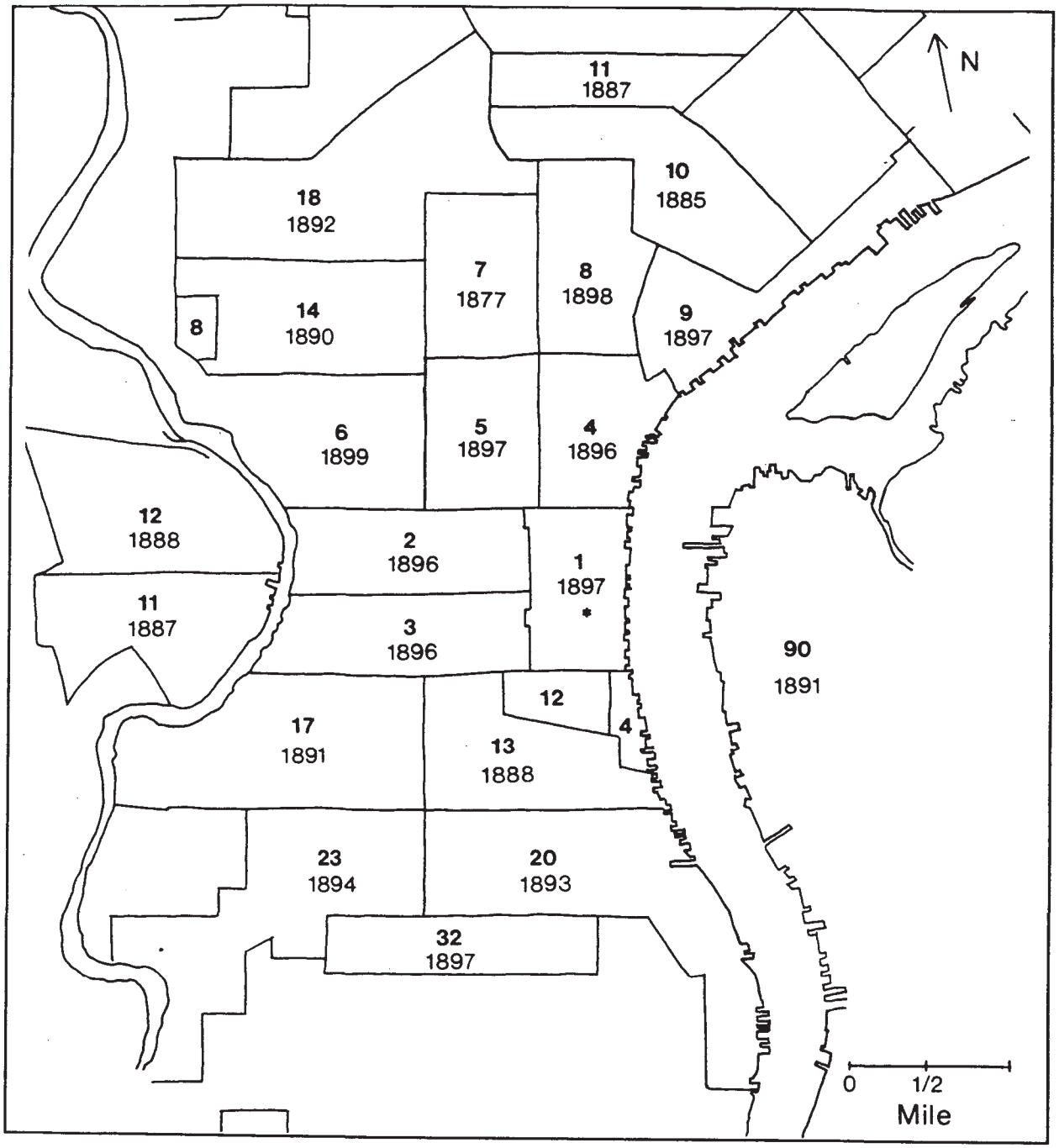
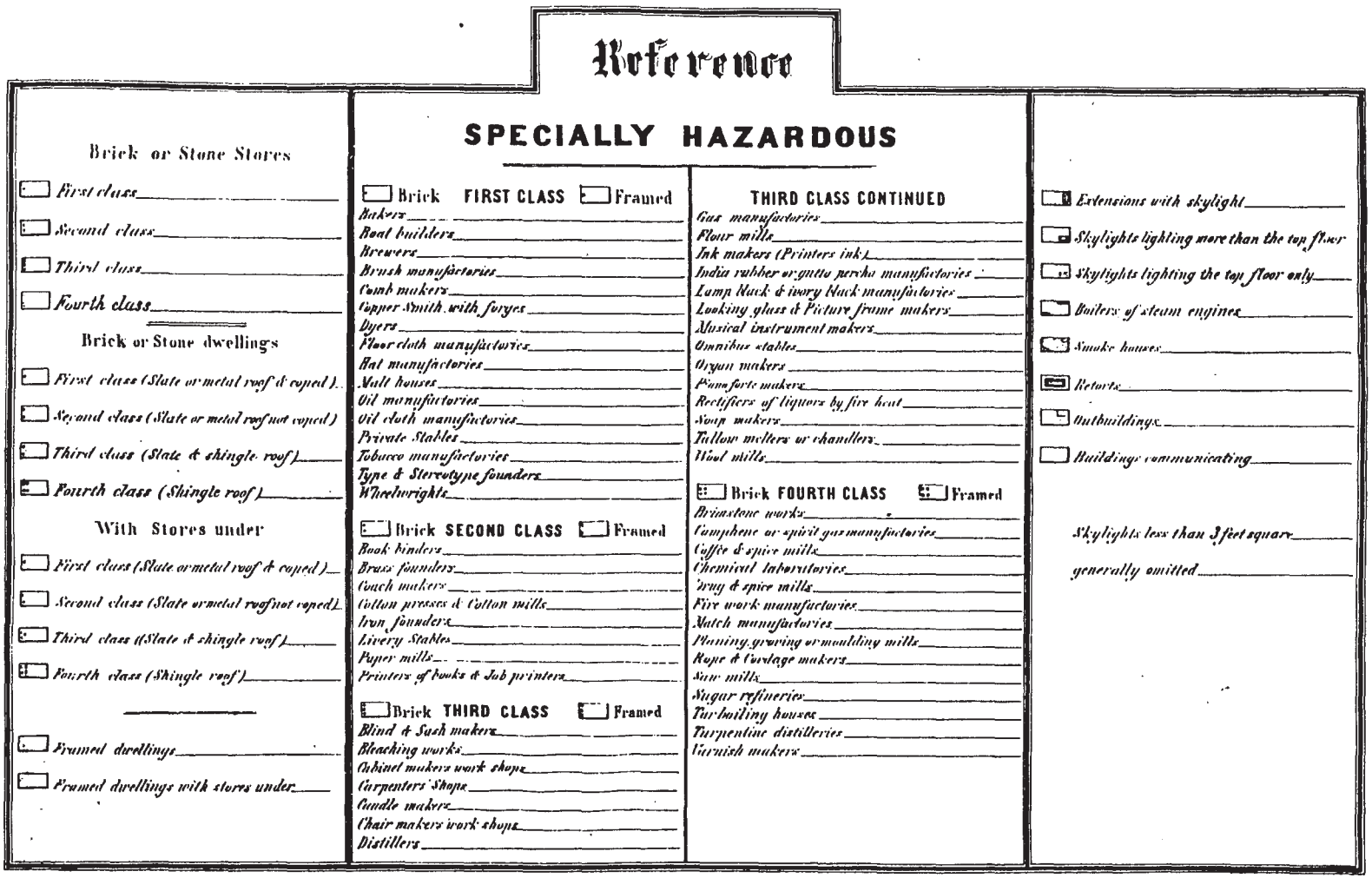


Figure C-I. *Hexamer Insurance Surveys - Dates of maps of insurance surveys used to estimate emission densities.*



Reference

Brick or Stone Stores

- First class
- Second class
- Third class
- Fourth class

Brick or Stone dwellings

- First class (Slate or metal roof & coped)
- Second class (Slate or metal roof not coped)
- Third class (Slate & shingle roof)
- Fourth class (Shingle roof)

With Stores under

- First class (Slate or metal roof & coped)
- Second class (Slate or metal roof not coped)
- Third class (Slate & shingle roof)
- Fourth class (Shingle roof)

- Framed dwellings
- Framed dwellings with stores under

SPECIALLY HAZARDOUS

Brick FIRST CLASS Framed

- Bakers
- Boat builders
- Brewers
- Brush manufactories
- Comb makers
- Copper Smith with forges
- Dyers
- Floor cloth manufactories
- Hat manufactories
- Malt houses
- Oil manufactories
- Oil cloth manufactories
- Private Stables
- Tobacco manufactories
- Type & Stereotype founders
- Wheelwrights

Brick SECOND CLASS Framed

- Book binders
- Brass founders
- Coach makers
- Cotton presses & Cotton mills
- Iron founders
- Livery Stables
- Paper mills
- Printers of books & Job printers

Brick THIRD CLASS Framed

- Blind & Sash makers
- Bleaching works
- Cabinet makers work shops
- Carpenters' Shops
- Candle makers
- Chair makers work shops
- Distillers

THIRD CLASS CONTINUED

- Gas manufactories
- Flour mills
- Ink makers (Printers ink)
- India rubber or gutta percha manufactories
- Lamp black & ivory black manufactories
- Looking glass & Picture frame makers
- Musical instrument makers
- Omnibus stables
- Organ makers
- Pianofortes makers
- Rectifiers of liquors by fire heat
- Soap makers
- Tallow melters or chandlers
- Wool mills

Brick FOURTH CLASS Framed

- Brimstone works
- Camphene or spirit gas manufactories
- Coffee & spice mills
- Chemical laboratories
- Drug & spice mills
- Fire work manufactories
- Match manufactories
- Planing, graving or moulding mills
- Rope & Cordage makers
- Saw mills
- Sugar refineries
- Turbailing houses
- Turpentine distilleries
- Varnish makers

- Extensions with skylight
- Skylights lighting more than the top floor
- Skylights lighting the top floor only
- Boilers of steam engines
- Smoke houses
- Retorts
- Outbuildings
- Buildings communicating

Skylights less than 3 feet square generally omitted

Table C-1. Hexamer Insurance Classification System.

classify buildings based upon type of construction material; but usually the type of industry or commercial activity is identified.

Data from the Sanborn and Hexamer atlases were treated as area sources. Because stack height is often not available, we assumed that the stacks were quite low and that emissions did not travel beyond the grid square. The following information was tallied from each map: the number of buildings categorized as "specially hazardous," the number of boilers (including boilers in commercial buildings which were not considered hazardous), the number of smokestacks, and the number of buildings of specific industries known to produce relatively large emissions. These industries included breweries, oil refineries, foundries, paper pulp mills, gas manufacturing, chemical laboratories, electric generating stations, and sugar refineries. Each individual map, covering a four to eight block square area, was treated as a unit. The irregular shapes of the map grids were normalized into a standard grid pattern, and boilers and smokestacks distributed as appropriate.

Emission densities were calculated based on the number of boilers in each grid cell and shown in Figures C-2 - C-4. Since the type of fuel used cannot be known in this spatial detail, two estimates were made; a) the best case assumption where all fuel was anthracite coal and b) the worst case, where the fuel used was completely bituminous coal. Reality is somewhere in the middle. If there was a geographic bias within the city in the type of fuel burned, then the emission density maps would not reflect the appropriate pollution distribution. However, with the exception of emissions from transportation systems, such a bias would be difficult to verify or refute. Table C-2 lists the emission factors assumed for the calculations.

As can be seen from the emission density maps (Figures 37, C-2 - C-4), the Exchange is located in the grid cell with the highest emissions. It is difficult to distinguish directionality within the grid square with the current data; it will be necessary to revaluate the primary source material to accomplish this. The high concentration of pollution in the same grid square of the Exchange may point to a need to collect data over the full time span of available data, if only for the single grid square, to evaluate the role of immediately proximate sources of pollution.

Contribution of Point Sources

In addition to the comprehensive mapping of all structures, particular industries were inventoried in much greater detail. Between 1866 and 1895, the Hexamer General Survey documented about 100 facilities per year, describing each facility in an oversize plate, which included an axiometric projection, a block map, and a table of data including number of employees, number of fire escapes, and most important for these purposes, the

	% sulfur in coal	Particulate Matter (PM) lbs/ton	SO_2 lbs/ton of coal	NO_x lbs/ton of coal
Anthracite coal	.6	9.1	23.4	10
Bituminous coal	2.0	60	72	14

Table C-2. Emission factors used for calculating strength of area sources in 1890s Philadelphia.

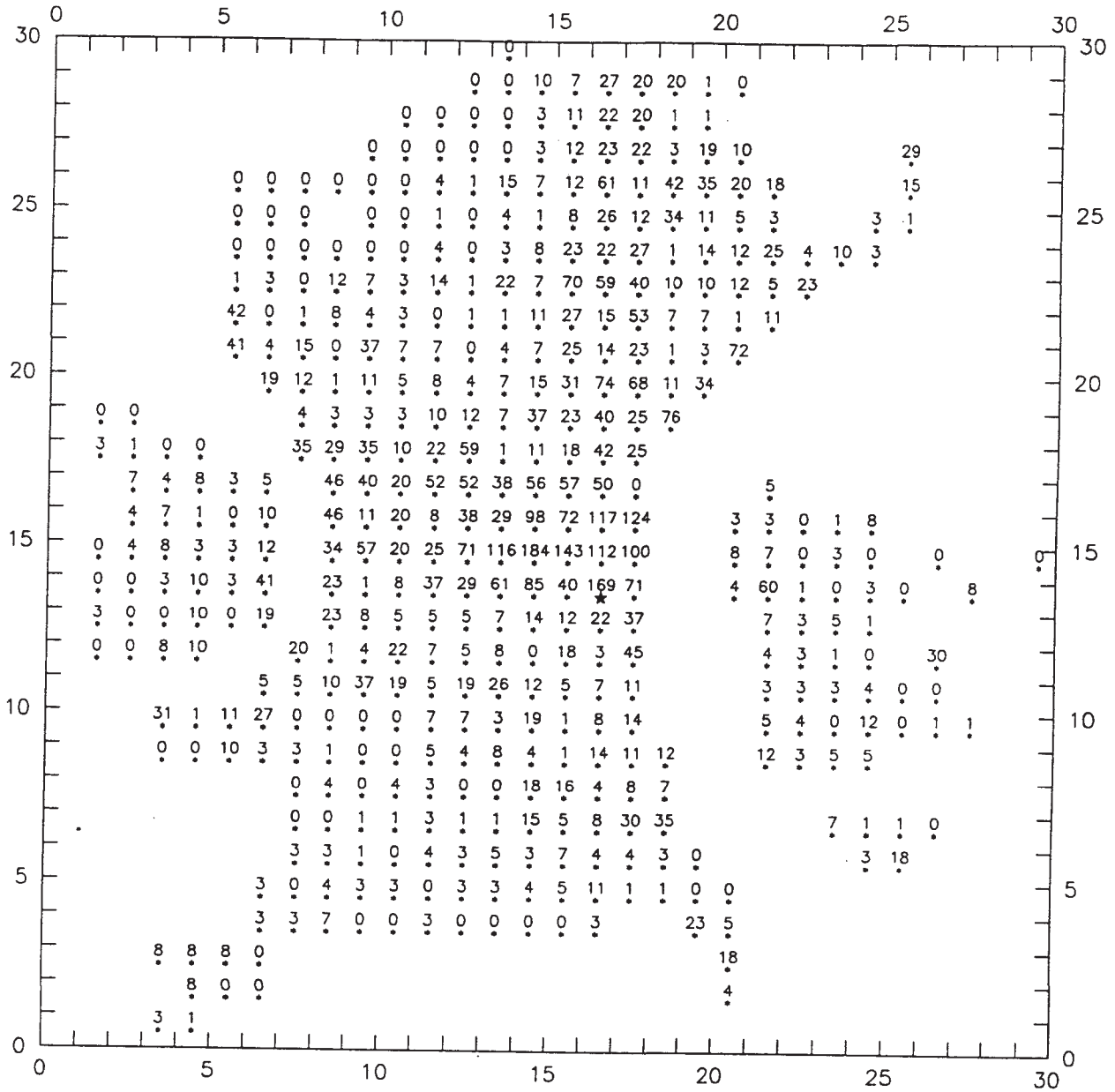


Figure C-2. *Particulate matter emission density, annual average lbs/hr, 1890s, estimated, assumes bituminous coal.*

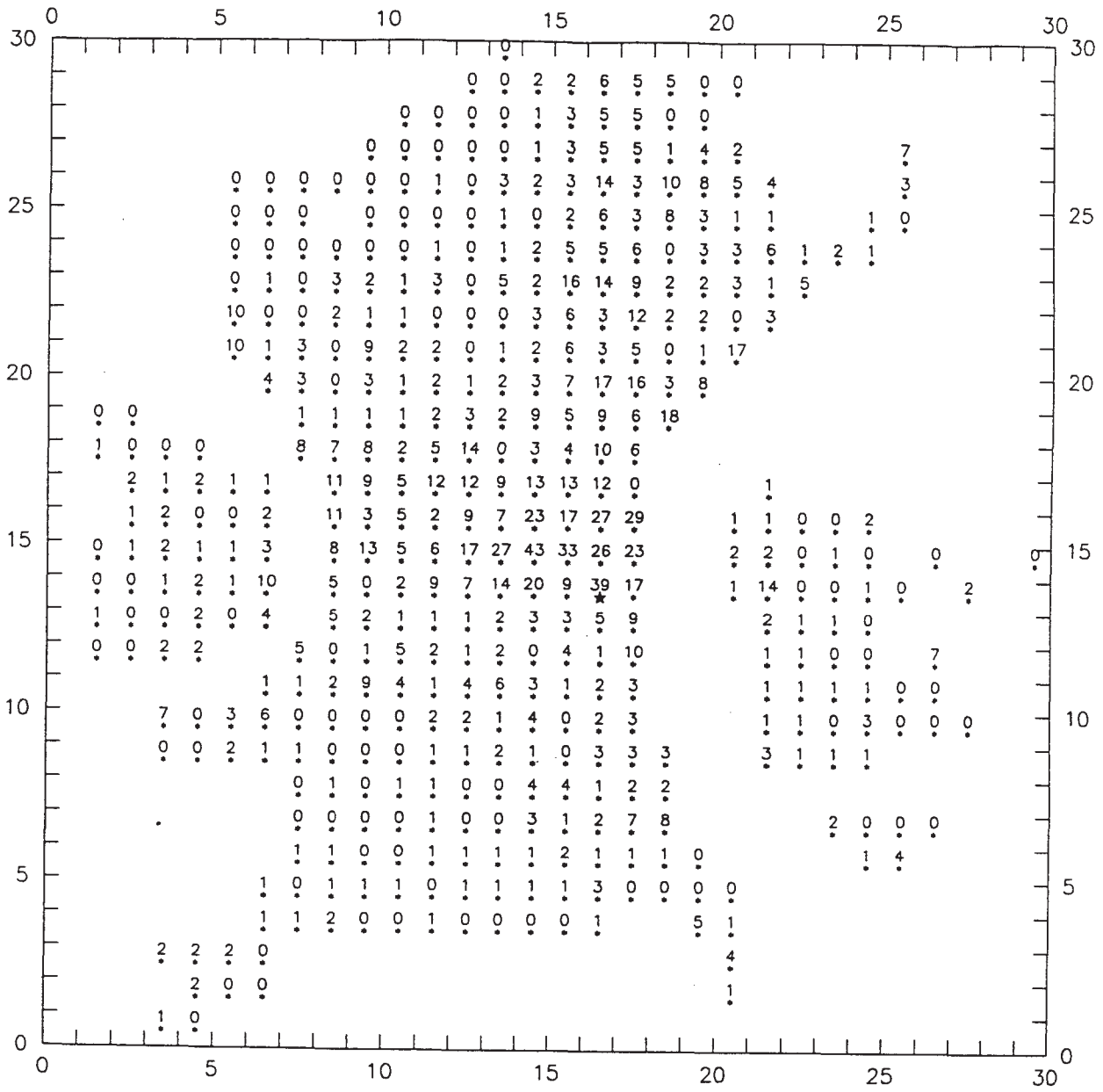


Figure C-3. *Nitrogen oxide emission density, annual average lbs/hr, 1890s, estimated, assumes bituminous coal.*

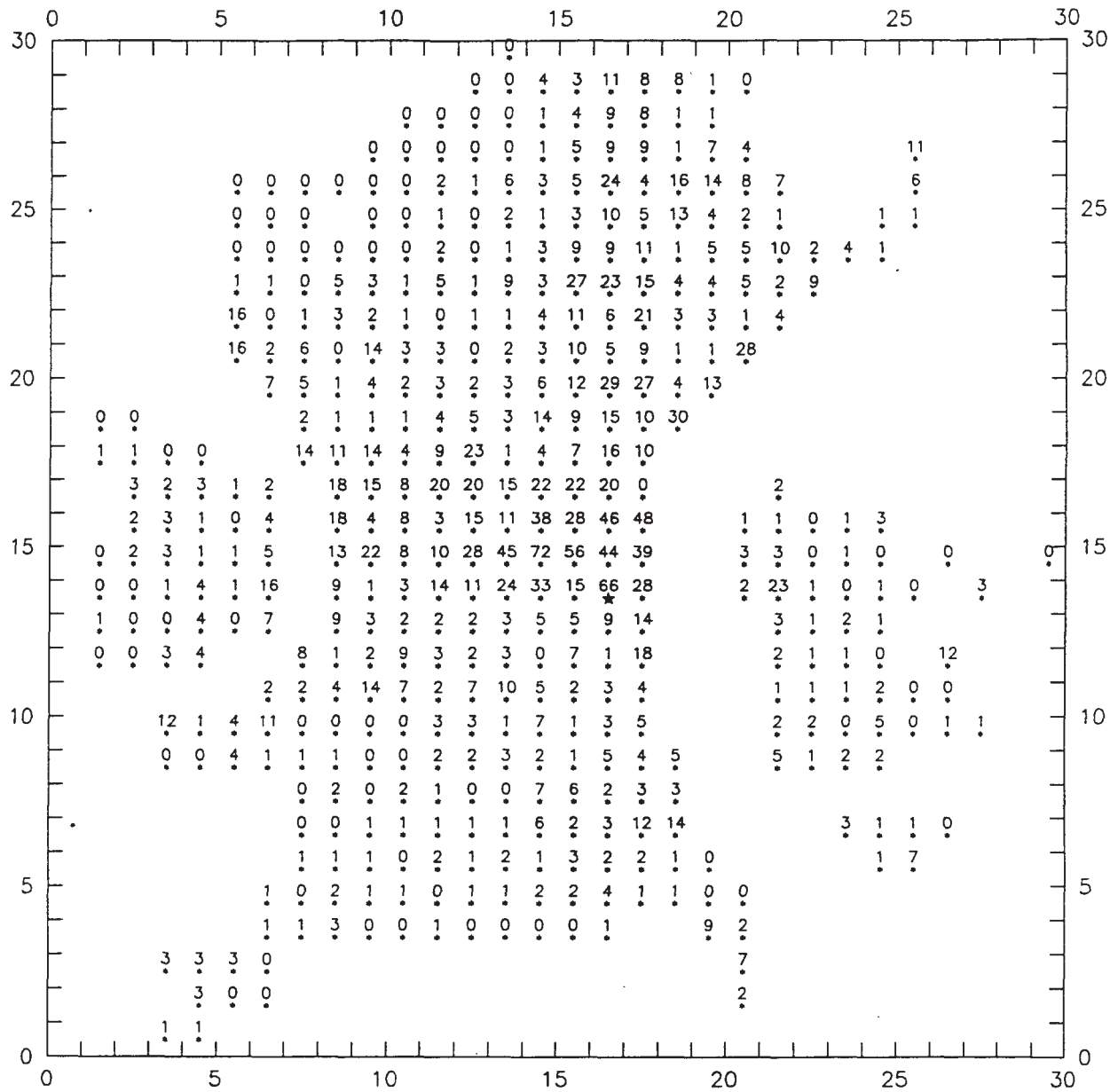


Figure C-4. *Sulfur dioxide emission density, annual average lbs/hr, 1890s, estimated, assumes anthracite coal.*

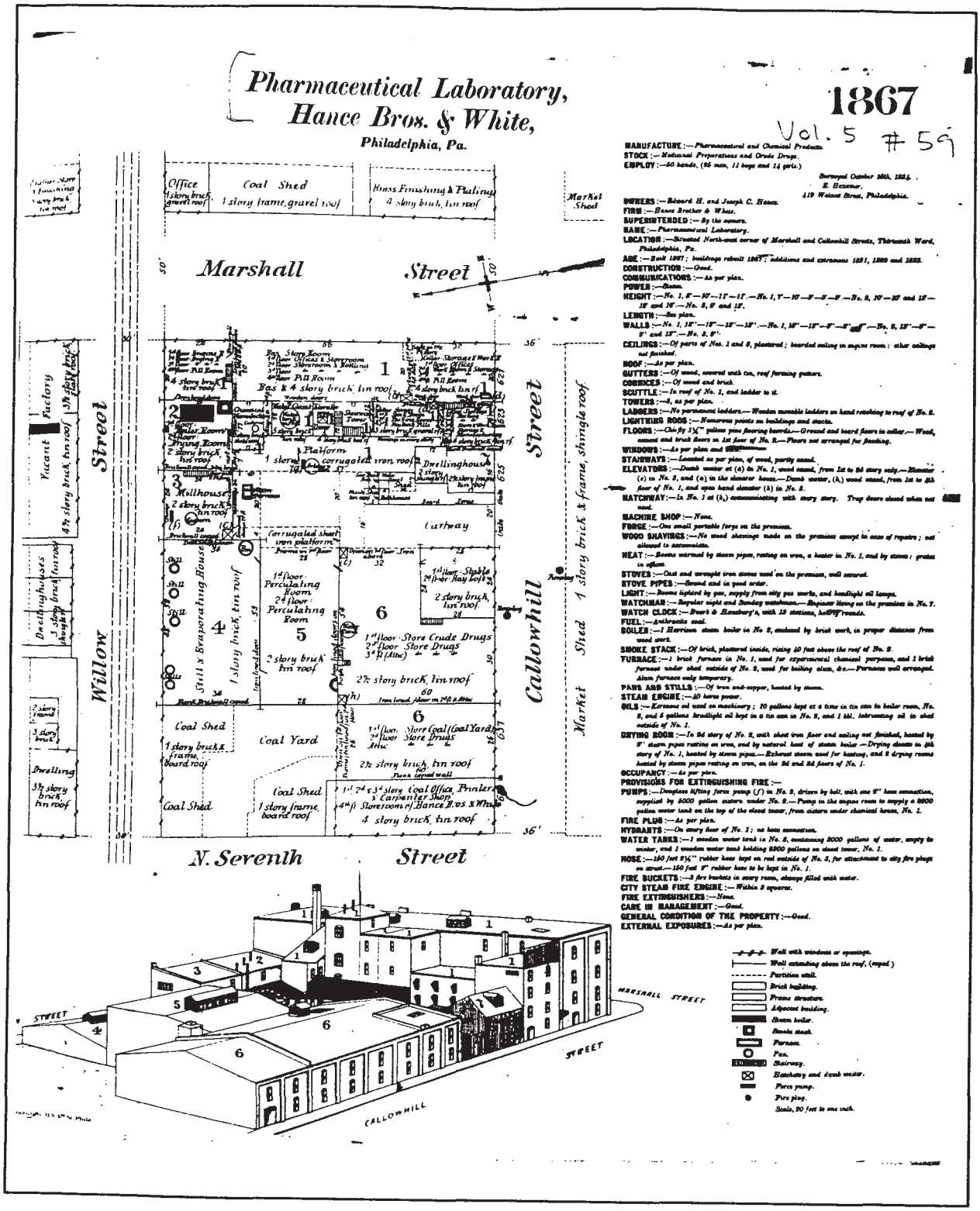


Figure C-5. *Hexamer General Survey - typical documentation of selected industries used in point source emissions analysis.*

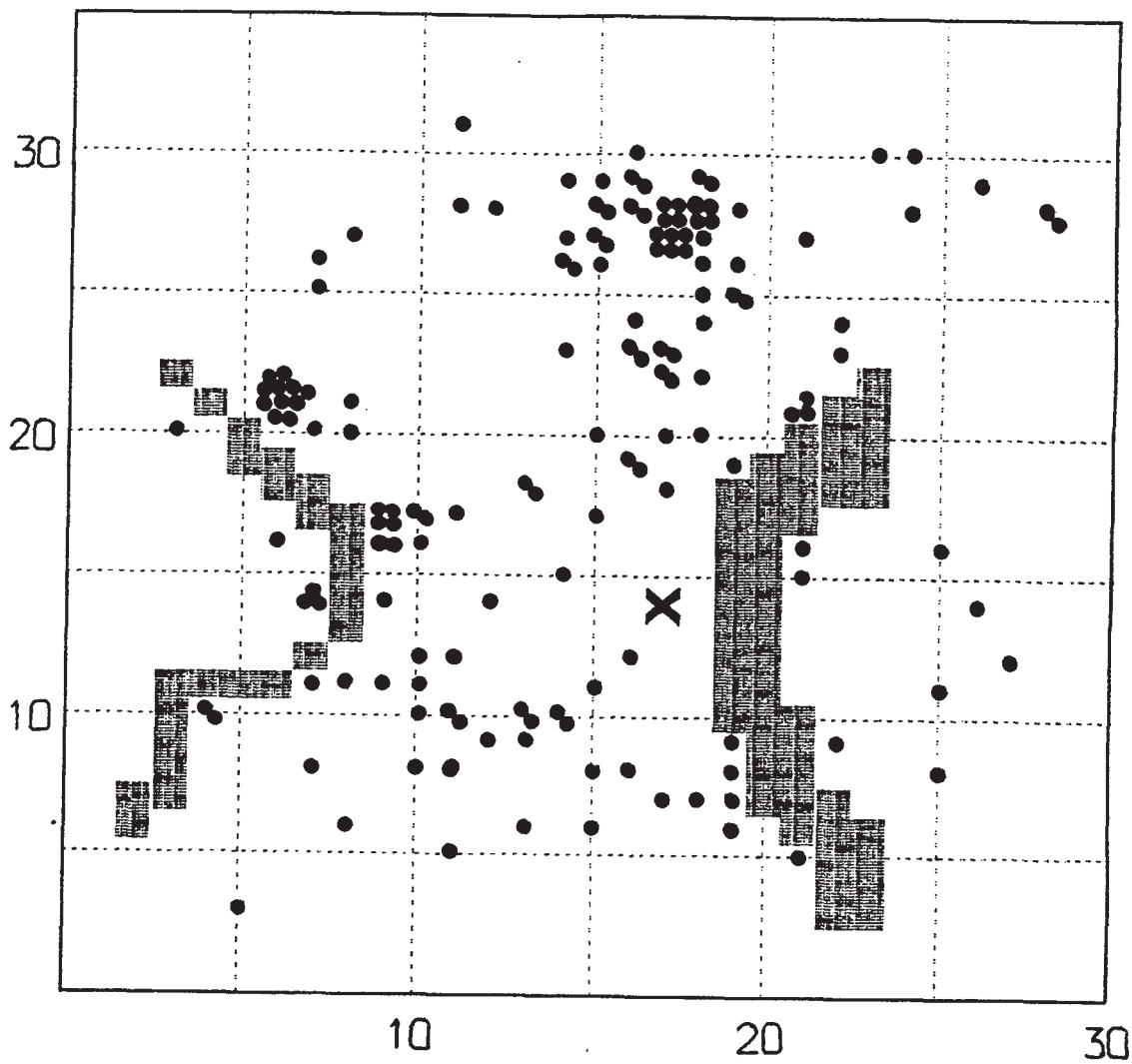


Figure C-6. Location of selected industries listed in Table C-3.

horsepower of the engines, the stack height, and occasionally the type of fuel used (Figure C-5). Comparable data from is not generally available for Camden. This introduces a potential bias in the results, where pollutants from the last are underestimated.

A selection of 153 industries from the Hexamer General Surveys with well-documented stack height and boiler horsepower were used in an air quality model as point sources to estimate their relative contribution to pollution at the Exchange (Figure C-6; Table C-3).

Annual average particulate matter concentrations in $\mu g/m^3$ were estimated using the Environmental Protection Agency's Industrial Source Complex Model (ISCST). This steady-state Gaussian model uses hourly wind speed and direction, temperature, mixing height, and atmospheric stability data to compute inert pollutant concentrations at distances out to 50 km away from their source. For the purposes of this analysis, a single receptor location was chosen; the Exchange. Data for ground level meteorology came from Philadelphia in 1986 and upper air data (atmospheric stability indicators) came from the same period at Dulles International Airport, Sterling, VA. The emissions inventory was based on 153 selected industries from the Hexamer General Survey listed in Table C-3. The relative contribution of each source can be tagged and identified. Sulfur and nitrogen oxide concentrations are estimated in a similar fashion. For the three pollutant species, estimates for all anthracite or all bituminous can be made.

The annual average particulate matter concentration at the Exchange was estimated to be about 25 $\mu g/m^3$. Around the Exchange, the estimated concentrations are:

North	10.8 $\mu g/m^3$
East	1.4 $\mu g/m^3$
South	3.2 $\mu g/m^3$
West	9.0 $\mu g/m^3$

This number is about 2 or 3 times less than would be expected, indicating that the emissions inventory is incomplete. The obvious gap is industrial emissions associated with chemical processes, not the combustion of coal for power. High sulfur process emissions are found in smelting, paper pulping, dye and ink manufacturing, and foundry operations.

Marine traffic

Records on marine traffic in the Port of Philadelphia in the 19th c. are quite detailed. Port authorities maintain data on country of origin and domestic versus Atlantic crossings for all cargo ships. We assumed that all foreign vessels burned sub-bituminous English coal and that all American vessels burned Pennsylvania anthracite coal. Further, we assumed that each ship took 3 hours to enter and leave the Port of Philadelphia, using their main boilers (plus 1.3 tugs on average) for that period only. Combustion during the stay in port was not considered. We assumed that on average ocean-going vessels used 4 Scotch marine boilers; that coastal cargo ships used 3 boilers, and that tugs used 2 boilers. Sailing ships were counted for the purpose of estimating emissions from escorting tugs during their entry and departure. Emission factors and boiler efficiency ratings were derived from the Babcox and Wilcox Steam handbook.

Data were collected from 1884-1898, to be consistent with the time period of the insurance data (Table C-4). A fifteen year average was used to calculate average total marine cargo vessel emissions for the suite of pollutants of interest, which were divided into six areas for plotting (using large type face) in Figures 37, C-2 - C-4. Given conservative assumptions about boiler efficiency, etc., and absent data on passenger ships, these probably approximate a minimum pollutant loading for comparison with industrial emissions.

HEXAMER REF #	INDUSTRY NAME	X	Y	QUADRANT	STACK IN FEET
2067	Gage Mill	21	16	E	80
2095	Arasapha Manufacturing Co.	25	11	E	65
2344	American Nickel Works	25	16	E	150
2594	The West Jersey Paper Manuf. Co.	21	15	E	100
2606	Steel Iron Co.	25	8	E	60
2741	Camden Chemical Works	26	14	E	125
2823	Aroma Mills	27	12	E	100
1861	Butterworth & S.Iron Foundry	22	23	N	70
1867	Pharmaceutical Laboratory	15	17	N	95
1903	Penn Works	21	21	N	50
1913	Kensington Beer, Ale & Porter B.	17	20	N	82
1917	Carpet Factory	15	28	N	130
1930	Glenmore Worsted Mills	14	27	N	76
1934	Stinson B. & Kurlbaum's Mill	16	28	N	85
1939	Diamond Carpet Works	18	28	N	113
1956	P's & P's Card Board Factory	17	22	N	90
1979	American Knitting Mills	17	23	N	102
1980	Bromley & Sons Carpet Factory	18	26	N	72
2015	Davenport's Mill	18	29	N	70
2021	Kensington Engine Works	21	21	N	70
2027	Pequod Mills	21	27	N	72
2032	Standard Worsted Mills	19	25	N	85
2047	Star & Crewscent Mill	18	28	N	40
2056	Star, Hampden & Malta Mills	18	22	N	80
2089	Somerset Carpet Mill	18	28	N	120
2090	Cambria Carpet Mills	14	29	N	100
2092	Columbia Iron Foundry	16	23	N	69
2104	N.E. Paul Mills	16	29	N	71
2119	Leibrandt & McDowel Stove Co.	21	21	N	50
2125	Oxford Carpet Mill	15	27	N	54
2127	Anchor Brewery	15	27	N	60

2138	Carey B. Paper Hanging Factory	14	26	N	90
2153	Phil 25th Gas Works	28	28	N	23
2180	York Carpet Co.	17	27	N	75
2211	Cresson Foundry & Machine	11	31	N	90
2216	Rock Carpet (Rickard's) Mill	18	28	N	100
2233	People's Works	18	20	N	35
2236	Rialto Mills	19	26	N	90
2258	Weaving Mill	17	28	N	90
2270	Howard Mills	17	28	N	90
2282	Keystone Carpet Mills	17	27	N	85
2297	Philadelphia Lead Works	22	24	N	60
2303	Plumbers' Metal Works	16	24	N	60
2320	Balfour's Paper Mill	28	28	N	125
2346	Craven & Dearnley's Mill	15	29	N	100
2357	Roehm's Brewery	16	19	N	112
2393	Whitaker's Sons Mill	23	30	N	75
2432	Dingee Brick Yard	8	27	N	72
2439	Orinoko Mills	11	28	N	100
2440	Bolt, Nut & Rivet Works	13	18	N	60
2452	Ivins, Dietz, Magee Carpet Fact.	15	28	N	130
2455	Collingwood Mills	17	28	N	60
2457	Bochmann & Co.'s Mill	17	28	N	70
2476	Class' Lager Beer Brewery	14	23	N	92
2482	Penn Lawn Mower Works	7	25	N	60
2492	Star Carpet Mill	18	24	N	74
2495	Scholes Woolen Yarn Mill	18	29	N	90
2501	Bridesbury Machine Works	15	20	N	76
2509	Reading Bolt & Nut Works	17	18	N	90
2524	Horner Bro. Carpet Co.	16	28	N	132
2542	Narrow Textile Factory	14	26	N	100
2561	Weisbrod & Hess Oriental Brew.	24	30	N	105
2570	Northern Liberties Gas Co. W.	19	19	N	56
2574	Linden Worsted Mills	17	22	N	100

2597	Nepaul Mills	16	29	N	91
2605	Park Carpet Mills	18	25	N	85
2625	Moore & White Co. Machine Works	12	28	N	50
2636	Ormiston Mills	15	26	N	100
2644	Dickey & McMaster's Mill	17	27	N	60
2645	Bavaria Brewery	16	30	N	120
2654	Hoyle, Harrison, Kaye's New Mill	19	28	N	150
2665	Nat'l Hardware & Iron Works	17	27	N	120
2683	Orianna Mills	17	27	N	75
2697	Abram Cox Stove Co.	17	27	N	82
2717	Glazier Hosiery Mills	19	25	N	90
2719	Colombia Carpet Mills	16	23	N	125
2720	Ontario Mills	17	23	N	70
2728	Belmont Carpet Mills	26	29	N	90
2783	Liberty Stove Works	16	19	N	60
2796	H. & T. Bolt, Nut & Rivet Works	13	18	N	100
2806	Rumpf & Witty's Mill	18	27	N	82
2812	Philadelphia Traction Company	7	26	N	132
2820	Union Knitting Mills	24	28	N	86
1858	Delaware River Chemical Works	19	7	S	70
1883	Enterprise Sugar Refinery	15	11	S	60
1975	Buteher's Oil Refinery	14	10	S	75
2003	West End Mills	16	12	S	75
2038	Triton Mills	14	10	S	100
2070	Southwark Mills #2	15	8	S	145
2072	Southwark Mills #1	17	7	S	80
2080	Persian Woolen & Cotton Mills	13	9	S	87
2140	Ship & Engine Building Co.	19	8	S	76
2158	Western White Lead Co.	18	7	S	60
2160	Delaware Sugar House	19	9	S	79
2264	Tygert's Phosphate Works	19	6	S	74
2294	Connelly & Son's Mill	11	5	S	90
2341	The River Iron Works	22	9	S	50

2560	Keystone Shovel Works	15	6	S	70
2592	Pascal Iron Works	16	8	S	140
2598	Victoria Mill	13	6	S	80
2603	Greenwich Chemical Works	21	5	S	100
	Brush Generation Station	10	16	W	139
	Ehret, Jr., & Co.	4	10	W	60
1862	Bergner & Engel Brewing Co.	6	21	W	60
1871	Wyeth & Bro. Manuf. Chemists	12	14	W	70
1872	Arnholt & Schaefer Brewing Co.	6	21	W	62
1876	Continental Worsted Mills	10	10	W	150
1880	Lager Beer Brewery	6	21	W	60
1944	Bonney Vice and Tool Co.	7	14	W	60
1952	Architectural Iron Works	9	16	W	60
1961	Gray's Ferry Chemical Works	4	10	W	160
1981	Eagle Brewery	6	21	W	81
1990	Penn Chemical Works	13	10	W	60
1994	Washington Iron Foundry	9	11	W	55
2014	The Machine Tool Works	9	17	W	70
2026	The American B.H.O. & Sewing M.	10	11	W	62
2044	New Castle Mills	13	10	W	70
2073	Kennebee Mills	10	12	W	72
2079	Schemm & S. Lager Beer Brewery	8	21	W	115
2081	Baltz's Brewing & Malt House	6	21	W	103
2111	Rosengarten & S. Manuf. Chemist	11	12	W	85
2171	Rooting Paper Mill	9	17	W	152
2178	Pennsylvania Woolen Co.	10	8	W	72
2183	The Ammonia Co. of Philadelphia	7	11	W	60
2203	American Galvanizing Works	11	10	W	70
2287	Smith India Pale Ale Brew Co.	3	20	W	65
2300	Red Star Mills	11	8	W	90
2343	Continental Carpet Mills	12	9	W	74
2348	F. A. Poth Brewing Co.	6	21	W	135
2372	Keller's Lager Beer Brewery	6	21	W	64

2381	Theis Lager Beer Brewery	6	21	W	70
2403	Lion Brewery	6	21	W	55
2427	Bement, Miles & Co. Machine Works	10	17	W	85
2447	Fairmount Av. Brewery	7	18	W	66
2456	Centennial Lager Beer Brewery	6	21	W	55
2460	Star Bolt Works	6	16	W	64
2462	City Mills	9	16	W	60
2463	Keystone State Brewery	8	20	W	60
2469	Wharton Jr. & Co. Inc.	8	11	W	60
2483	Park Paper Mills	9	17	W	152
2498	Weterill & Brother, W. Lead W.	7	14	W	62
2527	Union Malleable Iron Works	11	17	W	60
2550	Caledonia Worsted Mills	10	17	W	125
2612	Henderson Machine Tool Co.	9	14	W	100
2637	Furbush & Son Machine Co.	14	15	W	63
2670	Jarden Brick Co. Works	8	6	W	100
2709	Nat'l Wall Paper Co. Fact.	11	10	W	109
2712	Phil. Wagon Works	7	14	W	70
2747	Webster, Edmund Brick Works	7	8	W	50
2787	Burg & Pfaender, Lager Beer B.	6	21	W	85
2792	Manhattan Mills	9	17	W	80
2795	Point Breeze Gas Works	5	3	W	30
2802	City Park Brewery	7	20	W	100

Table C-3. Selected industries used for estimating point source emissions.

	BRITISH COAL		ANTHRACITE COAL		TOTAL #	TUGS	
YEAR	4 BOILERS	4 BOILERS	3 BOILERS	0 BOILERS	OF VESSELS	2 BOILERS	
1884	1654	704	3360	6892	12610	15132	
1885	1638	724	3340	6124	11826	14191	
1886	1648	677	3451	5443	11219	13463	
1887	1924	558	3358	5861	11701	14041	
1888	1562	599	3114	5163	10438	12526	
1889	1602	652	3090	5045	10389	12467	
1890	1947	587	2939	5070	10543	12652	
1891	1788	688	3158	5642	11276	13531	
1892	2314	734	3023	4881	10952	13142	
1893	1867	551	3025	5411	10854	13025	
1894	1638	564	3008	5818	11028	13234	
1895	1633	536	3289	5305	10763	12916	
1896	1484	347	3198	4365	9394	11273	
1897	1769	325	3012	4243	9349	11219	
1898	2431	205	2765	3936	9337	11204	
AVE	1793	563	3142	5280	10778	12934	
MIN	1484	205	2765	3936	9337	11204	
MAX	2431	734	3451	6892	12610	15132	
SO2 (T/Y)							TOTAL
AVE	193	36	152			418	799
MIN	160	13	134			362	669
MAX	262	48	167			489	965
NOX (T/Y)							
AVE	14.80	4.70	19.50			53.60	92.60
MIN	12.20	1.70	17.20			46.40	77.50
MAX	20.00	6.10	21.40			62.70	110.20
PM (T/Y)							

AVE	74.20	15.60	65.00			178.50	333.30
MIN	61.40	5.70	57.20			154.60	278.90
MAX	100.60	20.30	71.40			208.80	401.10
SO2(lb/h)							
AVE	48.53	9.15	38.27			105.03	200.98
MIN	40.23	3.34	33.69			90.97	168.24
MAX	65.80	11.94	42.04			122.88	242.67
NOX(lb/h)							
AVE	3.72	1.18	4.90			13.48	23.28
MIN	3.07	0.43	4.32			11.67	19.49
MAX	5.03	1.53	5.38			15.77	27.71
PM(lb/h)							
AVE	18.66	3.92	16.34			44.88	83.81
MIN	15.44	1.43	14.38			38.87	70.13
MAX	25.30	5.10	17.95			52.50	100.85

Table C-4. Port of Philadelphia marine traffic and associated emission estimates.

Train traffic

It is particularly important to take emissions from trains into account because railroad tracks ran within 10m to the east and north of the Exchange (Figure 36). The areas where the greatest marble deterioration is documented. These tracks were owned by the Delaware Avenue Beltline and the Dock Street spur, which operated from 1872 to World War II (Penrose (1988), Penrose (1989)). Before the 1870s, locomotives were not allowed in central Philadelphia (and most other densely populated cities) based on the danger of explosion and fire hazards. Long-distance trains were harnessed to mule and horse teams for the final leg of the journey to the center of the city. Thus, in the Exchange neighborhood, pollution from locomotives would not be a factor in the first 40 years of exposure. The Dock Street Spur was used for about 75 years to carry freight from the port to the Pennsylvania Railroad system.

This section will be expanded when additional data become available. It is anticipated that these emissions will include the greatest contribution to pollutant loadings at the Exchange in the 1890s.

Acknowledgements

Many thanks are due to assistance from NPS staff with encyclopedic knowledge, in particular Kevin Foster, Maritime Historian; David Orr, Mid-Atlantic Regional Archaeologist; Rebecca Schiffer, Technical Assistance Branch, Mid-Atlantic Regional Office.

In addition, thanks to the following individuals who were generous with their time and insights: Joel Tarr, Professor of Civil Engineering, Carnegie Mellon University; William Reilly, retired Chief of Air Management Services, City of Philadelphia, Gary Fitzpatrick of the Geography and Map Division of the Library of Congress; Rich

Boardman, Map Collection of the Free Library of Philadelphia; E. Ann Wilcox, Maritime Museum of Philadelphia; Richard Henderson, National Archives; Robert Penrose, Ted Xaras, and Frank Tartall, Philadelphia railroad buffs.

APPENDIX D: Microclimate/Pollution Measurement Methods

Donald A. Dolske

Introduction

Moisture cycling on building surfaces is a complex function of many variables including exposure to ambient winds, internal and surface thermal properties of various parts of the structure, relationship to other parts of the building, location relative to other buildings and nearby vegetation, insolation, and, of course, rainfall exposure. A limited amount of preliminary data (Dolske, 1987) at the Exchange demonstrated the range of variability in spatial and temporal patterns of surface moisture on the building (see Chapter 5, Figure 41). Further, mass-loss estimates developed in a survey of the condition of the marble exterior of the building conducted by Oehrlein and Associates (1988) showed that the parts of the building which tended to remain wet longer into the daytime hours (in the 1987 moisture study) have also eroded more rapidly.

This work, therefore, is an investigation of the correlation between the timing of surface moisture cycles and pollutant concentrations experienced by two selected locations on the building exterior. The microclimate / pollution concentration sampling points have similar exposure to wind and rainfall, but different exposure to some of the other moisture - cycle determinants. Two points on the east side of the building (see Chapter 5) are used for sampling: Column 9 which receives full sunlight immediately after sunrise in the summer months, and Column 16, which remains shaded until early afternoon. These measurements, which compare pollutant concentrations during the times the surfaces are moist or dry in combination with surface sampling techniques, will provide valuable information about the dry deposition process and its impact on the variable deterioration observed on the building. Background data on general meteorological parameters are collected via sensors mounted on the roof of the building.

Monitoring Techniques

Airborne pollutant concentrations

At each of two points selected for sampling, Columns 9 and 16, identical sets of pollutant sampling and microclimate sensing instrumentation has been installed (Figure D-1). The pollutant samplers consist of mass-flow controlled vacuum sources connected to series - filtration particle / gas units, or filterpacks. Each sampler controls two filtration units, one of which is connected to the sampling air stream when the surface is wet; the other is in line when the surface is dry. Wet and dry surface conditions are defined electronically by a surface moisture sensing system and the measured relative humidity of the air. The bimetallic grid sensors do not respond with absolute accuracy to the actual moisture content of the stone; however, the presence of sufficient moisture at the stone surface to affect pollutant deposition is reasonably well accounted for by this sensing technique. Thus, for each sample - integration period of one week, each sampling point provides two measurements of pollutant concentration: a "wet" period average concentration and a "dry" period average concentration.

A four-stage series filtration, "filterpack", method (Dolske, 1985; Dolske and Petuskey, 1984; Dolske and Stensland, 1983) is used to measure the airborne concentrations of particulate SO_4^{2-} and NO_3^- as well as HNO_3 and SO_2 gases. Air intake is controlled using MKS Instruments, Inc. Model 1259b electronic flow controllers (one for each column) ahead of a Gast Manufacturing model DOA-110A vacuum pump. The flow controllers compensate for variations in pressure drop in

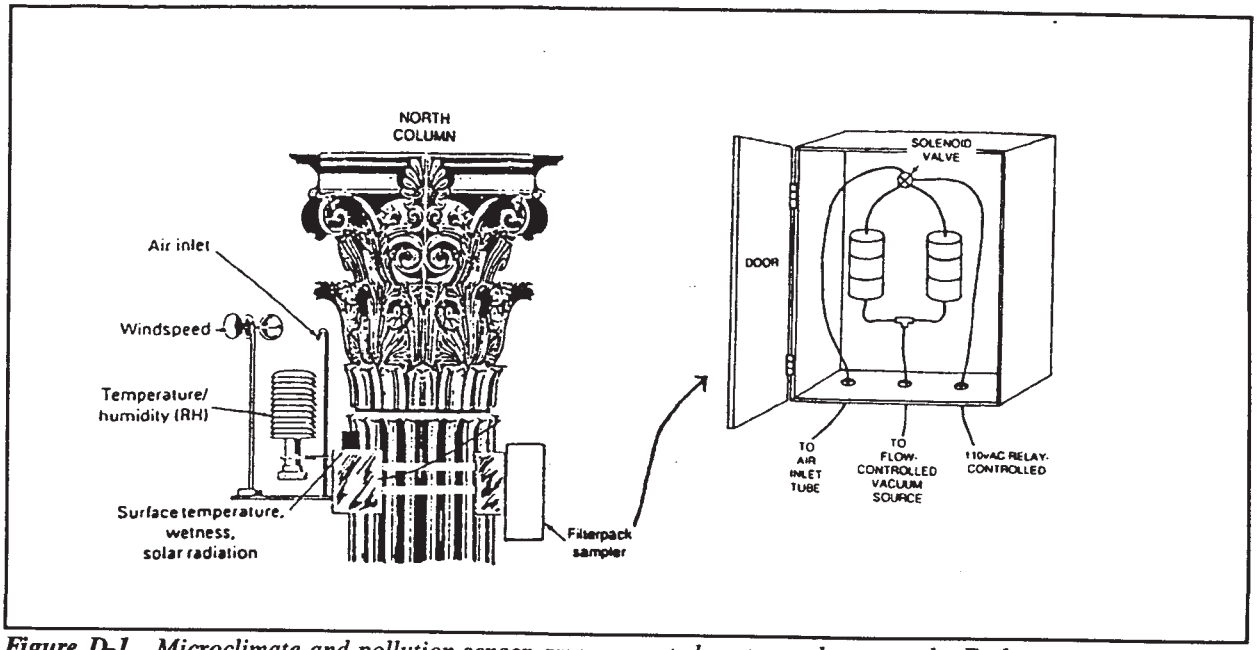


Figure D-1. Microclimate and pollution sensor array mounted on two columns at the Exchange.

the sampling system due to filter loading, humidity changes, and so on, keeping the flow rate constant (+/- 1/2 percent) at a nominal set point of 3.0 liters/min. Fittings and connectors in the system are stainless steel, and Tygon 3063R 1 cm diameter vacuum tubing is used throughout.

The filters are mounted in Nuclepore 47 mm in-line polycarbonate plastic multiple - filter aerosol - sampling holders. Pairs of holders with quick-release fittings and flow-dividing tubing are prepared in the Illinois State Water Survey (ISWS) laboratory to facilitate efficient handling by field site operators. Four types of filters are used in series within the holder, separated by polycarbonate support screens and sealed with silicone o-rings and flat gaskets. The first filter is an 8.0 um pore diameter Nuclepore, which collects large aerosol particles (diameter > 2.5 um), while allowing smaller particles to pass through to the second stage filter (Cahill, et al., 1977). The second filter is a 1.0 um Teflon membrane, which retains the remaining small particles with a very high collection efficiency, meaning that only gaseous components of the air stream pass through. These first two stages are made of materials which are relatively unreactive with the gaseous pollutants.

The third filter is a 1.0 um Nylasorb Nylon-membrane filter which selectively adsorbs nitric acid vapor (Goldan, et al., 1983). The sum of particulate nitrate from the first two filters and nitric acid from the third filter represents the total ambient nitrate concentration. It is difficult, however, to reliably use the data for particulate versus gaseous nitrate, because of artifact formation in series filtration sampling systems. Nitrate originally captured as particles can volatilize to maintain equilibrium with the sampled air stream passing over the filter; conversely, nitric acid can react with accumulated particles on the first two stages. Hence the use of nitrate data as total (gas plus particle) concentrations.

The fourth and last filter is a double layer of Whatman number 41 cellulose fiber paper which is doped with 25 percent (by volume) glycerol in water, saturated with K_2CO_3. The filters are dipped into the carbonate solution and then dried in an oven at 90°C for a few

minutes before loading into the filterpack. This treated-filter stage is used to selectively absorb sulfur dioxide (Johnson and Atkins, 1975).

Loading of clean filters is done shortly before shipment of the holder to the field site. The filter units are sealed in polyethylene bags and shipped to the field site within a few days of the scheduled installation. Exposed filterpacks are again sealed in several layers of polyethylene bags immediately after sampling to prevent contamination between the field site and laboratory.

Upon return to the ISWS laboratory, each of the filterpack stages is removed from the holder and placed in a 35 ml polyethylene bottle. For the first and second stages, extraction of the sample is done by adding 30 ml of the 20 mM carbonate / bicarbonate buffer used as the ion chromatograph eluant to the bottle. The bottle and filter are then sealed and placed in an ultrasonic bath for 30 minutes. This process removes and dissolves any particles trapped on the filters. The third and fourth stages are also extracted in an ultrasonic bath, but the extracting solutions are slightly different. The Nylasorb filter is subjected to 30 mM NaOH solution, to desorb the nitric acid from the Nylon membrane. The Whatman 41 filters are extracted in a 0.03 percent H_2O_2 solution to complete the oxidation of any SO_2 adsorbed on the filter to SO_4^{2-}. Analysis of the extracts for SO_4^{2-} and NO_3^- is done by automated ion chromatography, using a DIONEX 2110i chromatograph, Nelson Analytical Model 861A analog-to-digital interface, and an IBM PC/XT computer as system controller and data storage device. Standardization and calibration of analytical results is performed cooperatively with other laboratories at ISWS.

Building Microclimate

To provide additional information at each of the sampling points, identical arrays of microclimate sensors have been placed near each column's surface. The sensors are connected to a central digital datalogger (Campbell Scientific, Inc. model 21XL) which records the data on magnetic tape for retrieval on a weekly basis. The datalogger also

Sensor Code	Exposure and Compass Orientation	Location on Merchants Exchange Facade
X1	exposed - 270°	outside south column capital - west portico
X2	protected - 90°	inside south column capital - west portico
X3	exposed - 0°	outside north column capital - east portico
X4	protected - 180°	inside north column capital - east portico
X5	exposed -180°	outside south column capital - east portico
X6	protected - 0°	inside south column capital - east portico
X7	exposed - 25°	outside north-north-east antefix
X8	exposed - 65°	outside east-north-east antefix
X9	exposed - 115°	outside east-south-east antefix
X10	exposed - 155°	outside south-south-east antefix

Table D-1. Locations of sensors in 1987 ten-point moisture cycle survey.

controls the switching of filtration modules through a solid-state relay system, as described above. Microclimate sensors on each column include: air temperature (thermistor probe), relative humidity (capacitance sensors), stone surface temperature (copper-constantan thermocouple), stone surface wetness (Epitek Electronics, Ltd., Sereda SMMS-01 bimetallic grid), wind velocity (MetOne magnetic reed closure cup anemometer), and solar radiation intensity (Li-Cor LI2000S silicon pyranometer), shown in Figure D-1.

Surface deposit sampling

Soluble surface accumulation sampling techniques using deionized water washings are conducted once every four to six weeks during warm (above freezing) weather. These samples provide a measure of the accumulation of pollutants on the stone surface at each of the sampling points. At the top of each of the columns, individual samples are collected within one central each flute. A known volume (150 mL) of deionized water is be used to flush a measured area (100cm^2) of the stone surface. The runoff water is collected in a polyethylene funnel-and-bottle device, fitted with a flexible gasket to prevent loss of any liquid. The samples are returned to the laboratory for automated ion chromatographic analyses of inorganic anions and cations, including sulfate, nitrate, chloride, potassium, ammonium, calcium and magnesium, as well as volume and pH determinations.

Rooftop meteorology and precipitation collection at the Exchange

A set of meteorological sensors, compatible in response and precision with the microclimate equipment, is installed on the roof of the Exchange. Parameters monitored include temperature and humidity, wind velocity and direction, and precipitation rate (tipping bucket gauge) A Campbell Scientific, Inc. model CR21 datalogger records hourly averages of these parameters on magnetic tape. An automatic opening, quasi wet-only rain collector is also located on the roof. The rain collector is held closed in dry weather to prevent accumulation of dry deposited materials on the funnel and sample bottle inside. At the onset of rain, a small soluble paper strip holding the lid closed disintegrates, and the spring - loaded lid flips open. The site operator retrieves the sample as soon as possible after the cessation of rain and returns the sample to the laboratory for analysis (as the surface accumulation samples) (Dugan & Dolskey, 1990).

References

Cahill, T.A., L.L. Ashbaugh, J.B. Barone, R.A. Eldred, P.J. Feeny, R.J. Flocchini, and C. Goodart, 1977. Analysis of respirable fractions in atmospheric particulate via sequential filtration, *J. Air Pollut. Control Ass., 27*, 675-681.

Dolske, D.A., and G.J. Stensland, 1983. A comparison of ambient airborne sulfate concentrations determined by several different filtration techniques, In Proc. 3rd National Symposium on Recent Advances in Pollutant Monitoring of Ambient Air and Stationary Sources. Raleigh, NC, 3-6 May 1983.

Dolske, D.A., 1985. A Field Study of Dry Deposition of Airborne Materials to Soybeans and Corn: Measurement Of Accumulation Rates And Assessment Of Acid Precipitation Interactions. Terrestrial Effects Task Group Project Review, Brookhaven National Lab, Upton, NY.

Dolske, D. A., 1987. Preliminary Data Summary: Philadelphia Merchant's Exchange Surface Moisture Study. Report to U.S. National Park Service / Preservation Assistance Division, Washington, DC. 18pp.
Dugan, C.O., D.A. Dolske, 1990. Twelve Years of Rain Chemistry in Philadelphia. *APT Bulletin*, 26.

Goldan, P.D., W.C. Kuster, D.L. Albritton, F.C. Fehsenfeld, P.S. Connell, R.B. Norton,

and B.J. Huebert, 1983. Calibration and tests of the filter - collection method for measuring clean-air, ambient levels of nitric acid, *Atmos. Environ., 17,7,* 1355-1364.

Johnson, D.A., and D.H.F. Atkins, 1975. An airborne system for the sampling and analysis of SO2 and atmospheric aerosols, *Atmos. Environ., 9,* 825-833.

Appendix E: Estimating Sulfur Deposition to the Marbles

Donald A. Dolske

SO_2 is one of the major pollutants whose deposition is significantly increased by surface moisture cycle variations. Particulate $SO_4^=$ and NO_3^-, whether in gaseous HNO_3 or particulate NO_3^- form, may also potentially accelerate carbonate stone deterioration. The influence of surface moisture on the deposition of these species, however, is not well understood.

Measuring dry deposition fluxes to marbles at the Exchange

Four faces or "exposures" at the two columns are sampled as shown in Figure E-1a. The *protected* face of the capitals are partially sheltered from rain by projections from the upper capital, while the *exposed* face of the columns are fully washed by rain. This distinction applies to a lesser degree to the *east* and *west* sample locations, where both columns and capitals can be partially exposed or sheltered by their position within the colonnade with respect to the incoming rain. The *protected* column and capital sample locations are both fully sheltered from rain.

To collect a washdown sample, a known volume (150 ml) of deionized water is used to flush the defined area of stone, approximately 100 cm^2 (Figure E-1b). A narrow stream from a laboratory squeeze-wash bottle is applied for 60 seconds. The resulting runoff water is collected in a polyethylene and mylar funnel-and-bottle device, fitted with a flexible gasket at the stone-mylar junction to minimize loss of liquid. Washdown solutions are returned to the laboratory for ion chromatographic analyses of inorganic anions and cations (including $SO_4^=$, NO_3^-, Cl^-, NH_4^+, Ca^{++}, Mg^{++}, Na^+, and K^+).

Principles of estimating deposition to marble

The deposition of pollutants to building surfaces is normally expressed as a flux (mass deposited to a unit area per unit time). The relationship between the air concentration in the vicinity of a structure and the areally-averaged flux to the surface is expressed as follows:

$$\text{Deposition velocity} = \text{Flux}/\text{Concentration}$$

Dry deposition velocities, v_d, were derived for Carrara and Pennsylvania Blue marble using monument runoff compositions at Gettysburg National Military Park, Pennsylvania, are briefly described below. The relative effective deposition velocity can be calculated, if concentrations are measured and flux is measured or estimated. At Gettysburg, the flux is estimated by analogy to runoff concentrations of sulfate and nitrate; at Independence, by washdown concentrations of sulfate.

The impact of acidic precipitation on c. 100 year old marble monuments at Gettysburg NHP was measured during 40+ individual rain storms from mid-1986 through late 1988. Gutters to collect runoff from small catchment areas were fitted to two Carrara marble statues, a Carrara marble obelisk, and a Pennsylvania Blue marble obelisk. Incident rain and runoff from marble surfaces were collected for individual rainstorms or events. Calcium removed from the surface, as one indicator of marble decay, was measured using the concentration differences between incident rain and monument runoff. Calcium loss from the Carrara statues is about 3 times greater than for the vertical obelisk, whereas there is no difference in the mass losses for the Carrara and Pennsylvania obelisks. Over the course of the 2 1/2 year collection period, the

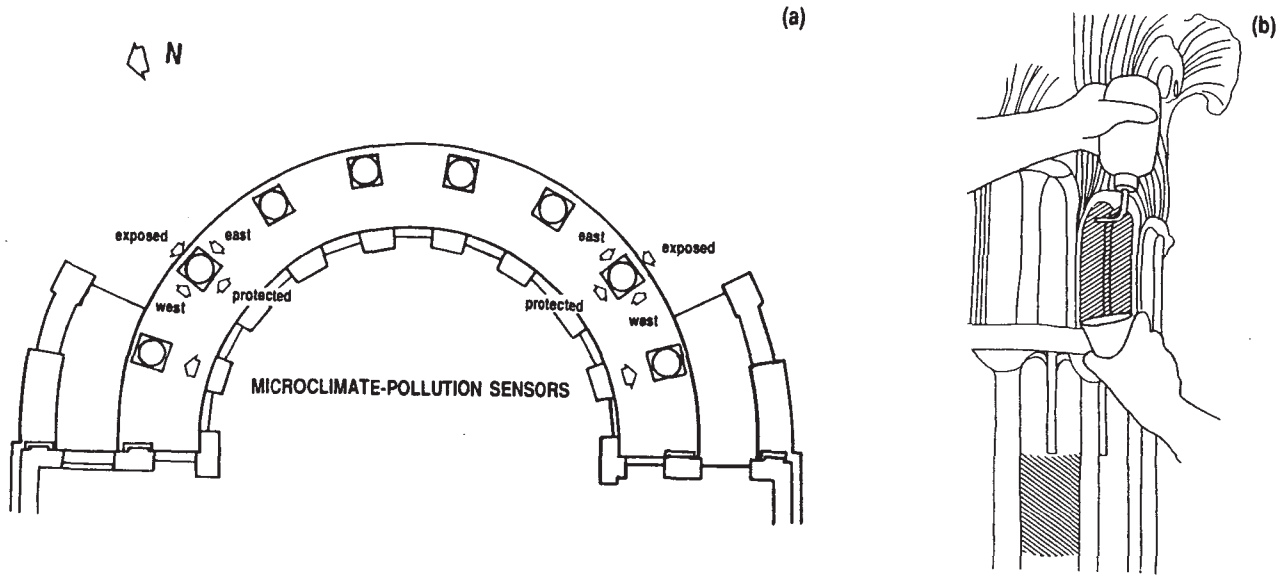


Figure E-1. *a) Washdown locations at the Exchange; b) washdown areas (c. 10 x 10cm) are shaded.*

net calcium lost per monument for every meter of rain varied as follows:

Pennsylvania obelisk	.02mg	7μm
Carrara obelisk	.02mg	7μm
Carrara statue - *History*	.22mg	8.2μm
Carrara statue - *War*	.22mg	9.1μm

Excess sulfate concentration in the runoff varies both as function of stone type and by configuration. The excess sulfate values for the two obelisks indicates the relative affinity of the coarse-grained Pennsylvania and fine-grained Carrara marbles for uptake of sulfur oxides. The median value for excess sulfate in runoff from the Pennsylvania blue marble is double that of Carrara. This finding that sulfur accumulates more readily on coarse grained stone compares well with findings from other groups (1).

Comparison of runoff sulfate for the two Carrara statues and the Carrara obelisk that the sulfate in runoff from the Carrara statues is even greater. These results confirm the aerodynamic predictions that the role of atmospheric sulfur is more significant for both rougher surfaces and complex shapes. The relative concentrations of airborne sulfur and nitrogen oxide species, in view of our understanding of the relative efficiency of delivery of these species to material surfaces (2), appear to correlate well with the observations of sulfate and nitrate in the runoff solutions described below (Figure E-2).

A large concentration difference (and the associated difference in dry deposition to marble surfaces) during the period immediately preceding a rain event might be expected to alter the chemical makeup of the runoff. The airborne concentrations during dry periods between rain events were calculated using time-weighted averages of the weekly filterpacks. Between rain-event periods ranged from several days to three weeks. Antecedent concentrations in $\mu g/m^3$ for SO_2, particulate sulfate, and total nitrate are summarized in Table E-1.

Relative effective deposition velocities were calculated as follows. First, the nitrate or sulfate in runoff from the monuments in excess of the concentration in the incident rain water

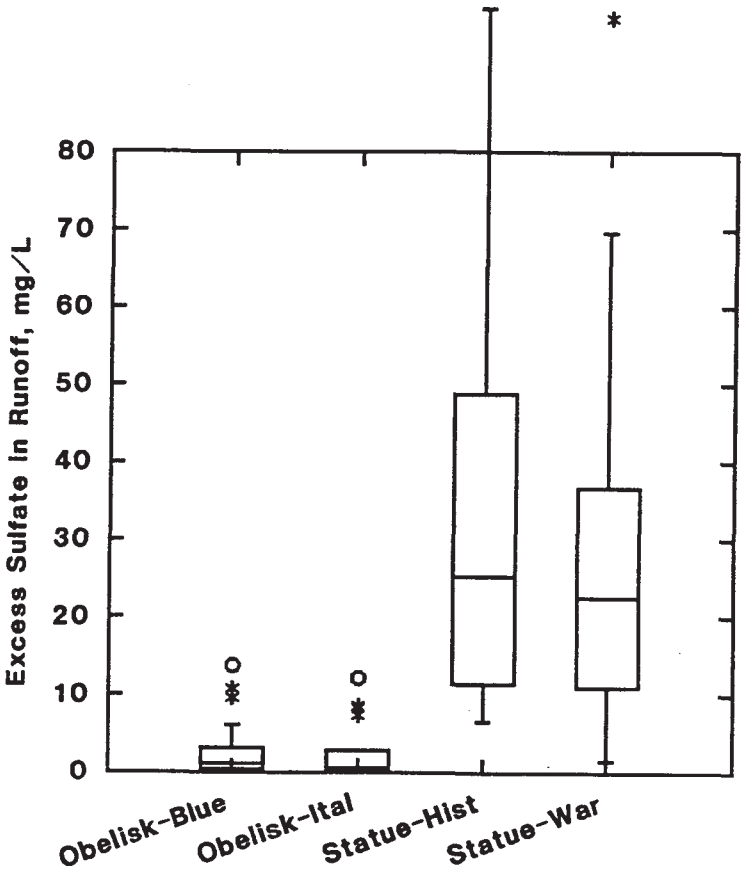


Figure E-2. Excess sulfate concentrations in runoff by Gettysburg monument.

was taken to be the contribution of dry deposited surface accumulations. These excess concentrations were normalized by catchment area and sample volume to arrive at a mass per unit area value. This number was then divided by the airborne concentration for the period preceding the rain event, and the length of time between rain events, to arrive at a v_d estimate. Appropriate unit conversions were made to arrive at v_d values in cm/s. Mean values for the various parameters used to compute these estimates are shown in Table E-1.

Mean values for the various parameters used to compute the v_d's are shown in Table E-1.

A difficulty of interpretation arises because sulfur in the runoff sample occurs as sulfate, which need to be related to distinct airborne concentrations of SO_2 and sulfate aerosol. Thus, three sulfur v_d values are presented: the first assumes that SO_2 and particulate $SO_4^=$ contribute to sulfate in the runoff, the second assumes all sulfate in runoff stems from SO_2 dry deposition, and the third assumes particulate $SO_4^=$ is the only contributor. This complexity is not present for nitrate, as the airborne measurements aggregate the gas and aerosol concentrations. These results suggest that the type of marble strongly influences the dry deposition of sulfate and nitrate.

Monument	Blue marble Obelisk	Carrara marble Obelisk
catchment area (m^2)	0.404	0.436
mean runoff sample volume, mL	213.4	151.0
excess concentration in runoff (mg/L):		
sulfate	1.12	0.56
nitrate	0.83	0.61
antecedent airborne concentrations ($\mu g/m^3$)		
nitrate	0.979	0.979
sulfate	1.389	1.389
sulfur dioxide	1.31	1.31
dry deposition velocity, v_d (cm/s):		
nitrate	0.43	0.20
(both SO_2 & $SO_4^=$) sulfate	0.10	0.03
(SO_2 only) sulfate	0.15	0.05
(particle $SO_4^=$) sulfate	0.40	0.13

Table E-1. *Values of parameters used to estimate dry deposition velocities to Carrara and Pennsylvania Blue Marble Obelisks at Gettysburg, Pennsylvania.*

Using the estimated v_d values from the Gettysburg measurements and the airborne concentration measurements at Independence, a sulfur dry deposition flux to the marbles at the Exchange was computed for each bi-weekly measurement interval. The calculation assumes that a rain event flushes all the sulfate from the marble surface (3); thus the flux estimates represent recent deposition of sulfate, not an aggregate accumulation. A fixed period between rain events (5 days) was selected based on the long-term regional average to simplify the calculation of sulfate accumulation for these preliminary estimates. Future calculations will be based on the actual intervals between rain. The algorithm also assumes that the deposition velocity during dry surface conditions is 10% of the v_d for wet marble, by analogy with laboratory determinations of v_d for Vermont marble and Indiana limestone (4). Table E-2 presents the long-term average of the estimated sulfur deposition.

The results in Table E-2 demonstrate that a relatively small difference in wetness has a large influence the deposition of SO_2, with the south side receiving about 60% more deposition to wet surfaces than the north side. As expected from the 1:3 ratio of the v_d's, the net sulfur flux to the fine grained Carrara marble is about one-third that to coarse-grained Pennsylvania blue marble. The sulfur flux estimates indicate that while deposition to wet marble is more efficient, the bulk of sulfur is deposited when marble is dry.

	North Side		South Side	
percent time surface wet	11.1		16.7	
SO_2 WET	1.0		1.6	
(μg/m3) DRY	11.1		12.3	
marble type	Carrara	Blue	Carrara	Blue
v_d wet	0.15	0.45	0.15	0.45
v_d dry	0.017	0.05	0.017	0.05
SO_2 Flux, wet	7.2	21.6	17.3	51.8
ng/cm^2 dry	71.8	210.0	75.2	222.0
total	79.0	231.6	92.5	273.8

Table E-2. Calculated sulfur fluxes to the north and south sides of the Exchange.

References

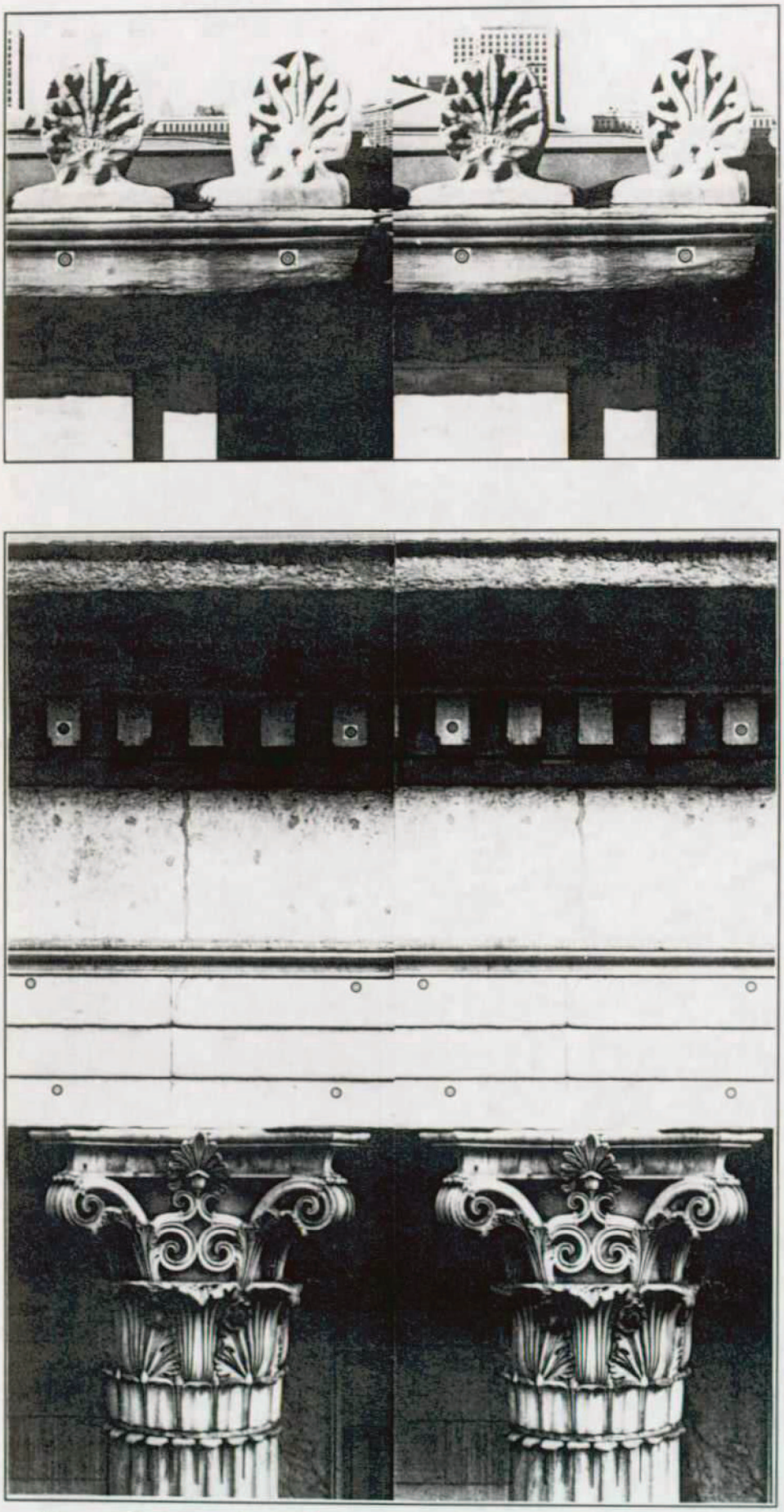
1. Furlan, V., and Giradet, F., Vitesse d'accumulation des composes atmospheriques du soufre sur diverses natures de pierre. Proc. 6th Int'l Congress on Deterioration and Conservation of Stone, Torun, Poland, 12-14 Sept. 1988, pp. 187-196; Spedding, D. J., The nature of water associated with atmospheric particulate material. Extended abstract. Proc. Conf. Gas Liquid Chemistry of Natural Waters, Univ. of Aukland, Auckland, New Zealand, April 1984; Zallmanzig, J., Investigations on the rates of emission and effects in selected places of Europe for the quantitative examination of the influence of air pollution on the destruction of ashlar. NATO report of the NATO/CCMS Pilot Study on Conservation and Restoration of Monuments, Number 158, 1985, 216p.

2. Judeikis, H. S., and Wren, A. G., Laboratory measurements of NO and NO_2 depositions onto soil and cement surfaces. Atmos. Environ., 1978, Vol. 12, pp. 2315-2319; Livingston, R. A., The role of nitrogen oxides in the deterioration of carbonate stone. Proc. 5th Int'l Congress on Deterioration and Conservation of Stone, 25-27 Sept. 1985, Lausanne, Switzerland, pp. 509-516. Sherwood, S. I., Gatz, D. A., Hosker Jr., R. P., et al., Processes of deposition to structures. NAPAP SOS/T Report 20, National Acid Precipitation Assessment Program, Acidic Deposition: State of Science and Technology, 1990, Vol. III.

3. White, W. B., Rate processes: chemical kinetics and karst landform development. Groundwater as a Geomorphic Agent, R. G. LaFleur, ed., Allen and Unwin, Inc. Boston, 1983, pp. 227-248.

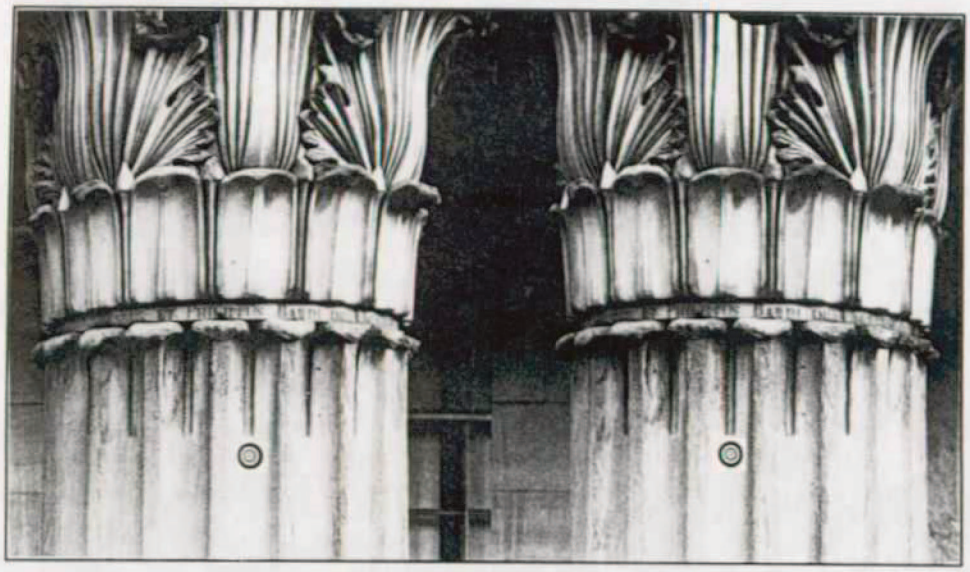
4. Spiker, E. C., Comer, V. J., Hosker, R. P., and Sherwood, S. I., Dry deposition of SO2 on limestone and marble: role of humidty. Proceedings of the 7th Intl Congress on Deterioration and Conservation of Stone, Lisbon, June 1992.

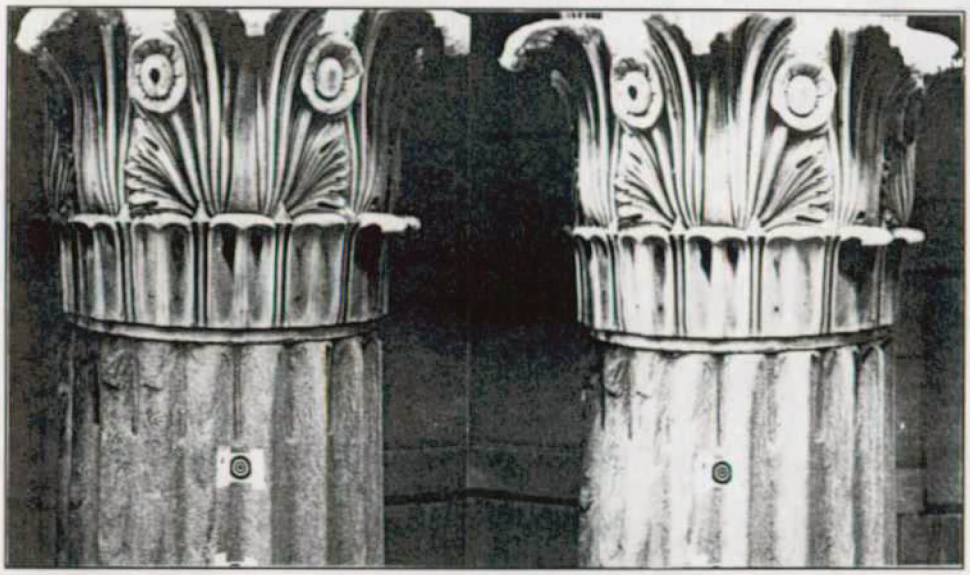
PLATE 1 - UPPER SECTION

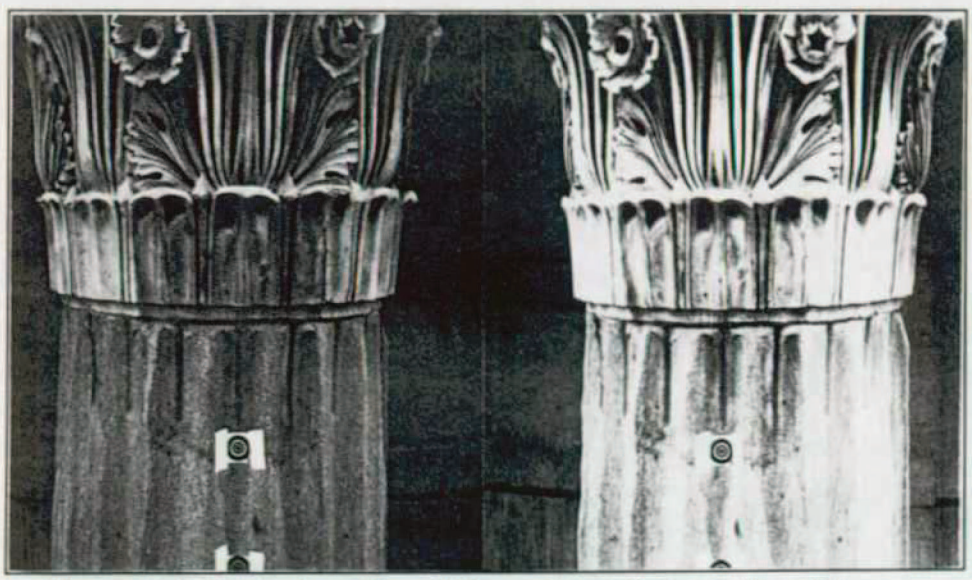


Top: antefixes, east facade; *bottom:* west entablature and capital.

PLATE 2 - LOWER CAPITALS/UPPER COLUMNS

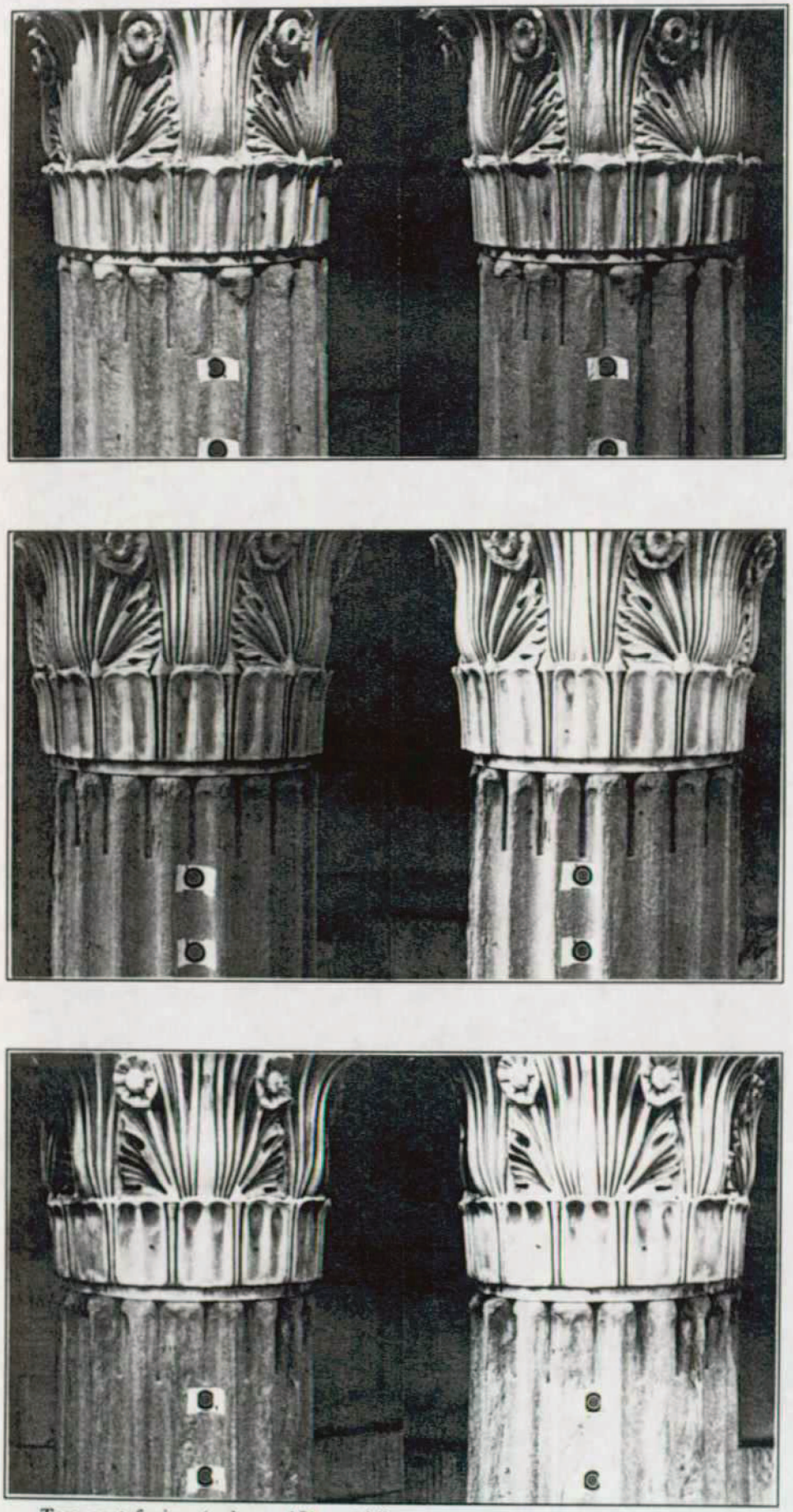






Top: west facing (column 3); *middle*: northeast facing (column 9); *bottom*: northeast east facing (column 10).

PLATE 3 - LOWER CAPITALS/UPPER COLUMNS



Top: east facing (column 12); *middle*: southeast east facing (column 15); *bottom*: southeast facing (column 16).